BIBLIOGRAPHIC INFORMATION

PB92-189109

Report Nos: CCEER-92-1

Title: Scale Model Testing of One-Way Reinforced Concrete Pier Hinges Subjected to Combined Axial Force, Shear and Flexure.

Date: Mar 92

Authors: D. L. Straw, M. Saiidi, and D. N. O'Connor.

Performing Organization: Nevada Univ., Reno. Center for Civil Engineering Earthquake Research.

Sponsoring Organization: *National Science Foundation, Washington, DC.

Grant Nos: NSF-CES-870062

Supplementary Notes: Sponsored by National Science Foundation, Washington, DC.

NTIS Field/Group Codes: 50A, 50C

Price: PC A03/MF A01

Availability: Available from the National Technical Information Service, Springfield, VA. 22161

Number of Pages: 47p

Keywords: *Model tests, *Reinforced concrete, *Bridge piers, *Hinges, *Dynamic response, Deformation, Reinforcing steels, Computer programs, Loads(Forces), Earthquake engineering, Structural vibration, Displacement, Structural members, Cyclic loads, Seismic waves, Earthquake damage, Shear properties.

Abstract: The report presents the results of the second phase of an ongoing study at the University of Nevada, Reno. The phase involved laboratory and analytical evaluation of one-way reinforced concrete pier hinges subjected to a combination of uniaxial moment transfer, shear, and axial compression. Four one-sixth scale hinge models were built and tested in the strong direction. There were two primary variables in the testing sequence; shear-span to depth ratio (aspect ratio), and monotonic versus cyclic loading. Analysis of the hinged specimens involved determining flexural and shear strengths, concentrated hinge rotations, and displacement of the column elements. A comparison between the measured and the calculated yield and failure loads is presented for each specimen. Various shear capacity equations and their accuracies are also examined relative to the measured data. Hinge rotation and column deflection consisted of two components: reinforcement bond slippage and plastic deformation. Flexural displacements were determined from the curvature distribution along the column and included elastic deformation of the column and plastic deformation of the hinge. Empirical formulas used to estimate the rotations and displacements are discussed.

Center for Civil Engineering Earthquake Research

• Reno

Engineering Research and Development Center
College of Engineering
University of Nevada Reno

Report Number CCEER-92-1

Scale Model Testing of One-Way Reinforced Concrete Pier Hinges Subjected to Combined Axial Force, Shear and Flexure

D. L. Straw, Graduate Assistant
M. "Saiid" Saiidi, Professor and Chairman

Edited by D. N. O'Connor, Engineering Research Assistant

Center for Civil Engineering Earthquake Research
Department of Civil Engineering
University of Nevada
Reno, Nevada 89557

March 1992

Abstract

This report presents the results of the second phase of an ongoing study at the Univerisity of Nevada, Reno. This phase involved laboratory and analytical evaluation of one-way reinforced concrete pier hinges subjected to a combination of uniaxial moment transfer, shear, and axial compression. Four one-sixth scale hinge models were built and tested in the strong direction. There were two primary variables in the testing sequence: shear-span to depth ratio (aspect ratio), and monotonic versus cyclic loading.

Analysis of the hinged specimens involved determining flexural and shear strengths, concentrated hinge rotations, and displacement of the column elements. A comparison between the measured and the calculated yield and failure loads is presented for each specimen. Various shear capacity equations and their accuracies are also examined relative to the measured data.

Hinge rotation and column deflection consisted of two components: reinforcement bond slippage and plastic deformation. Flexural displacements were determined from the curvature distribution along the column and included elastic deformation of the column and plastic deformation of the hinge. Empirical formulas used to estimate the rotations and displacements are discussed.

Results of the testing indicate that cyclic loading reduces the stiffness of the connection substantially and reduces the energy absorbing capabilities of the hinge.

Acknowledgements

This study was conducted under grant number CES-870062 from the National Science Foundation. The opinions expressed in this paper belong solely to the authors, and do not represent the official position of either the University of Nevada, Reno (UNR), or the National Science Foundation.

The authors would like to express their appreciation to Mr. Joseph Shields, a former graduate student at UNR, for his assistance during the initial stages of this project. Special thanks are due to Mr. Jesus Pedroarena, Civil Engineering Technician, for his careful work in constructing, instrumenting, and testing of the specimens.

This report is based on a Master of Science thesis written by the first named author, under the direction of M. Saiidi.

Contents

Abstract . . . iii

Acknowledgements . . . iv

List of Tables . . . ix

List of Figures . . . ix

Notations . . . xiii

Chapter 1 Introduction . . . 1
- 1.1 Background . . . 1
- 1.2 Previous Work . . . 2
- 1.3 Object and Scope . . . 4

Chapter 2 Experimental Study of Hinged Specimens . . . 7
- 2.1 Introduction . . . 7
- 2.3 Materials and Fabrication . . . 8
- 2.4 Instrumentation . . . 9
- 2.5 Test Procedure . . . 10

Chapter 3 Results of Hinged-Specimen Testing . . . 11
- 3.1 Introduction . . . 11
- 3.2 Specimen SD1M . . . 12
  - 3.2.1 Load-Deflection Response . . . 12
  - 3.2.2 Load-Strain Response . . . 12
  - 3.2.3 Load-Rotation Response . . . 13
  - 3.2.4 Load-Horizontal Slip Response . . . 13
  - 3.2.5 Axial Load-Deformation Response . . . 13
  - 3.2.6 Load-Column Twist Response . . . 14
- 3.3 Specimen SD2M . . . 14
  - 3.3.1 Load-Deflection Response . . . 14
  - 3.3.2 Load-Strain Response . . . 14
  - 3.3.3 Load-Rotation Response . . . 15
  - 3.3.4 Load-Horizontal Slip Response . . . 15
  - 3.3.5 Axial Load-Deformation Response . . . 15
  - 3.3.6 Load-Column Twist Response . . . 16
- 3.4 Specimen SD1C . . . 16
  - 3.4.1 Load-Deflection Response . . . 16
  - 3.4.2 Load-Strain Response . . . 17
  - 3.4.3 Load-Rotation Response . . . 17

3.4.4 Load-Horizontal Slip Response . . . 18
3.4.5 Axial Load-Deformation Response . . . 18
3.4.6 Load-Column Twist Response . . . 18
3.4.7 Load-Base Rocking Response . . . 18
3.5 Specimen SD2C . . . 19
3.5.1 Load-Deflection Response . . . 19
3.5.2 Load-Strain Response . . . 19
3.5.3 Load-Rotation Response . . . 20
3.5.4 Load-Horizontal Slip Response . . . 20
3.5.5 Axial Load-Deformation Response . . . 20
3.5.6 Load-Column Twist Response . . . 21
3.5.7 Load-Base Rocking Response . . . 21

Chapter 4 Analysis of Specimens . . . 23
4.1 Introduction . . . 23
4.2 Flexural Analysis . . . 23
4.3 Shear Analysis . . . 25
4.4 Rotation Analysis . . . 26
4.4.1 Specimen SD1M . . . 28
4.4.2 Specimen SD2M . . . 28
4.4.3 Specimen SD1C . . . 28
4.4.4 Specimen SD2C . . . 29
4.4.5 General Comments . . . 29
4.5 Deflection Analysis . . . 29
4.5.1 Specimen SD1M . . . 30
4.5.2 Specimen SD2M . . . 30
4.5.3 Specimen SD1C . . . 30
4.5.4 Specimen SD2C . . . 31
4.5.5 General Comments . . . 31

Chapter 5 Comparison with Previous Testing . . . 33
5.1 Introduction . . . 33
5.2 Comparison of Test Specimens . . . 33
5.3 Failure Modes . . . 34
5.3.1 Original Concrete Hinge Series . . . 34
5.3.2 Standard Detail Series . . . 35
5.4 Scale Effect . . . 35
5.5 Effects of the use of Deformed Bars . . . 35

Chapter 6 Summary and Conclusions . . . 37
6.1 Summary . . . 37
6.2 Observations . . . 37
6.3 Conclusions . . . 38

References . . . 41

Appendix A Aggregate Properties 107

Appendix B Concrete Mixture Design 109

Appendix C Concrete Properties 111

Appendix D Reinforcing Steel Properties 113

Appendix E Listing of *PIERHINGE* Computer Program 115

Appendix F *PIERHINGE* User's Guide 131

Appendix G List of CCEER Publications 137

List of Tables

4-1	Measured and Computed Yield Loads for Specimen SD1M	44
4-2	Measured and Computed Yield Loads for Specimen SD2M	44
4-3	Measured and Computed Yield Loads for Specimen SD1C	45
4-4	Measured and Computed Yield Loads for Specimen SD2C	45
4-5	Shear Strength Analysis based on Different Methods	46

List of Figures

1-1	Typical Reinforced Concrete Hinge	47
1-2	Shear Friction Mechanism	47
1-3	One-Way Hinge Failure Mechanism	48
2-1	Cross-Sections of the Rose Creek Interchange	49
2-2	Typical Hinge Cross-Section and Elevation of SD-Series Test Specimens	50
2-3	Typical Foundation Segment after Curing	51
2-4	Flowchart for Data Acquisition Software Program *PIERHINGE*	52
2-5	Instrumentation Detail for Specimens SD1M and SD2M	53
2-6	Instrumentation Detail for Specimens SD1C and SD2C	53
2-7	Instrumentation Detail for Measuring Column Twist	54
2-8	Instrumentation Detail for Measuring Base Rocking	54
2-9	Test Frame Setup	55
2-10	Hydraulic Ram Collar	56
3-1	Dowel Numbering for Test Specimens	57
3-2	Load-Deflection Diagram for Specimen SD1M	57
3-3	Cracking Pattern of Specimen SD1M	58
3-4	Load-Strain Diagram for SD1M, Bar 1 (Avg. of Gages 1 and 2)	58
3-5	Load-Strain Diagram for SD1M, Bar 1 (Avg. of Gages 3 and 4)	59
3-6	Load-Strain Diagram for SD1M, Bar 1 (Avg. of Gages 5 and 6)	59
3-7	Load-Strain Diagram for SD1M, Bar 2 (Avg. of Gages 7 and 8)	60
3-8	Load-Strain Diagram for SD1M, Bar 2 (Avg. of Gages 9 and 10)	60
3-9	Load-Strain Diagram for SD1M, Bar 3 (Avg. of Gages 11 and 12)	61
3-10	Load-Strain Diagram for SD1M, Bar 4 (Avg. of Gages 13 and 14)	61

3-11 Load–Strain Diagram for SD1M, Bar 5 (Avg. of Gages 15 and 16) 62
3-12 Load–Strain Diagram for SD1M, Bar 5 (Avg. of Gages 17 and 18) 62
3-13 Load–Strain Diagram for SD1M, Bar 6 (Avg. of Gages 19 and 20) 63
3-14 Load–Strain Diagram for SD1M, Bar 6 (Avg. of Gages 21 and 22) 63
3-15 Load–Strain Diagram for SD1M, Bar 6 (Avg. of Gages 23 and 24) 64
3-16 Load–Rotation Diagram for Specimen SD1M 64
3-17 Load–Horizontal Slip Diagram for Specimen SD1M 65
3-18 Axial Load–Deformation Diagram for Specimen SD1M 65
3-19 Load–Column Twist Diagram for Specimen SD1M 66
3-20 Load–Deflection Diagram for Specimen SD2M 66
3-21 Cracking Pattern of Specimen SD2M 67
3-22 Load–Strain Diagram for SD2M, Bar 1 (Avg. of Gages 1 and 2) 67
3-23 Load–Strain Diagram for SD2M, Bar 1 (Avg. of Gages 3 and 4) 68
3-24 Load–Strain Diagram for SD2M, Bar 1 (Avg. of Gages 5 and 6) 68
3-25 Load–Strain Diagram for SD2M, Bar 2 (Avg. of Gages 7 and 8) 69
3-26 Load–Strain Diagram for SD2M, Bar 2 (Avg. of Gages 9 and 10) 69
3-27 Load–Strain Diagram for SD2M, Bar 3 (Avg. of Gages 11 and 12) 70
3-28 Load–Strain Diagram for SD2M, Bar 4 (Avg. of Gages 13 and 14) 70
3-29 Load–Strain Diagram for SD2M, Bar 5 (Avg. of Gages 15 and 16) 71
3-30 Load–Strain Diagram for SD2M, Bar 5 (Avg. of Gages 17 and 18) 71
3-31 Load–Strain Diagram for SD2M, Bar 6 (Avg. of Gages 19 and 20) 72
3-32 Load–Strain Diagram for SD2M, Bar 6 (Avg. of Gages 21 and 22) 72
3-33 Load–Strain Diagram for SD2M, Bar 6 (Avg. of Gages 23 and 24) 73
3-34 Load–Rotation Diagram for Specimen SD2M 73
3-35 Load–Horizontal Slip Diagram for Specimen SD2M 74
3-36 Axial Load–Deformation Diagram for Specimen SD2M 74
3-37 Load–Column Twist Diagram for Specimen SD2M 75
3-38 Cyclic Loading for Test Specimen SD1C 75
3-39 Load–Deflection Diagram for Specimen SD1C 76
3-40 Cracking Pattern of Specimen SD1C 76
3-41 Failure of SD1C Bar Number 1 in Tension 77
3-42 Load–Strain Diagram for SD1C, Bar 1 (Avg. of Gages 1 and 2) 77
3-43 Load–Strain Diagram for SD1C, Bar 2 (Avg. of Gages 3 and 4) 78
3-44 Load–Strain Diagram for SD1C, Bar 3 (Avg. of Gages 5 and 6) 78
3-45 Load–Strain Diagram for SD1C, Bar 4 (Avg. of Gages 7 and 8) 79
3-46 Load–Strain Diagram for SD1C, Bar 5 (Avg. of Gages 9 and 10) 79
3-47 Load–Strain Diagram for SD1C, Bar 6 (Avg. of Gages 11 and 12) 80
3-48 Load–Strain Diagram for SD1C, Bar 1 (Gage 13) 80
3-49 Load–Strain Diagram for SD1C, Bar 2 (Gage 14) 81
3-50 Load–Strain Diagram for SD1C, Bar 3 (Gage 15) 81
3-51 Load–Strain Diagram for SD1C, Bar 4 (Gage 16) 82
3-52 Load–Strain Diagram for SD1C, Bar 5 (Gage 17) 82
3-53 Load–Strain Diagram for SD1C, Bar 6 (Gage 18) 83
3-54 Load–Rotation Diagram for Specimen SD1C 83
3-55 Load–Horizontal Slip Diagram for Specimen SD1C 84

3-56 Axial Load-Deformation Diagram for Specimen SD1C 84
3-57 Load-Column Twist Diagram for Specimen SD1C 85
3-58 Load-Base Rotation Contributing to Total Deflection for SD1C 85
3-59 Cyclic Loading for Test Specimen SD2C 86
3-60 Load-Deflection Diagram for Specimen SD2C 86
3-61 Cracking Pattern of Specimen SD2C 87
3-62 Load-Strain Diagram for SD2C, Bar 1 (Avg. of Gages 1 and 2) 87
3-63 Load-Strain Diagram for SD2C, Bar 2 (Avg. of Gages 3 and 4) 88
3-64 Load-Strain Diagram for SD2C, Bar 3 (Avg. of Gages 5 and 6) 88
3-65 Load-Strain Diagram for SD2C, Bar 4 (Avg. of Gages 7 and 8) 89
3-66 Load-Strain Diagram for SD2C, Bar 5 (Avg. of Gages 9 and 10) 89
3-67 Load-Strain Diagram for SD2C, Bar 6 (Avg. of Gages 11 and 12) 90
3-68 Load-Strain Diagram for SD2C, Bar 1 (Gage 13) 90
3-69 Load-Strain Diagram for SD2C, Bar 2 (Gage 14) 91
3-70 Load-Strain Diagram for SD2C, Bar 3 (Gage 15) 91
3-71 Load-Strain Diagram for SD2C, Bar 4 (Gage 16) 92
3-72 Load-Strain Diagram for SD2C, Bar 5 (Gage 17) 92
3-73 Load-Strain Diagram for SD2C, Bar 6 (Gage 18) 93
3-74 Load-Rotation Diagram for Specimen SD2C 93
3-75 Load-Horizontal Slip Diagram for Specimen SD2C 94
3-76 Axial Load-Deformation Diagram for Specimen SD2C 94
3-77 Load-Base Rotation Contributing to Total Deflection for SD2C 95
4-1 Idealized Stress-Strain Curve for Concrete .95
4-2 Axial Load-Moment Interaction Diagram for Specimen SD1M 96
4-3 Axial Load-Moment Interaction Diagram for Specimen SD2M 96
4-4 Axial Load-Moment Interaction Diagram for Specimen SD1C 97
4-5 Axial Load-Moment Interaction Diagram for Specimen SD2C 97
4-6 Moment-Curvature Diagram for Specimen SD1M 98
4-7 Moment-Curvature Diagram for Specimen SD2M 98
4-8 Moment-Curvature Diagram for Specimen SD1C 99
4-9 Moment-Curvature Diagram for Specimen SD2C 99
4-10 Mechanisms for Dowel Action 100
4-11 Measured versus Calculated Load-Rotation Diagrams for SD1M 101
4-12 Measured versus Calculated Load-Rotation Diagrams for SD2M 101
4-13 Measured versus Calculated Load-Rotation Diagrams for SD1C 102
4-14 Measured versus Calculated Load-Rotation Diagrams for SD2C 102
4-15 Idealized Curvature Distribution Along Cantilevered Element 103
4-16 Bar Slip Mechanism in in a Typical Reinforced Concrete Beam 103
4-17 Assumed Bar Slip Mechanism in Hinged Specimens 104
4-18 Measured versus Calculated Load-Deflection Diagrams for SD1M 104
4-19 Measured versus Calculated Load-Deflection Diagrams for SD2M 105
4-20 Measured versus Calculated Load-Deflection Diagrams for SD1C 105
4-21 Measured versus Calculated Load-Deflection Diagrams for SD2C 106
4-22 Cantilevered End Element 106

Notations

A_{st}	Area of tensile steel.
a	Depth of rectangular stress distribution from compression face.
a_y	Stiffness reduction at yielding.
b	Width of compression face of member.
d	Distance from the extreme compression fiber to the centroid of tension reinforcement. Also called effective depth of the section.
d''	Distance from the centroid of compression steel to centroid of tension reinforcement.
e	Steel elongation due to bar slippage.
E_c	Modulus of elasticity of concrete.
E_s	Modulus of elasticity of steel.
f'_c	Compressive strength of concrete.
f_s	Steel tensile stress.
f_y	Yield strength of steel.
h	Overall section depth.
I_g	Gross section moment of inertia, in^4.
k_1, k_2, k_3	Factors for Baker's equation (Ref. 18).
kd	Distance from extreme compressive fiber to the neutral axis.
L	Span length measured from the center of the support to the hinge face.
l_d	Reinforcing steel development length.
l_p	Equivalent plastic hinge length.
M_y	Yield moment.
P_o	Axial strength of member under pure compression.

P_u Axial compressive force applied to member.

z Distance from critical section to point of contraflexure.

δ_s Displacement due to steel reinforcement bond slip.

ϵ_c Concrete strain at the extreme compression fiber.

ϕ_y Curvature at yielding.

θ_s Rotation due to bond slip.

θ_y Rotation at yielding.

Chapter 1

Introduction

1.1 Background

Reinforced concrete hinges have been extensively used in structures for the past 70 years. In many reinforced concrete highway bridges, hinge details are used to connect foundations to columns and columns to decks. Column hinges fall into two categories, one-way and two-way hinges, as illustrated in Figure 1-1.[21] A one-way hinge will prevent moment transfer in the weak direction, i.e., intended direction of rotation, while resisting bending moments in the strong direction. To induce hinge action in one-way pins, the column dimension is decreased in the direction of rotation and the reinforcing steel is aligned in a single row. In a two-way hinge connection, the column section is reduced in both directions and the reinforcing steel is grouped at the center. Two-way hinges are usually used in circular columns; one-way hinges are used in both rectangular and circular columns.[21]

In the actual construction of a bridge, concrete is placed separately for the foundation and the columns, resulting in a construction joint between the column and the footing. A shear key is incorporated at the joint to transfer horizontal forces from the column to the foundation. To allow the column to rotate with respect to the footing, the hinge "throat" typically has a depth of 1 to 4 inches.

One-way hinges in bridge columns may be subjected to a combination of loads, such as axial compressive force due to the dead load of the bridge superstructure, shear forces in the hinge in the two principal directions, and bending moments in the strong direction. The latter two loads may be due to lateral loading caused by either ground motion or wind.

One-way hinge connections are designed to carry axial compressive forces according to Sec. 10.3.5 of the American Concrete Institute (ACI) building code,[1] commonly referred to as ACI-318. Sec. 11.7, which describes the shear friction method (SFM), is used to design for shear.[1]

Many modern highway bridges in areas of high seismic risk are supported by bents consisting of one or more columns. Seismic design of highway bridge columns is usually based on building codes for columns in frame buildings. However, the basis for designing bridge columns using building codes may not be valid due to several important differences which exist between bridge and building columns:[5]

1. Building columns usually have smaller cross-sections than bridge columns.

2. Because of their smaller dimensions and more complex beam to column joint details, the use of reinforcing steel greater than No. 11 bars is not a common practice in building columns; however, No. 14 and No. 18 bars are frequently used in bridge columns. The differences in bonding characteristics between the smaller and the larger bars may also contribute to performance differences.

3. Building columns typically carry higher axial stresses than bridge columns.

4. The general design approach for building frames is based on developing plastic hinges in beams and not in columns. In contrast, development of plastic hinges in bridge columns is necessary for energy dissipation under lateral loads.

5. The reinforcement ratio in bridge columns is smaller than in building columns. Bridge columns typically have a reinforcement ratio of less than 2 percent.

Because of the devastating effects on highway bridges of the 1971 San Fernando earthquake, seismic design procedures for bridges in the United States have changed significantly. Damage to highway bridges from the earthquake included five collapsed bridges and 42 which suffered major damage.[11] The primary causes of pier damage were identified as:

1. Insufficient ductility of bridge columns to absorb the inelastic displacements experienced.

2. Shear dominated failures in shorter columns.

3. Anchorage failures of longitudinal reinforcement in the plastic hinge locations formed at the base of columns.

1.2 Previous Work

Very little research has been done on bridge column-to-foundation one-way hinge connections subject to a combination of axial, shear, and flexural loadings in the moment-resisting direction. However, there has been extensive research and testing to determine the bearing, shear, and flexural capacity under monotonic and cyclic loading induced in the weak direction.

In 1965, G. D. Base conducted research on four prototype reinforced concrete hinges with the loading applied in the rotation direction (about the weak axis).[3] He tested three different types of hinges: a Freyssinet hinge, which has very little reinforcement through the hinge section; a Messanger hinge; and a saddle bearing hinge. Base induced a series of different loadings on the reinforced concrete hinges: axial load only, combined axial and shear loadings, and axial loading with cyclic flexural loadings.

The results of these tests indicate that the specimens were able to carry design loads with substantial factors of safety and allow for rotations greatly in excess of the design requirements. Concrete compressive stresses in the hinge throats reached values several times the compressive strength of the concrete without causing crushing. Base also discovered that the reinforcing steel through the hinge throat appeared to be unnecessary. The static shear resistance of the hinge section appeared sufficiently adequate, and only the consideration of impact shear would create a need for diagonal reinforcement to assist in shear resistance.

A preliminary study was conducted on one-eighth scale reinforced concrete bridge piers at the University of Nevada in 1988; four model bridge piers were built and tested. Three of the specimens with shear-span to depth ratio (aspect ratio), *l/h*, varying from 1 to 3 were loaded monotonically to failure. The fourth specimen had an aspect ratio of 3 and was tested cyclically. The scope of the research was to subject a typical one-way bridge pier hinge to lateral loads and determine if the shear friction theory was indeed valid for this type of application. The results of these tests indicated that the shear friction method can overestimate the shear capacity of a typical one-way hinge by as much as 100 percent.[21]

The pilot study showed that the mechanism for shear resistance in a one-way hinge is different than what the shear friction theory has indicated. The shear friction method assumes that aggregate interlock takes place over the entire length of the crack in the hinge region. According to this method, when an initially cracked reinforced concrete specimen is loaded monotonically in shear, slippage will occur along the crack interface.[2,13,14,28] As the two concrete segments on opposite sides of the crack slide relative to each other, tension is introduced into the reinforcement bars, as shown in Figure 1-2.[21] To maintain equilibrium, the reaction from this tensile force is a net compressive force normal to the crack. This net compressive force is multiplied by a friction factor; the product is the shear resistance of the section.

The sliding mechanism along the crack face subjects the reinforcing steel to a shearing action, commonly referred to as "dowel action." Dowel action can be developed by three mechanisms: flexure of the reinforcement, shear stress across the steel bars, and kinking of the reinforcing steel.[18]

Initially-cracked reinforced concrete members behave differently under cyclic loading. After one cycle, the specimen builds up residual tensile strain in the reinforcing steel which prevents the crack along the shear plane from closing immediately after the load has reversed.[6,17,22] This results in shear transfer by dowel action as well as aggregate interlock. After the initial cycle is completed, the shear stiffness of the specimen is much lower than the stiffness during the previous loading cycle. The specimen experiences slip equal to the previous maximum slip until the contact sections again come into bearing. The resistance of the contact areas to deformation results in an increase in shear resistance. Further cyclic motion results in similar behavior until the two surfaces in contact are worn smooth, thus reducing the portion of shear resistance normally provided by aggregate interlock.

The mechanical behavior of a one-way hinge, shown in Figure 1-3, is considerably different than that discussed in the shear friction method.[21] Usually, a large flexural crack forms in the concrete, limiting the contact area for aggregate interlock to the compression zone of the section. The net compressive force is the summation of the reinforcing steel force and the concrete force crossing this compression region. Thus, the resultant compressive force may be very different from that obtained when all bars are acting in tension as indicated by the shear friction method.[21]

Researchers at Washington State University in Pullman are developing a modified hinge detail to reduce the size of the foundation for economic reasons.[15] Their objective is to build forty, one-twentieth scale and six one-sixth scale specimens and subject them to cyclic loadings that will produce lateral deflections of up to 14 times the yield displacement. Preliminary findings of the small-scale study indicate that the modified hinge detail appears to be better than the unmodified hinge detail in absorbing the energy induced by lateral forces. This improvement is a result of the confinement provided around the hinge throat by the addition of an outer segment of the architectural column. At the time of this writing, work is being conducted on the one-sixth scale models to substantiate the findings of the small scale specimen tests.

1.3 Object and Scope

A continuation of the research which started at the University of Nevada in 1985, the present study involves testing hinge details for bridge column-to-foundation connections subjected to lateral loading in the strong direction. The objective of this part of the study was to determine the effects of pier aspect ratio and cyclic loads on the lateral response of one-way hinges in the presence of a constant axial load.

The major differences between the current study (Standard Detail specimens) and the pilot study[21] (Concrete Hinge specimens) are the following: the scale of SD specimens is one-sixth compared to one-eighth scale for the CH series; deformed No. 3 reinforcing bars were used in the SD specimens, whereas plain No. 2 bars were used in the original study; and a constant axial load was applied to the SD specimens, whereas there was no axial load for the CH series.

In the current study, two test variables were considered: monotonic versus cyclic loading and shear-span to depth ratio (aspect ratio). The shear-span to depth ratio is defined as the distance from the point of zero moment to the point of maximum moment, l, divided by the total depth of the section in the strong direction, h. The first two specimens, with aspect ratios of 1 and 2, were loaded monotonically to failure. The last two test specimens, also with aspect ratios of 1 and 2, were subjected to cyclic lateral deformations with increasing amplitude levels until failure. The shear-span to depth ratio was varied to determine its effects on shear and flexural capacity of the hinge and to determine a limiting shear span to induce a shear failure. By decreasing the shear span of the column, the shearing effect in the hinge region will become more dominant.[20]

Previous research has shown that the strength of columns having a shear-span to depth ratio less than 2.5 is controlled by shear related failures.[12,25,27]

During testing, specimens subjected to cyclic lateral loading experienced ultimate displacements of up to four times the yield displacement. It should be noted, however, that very slow static lateral displacements were applied to each test specimen. This was done to monitor the cracking pattern and the overall response of each specimen. The cyclic testing was performed to obtain a general insight into the effects that load reversals have on shear and flexural strengths and to give an indication of energy dissipation in the hinge section.

The long-term goal of this project is to develop a method for estimating the shear behavior of common reinforced concrete hinge details subjected to lateral loads, and to develop details that will improve the energy dissipation capacity of one-way hinges.

Chapter 2

Experimental Study of Hinged Specimens

2.1 Introduction

Four one-sixth scale model foundation-to-column hinge connections were tested. These models were designed to represent piers 2 and 3 of the Rose Creek Interchange (I-862) located on Interstate-80 in Winnemucca, Nevada, shown in Figure 2-1. The test specimens, shown in Figure 2-2, consist of two elements: a lower portion, representing the foundation, and an upper portion, representing the column. All specimens were tested in the upright position with an axial load applied at the top of the column to simulate the dead load of the bridge deck. Specimens were laterally loaded (combined shear and flexure) in the strong direction.

This chapter describes the test specimens, equipment, and procedure used in the testing program.

2.2 Test Specimens

Four standard detail (SD) specimens were tested: SD1M, SD2M, SD1C and SD2C. The first two specimens were loaded monotonically; the last two specimens were loaded cyclically. The first and third specimens had a shear span to depth ratio (aspect ratio), l/h, of 1; the ratio for the second and fourth specimens was 2.

All specimens had a 14.5-inch by 18-inch by 24-inch footing section. The column section measured 6.5 inches by 16 inches by 22 inches for specimens SD1M and SD1C and 6.5 inches by 16 inches by 38 inches for SD2M and SD2C. Six No. 3 deformed Grade 60 reinforcing bars were used to connect the footing to the column. Concrete cover was 1 inch for the outer two dowels. Inner dowels were spaced at approximately 2.75 inches, on center.

The six reinforcing dowels had 90 degree, 6-inch standard hooks on either end with a straight segment of 8 inches in the footing section. Test specimens SD1M and SD2M had No. 3 Grade 60 deformed bars for U-stirrups and no horizontal ties located in the column section. In specimens SD1C and SD2C, both U-stirrups and horizontal ties were used, to enhance concrete confinement in the column section. Horizontal ties were plain No. 2 bars, spaced at 6.5 inches, on center, with 1 inch of concrete cover both top and bottom. The connection between the footing and the column was formed with a 2.5-inch by 16-inch by ½-inch keyway. The hinge throat was fabricated by placing a ½-inch thick piece of styrofoam in the base section prior to concrete placement. Two ⅝-inch thick styrofoam inserts were placed on either side of the keyway to ensure no bonding occurred between the outer portions of the column and the footing. After the footing section was poured, the throat area was scraped to achieve a roughness amplitude of approximately ½-inch before the upper section was poured. Figure 2-3 is a photograph of the base segment after curing. The reinforcing bars, the upper strain gage location, the keyway, and the styrofoam used to keep the column and the footing from adhering to each other can be seen. The cross-sectional area of concrete at the keyway was 40 square inches. The reinforcement ratio at the hinge throat was 1.65 percent; the steel ratio in piers 2 and 3 of the Rose Creek Interchange is 1.30 percent.

2.3 Materials and Fabrication

Fine and coarse aggregates for the concrete were obtained from a local pit in the Reno area. The coarse aggregate was sieved to remove material larger than ½-inch. The coarse aggregate failed to meet the requirements of American Society for Testing and Materials (ASTM) Specification C33 on the No. 8 sieve; the fine aggregate did meet all requirements for ASTM C33. Further information concerning the aggregates is contained in Appendix A. The concrete mixture used type I-II low-alkali portland cement; proportions for the four specimens are listed in Appendix B.

The concrete was batched in a 4-cubic foot revolving drum mixer with a mixing time of approximately 10 minutes. Three 6-inch diameter by 12-inch high cylinders were cast during both footing and column pours. Compressive strength testing was performed after 7 days, after 28 days, and on the day the corresponding specimens were tested. Appendix C lists the results of the compressive strength testing.

Reinforcing dowels for the four test specimens consisted of No. 3 Grade 60 deformed bars. The yield stress was 58,000 psi for the bars used in SD1M and SD2M and 57,000 psi for the bars in SD1C and SD2C. Detailed information about the steel properties is contained in Appendix D. The horizontal ties used in specimens SD1C and SD2C were plain, i.e., non-deformed, No. 2 Grade 40 bars.

Forms were constructed using 2×4 lumber and ¾-inch plywood. To allow easy removal of the forms after concrete placement, screws were used in the side panels. The forms were cleaned and coated with polyurethane to reduce water absorption and ease form stripping.

The two portions of the model bridge pier were poured separately to simulate field construction. The footing section was first poured and moist-cured for 24 hours. The styrofoam used to form the keyway was then removed and a chisel used to roughen the concrete until the keyway had an amplitude of approximately ½-inch, to ensure good bonding between the foundation and the column. After an additional 48 hours of moist-curing, the column was cast onto the footing. The entire specimen was then moist-cured for an additional four days. After the moist-curing period, the forms were removed and the specimens were allowed to cure at room temperature until testing.

2.4 Instrumentation

A Hewlett-Packard 9000 Series microcomputer interfaced with a 3054 data acquisition system was used to record electrical strain gage and linear variable differential transformer (LVDT) measurements for the test specimens. A computer software program named *PIERHINGE*, listed in Appendix E, was developed to convert, collect, and store the test data (strains, displacements, and loads). A flow chart for the computer program is shown in Figure 2-4. The user's manual for *PIERHINGE* is presented in Appendix F.

An MTS structural testing system was used to laterally load the test specimens. The MTS system has a 55,000-pound load cell and an actuator arm with a stroke of ± 3 inches. The hydraulic arm is displacement controlled from a 458.20 microconsole. An axial load of 26,000 pounds was applied by means of a 300,000-pound Riehle machine. The test specimens were thus loaded with a combination of flexure, shear, and axial force.

Instrumentation for the different specimens varied slightly: specimens SD1M and SD2M had 24 electrical resistance strain gages while SD1C and SD2C had 18 strain gages. The strain gages were mounted on the reinforcing bars, within each specimen. Twelve gages were located in the hinge region; the remaining gages were located above the hinge throat, at 3-inch intervals (See Figures 2-5 and 2-6). The bars in the columns of specimens SD1M and SD2M had one gage on both front and back face to compensate for out-of-plane bending. Fewer gages were used in SD1C and SD2C because out-of-plane bending was found to be negligible. The deformed bars were ground smooth and thoroughly cleaned at the strain gage locations. The strain gages were bonded to the reinforcing steel using an epoxy adhesive.

Specimens SD1M and SD2M used two 2-inch LVDTs to measure the rotation of the column section relative to the foundation and one 1-inch LVDT to measure the horizontal slippage of the column with respect to the base. In addition to the LVDTs, two 1-inch dial gages were used to observe torsional effects from the lateral loading. Figure 2-7 shows this instrumentation.

To achieve better sensitivity for specimens SD1C and SD2C, two 1-inch LVDTs were used to measure the rotation of the column and one ½-inch LVDT was used to measure horizontal slip of the column relative to the footing. In addition to the dial gages described above, two 1-inch dial gages were used to monitor foundation movement relative to the column, to check whether the footing was rocking under load, and contributing to the lateral displacement of the column. The additional dial gages were placed as shown in Figure 2-8.

The test specimens were connected to the load frame by eight 1-¼ inch diameter, 125,000 psi (tensile strength) threaded rods. To create a passageway for the threaded rods in base section of the test specimen, eight 24-inch long segments of 1-¼ inch

Schedule 40 PVC pipe were included in the foundation formwork. A 1-inch thick steel bearing plate was used at the end of the test specimens to distribute the load across the face of the foundation. Figure 2-9 illustrates the test frame setup.

A steel collar, designed to carry a load of 55,000 pounds, was built to connect the hydraulic ram to the column section of the specimen. The collar was built from ½-inch thick by 5-inch wide steel plates, with four 1-inch A325 bolts on each side. Two 1.875-inch diameter pins were attached to allow for rotation as the ram pushed and pulled the specimen. Two sections of C6×13 channel were used to connect the collar to the hydraulic ram. Figure 2-10 illustrates the details of the collar.

2.5 Test Procedure

The test procedure was essentially the same for all four specimens; however, the loading was monotonic for SD1M and SD2M and cyclic for SD1C and SD2C. The specimens were laterally displaced a predetermined amount, the displacement halted, and the computer triggered to record electrical strain gage measurements, center span deflection, lateral load, and LVDT displacements. A pen plotter was used to simultaneously plot lateral load versus center span deflection. Dial gage readings were also taken and recorded on data sheets. The applied vertical load was 26,000 $\pm$ 1000 pounds, representing the same stress in the hinge throat as the Rose Creek Interchange. An outline for the loading procedure and failure modes for each specimen follows.

The first step in the testing procedure was to apply the axial load of 26,000 pounds in increments of approximately 5000 pounds. Once the total axial load was applied, the threaded rods were tightened to prevent movement during loading. The hydraulic ram was then bolted to the column collar and the actual test was ready to proceed.

Chapter 3

Results of Hinged-Specimen Testing

3.1 Introduction

The results presented in this chapter describe the experimental data recorded during each of the model tests. The following are discussed:

1. Lateral load versus deflection.
2. Lateral load versus strain.
3. Lateral load versus rotation.
4. Lateral load versus slip.
5. Axial load versus deformation.
6. Column twist and base rotation contributing to total lateral deflection.

These data give an indication of the stiffness characteristics and strength decay for each test specimen.

Before testing, each specimen was inspected for unusual or dominant cracking patterns. There were no major visible cracks in any of the test specimens; however, there were some minor shrinkage cracks.

Specimens SD1M and SD2M were monotonically loaded to failure, where failure is defined as the point where the lateral load has decreased to 85 percent of the maximum load. Points at which individual bars yielded are indicated on the measured response curves for specimens SD1M and SD2M. The number indicates which layer of steel yielded in tension during loading.

The cyclically-loaded specimens, SD1C and SD2C, were subjected to several cycles of increasing lateral displacement amplitudes and ductility levels. No particular earthquake response history was simulated during the testing phase. Figure 3-1 shows the numbering system used for the reinforcing steel located within each specimen: bar 1 being on the front face (right side of the diagram) of the column; bar 6 on the back face of the column (far left side).

3.2 Specimen SD1M

3.2.1 Load-Deflection Response

Figure 3-2 shows the load-deflection curve for specimen SD1M, which had an ultimate lateral load of 25,300 pounds. The specimen cracked at a load of 3600 pounds as indicated by the change in the slope of the load-deflection diagram. Yielding of bar 1 in tension occurred at a load of 18,240 pounds, corresponding to a lateral displacement of 0.20 inches. Failure of the specimen occurred at 21,500 pounds and a lateral displacement of 1.54 inches; this displacement corresponds to an apparent displacement ductility factor of 7.70. Displacement ductility is defined as the maximum lateral deflection divided by the yield deflection.

Figure 3-3 shows the actual cracking pattern of the specimen near the failure point. The photograph was taken at a load of 25,300 pounds and a lateral deflection of 1.29 inches. The photograph shows that there was major cracking on the compression side of the hinge just above the interface between the column and the foundation. The cracks propagate up the column face, indicating severe stresses in the upper part of the column. The severity of cracking is partly due to the absence of horizontal ties in the column region which would have provided some confinement.

3.2.2 Load-Strain Response

Figures 3-4 through 3-15 illustrate the relationships between lateral load and strain distribution in the reinforcing steel.

After the initial axial loading of the model with the 26,000-pound axial load, all of the bars in the hinge throat were in compression. As the lateral load was applied, the strain distribution changed from compression to tension in bars 1 through 5. Because of its location, bar 6 remained in compression.

To explain the load-strain curves, the curves for bars 4, 5, and 6 can be examined. Figure 3-10 shows the relationship for bar 4, and is composed of three distinctly different segments. The first segment, from point A to B, indicates that the lateral load creates negligible strain in the bar; the strain is mainly a result of the applied axial load. Between points B and C, the lateral load becomes sufficiently large to overcome the compressive stress from the axial load, causing tensile strains to develop in the bar. The last segment, from point C to point D, shows large strains due to the rotation of the column section and separation of the column from the footing; there is no concrete contact between the foundation and the column except in the compression zone at the far left end of the specimen. The reinforcing bar eventually yields, and large strains develop with little increase in section load capacity.

Figure 3-12, representing bar 5, also has three distinct regions. The first region, from point A to point B, shows the response from the initial axial loading. As the lateral load is increased, compressive strain increases to a maximum at point B, where the applied lateral load is approximately 11,000 pounds. The second region, from point B to C, shows that the lateral load is large enough to cause tension and a decrease in the compressive strain in the bar. At a lateral load of approximately 20,000 pounds, the bar undergoes a stress reversal to tension. The final region, from point C to D, shows that the bar is undergoing large strains with little increase in lateral load. The bar eventually yields in tension. This is a result of the large relative rotations present, which limit the contact area between the column and the foundation.

Figures 3-13 through 3-15 show that bar 6 remains in compression. This bar is located on the left end of the column, where the large rotations cause the concrete column and footing to bear against each other.

The extent of yielding penetration can be observed in Figure 3-4, for tension, and in Figure 3-13, for compression. The bars yielded at a distance up to 6 inches from the hinge throat, as the lower sections underwent strain-hardening.

3.2.3 Load-Rotation Response

Figure 3-16 shows the load-rotation curve for specimen SD1M. Up to yielding of bars 1 through 4, the specimen exhibited small rotations, but after yielding, large rotations developed. The initial yield rotation was 0.0044 radian. The rotation near the end of the test, when the load dropped to 85 percent of the peak load, was 0.083 radian. This corresponds to a rotation ductility of 18.9, which is quite high for a specimen with an aspect ratio of 1.

3.2.4 Load-Horizontal Slip Response

The load-horizontal slip curve, Figure 3-17, shows that up to yielding very little slip has occurred between the column and the footing. After bars 1 through 4 yielded in tension, and the column had separated from the footing over most of the hinge area, large horizontal slips were recorded. The initial yield slip was 0.014 inch; the slip at failure was 0.152 inch. The slip ductility factor was 10.9.

3.2.5 Axial Load-Deformation Response

Figure 3-18 shows the relationship between axial force and axial deformation of the column section. The LVDTs that measured axial deformation were located approximately 6 inches from the top of the footing. Shortening was measured over a distance of 6.5 inches, including the ½-inch hinge throat depth. The discontinuity at 10,000 pounds applied lateral load is most likely due to the LVDT signal noise level.

3.2.6 Load-Column Twist Response

Two dial gages were used to monitor out-of-plane twisting caused by the hydraulic ram. As shown in Figure 3-19, the column experienced very little out-of-plane rotation relative to the footing. A column twist of 0.0005 radian was measured at the initial yield load, corresponding to a displacement component of 0.0016 inch at the corner of the column in the loading direction. This is negligible when compared to the yield displacement of 0.24 inch.

3.3 Specimen SD2M

3.3.1 Load-Deflection Response

The load-deflection curve for SD2M, Figure 3-20, shows that bar 1 yielded in tension at a lateral load of 9120 pounds and a corresponding deflection of 0.19 inch. The peak load was 13,100 pounds at a displacement of 1.0 inch. Failure occurred at a lateral load of 11,110 pounds with a corresponding displacement of 1.38 inches. This relates to a ductility factor of 7.26, which is close to the ductility factor of 7.70 observed for SD1M. Specimen SD2M initially cracked at 4500 pounds.

Figure 3-21 is a sketch of the cracking pattern for test specimen SD2M. Because the photographs taken during this test were of poor quality, a video tape was reviewed and a hand drawing was made to show the cracking pattern at the failure point. Major cracks are present on the compression face of the column. Vertical crack propagation is apparent on the compressive side of the column. The tests of other tied specimens revealed that the cracking of SD2M was a result of the lack of horizontal ties in the pier section. The cracking pattern for SD2M is similar to what was observed for SD1M.

3.3.2 Load-Strain Response

Figures 3-22 through 3-33 present the data collected for the load-strain response of specimen SD2M. The data can be grouped into three groups: the first for bars 1 through 4 (Figures 3-22 through 3-28); the second for bar 5 (Figures 3-29 through 3-30); and the last for bar 6 (Figures 3-31 through 3-33).

Figures 3-22 through 3-28 show three distinct line segments on the load-strain diagram; Figure 3-22 will be used to explain the load-strain response curve. Initially, as the axial load is applied the bar goes into compression (point A to point B). As the lateral load is applied, from point B to point C, the strain reverses from compression to tension. The last segment, from C to D, is a result of the large flexural crack which developed between the footing and the column. As the flexural crack propagates, large rotations are developed between the two concrete segments with minimal contact only in the compression region. Beyond this point, the reinforcing steel has yielded, and larger tensile strains are recorded with every increase in lateral load.

Figures 3-29 and 3-30 represent the load-strain response for bar 5. Again there are three distinct line segments to the curve. The first segment of Figure 3-30, from point A to point B, shows the application of the axial load. At point B (about 6000 pounds lateral load), the maximum compressive strain has been reached. A slow decrease in compressive strain is then seen, due to the increasing lateral load. The final segment, point C to point D, shows that the strain has reversed from compression to tension. The only concrete section of the column still in contact with the footing is the far left edge which contains bar 6.

Figures 3-31 through 3-33 show the data for bar 6, which remains in compression throughout the test. As the pier rotates counter-clockwise, the rear of the column is forced downward into the footing, resulting in increasing compressive strains.

3.3.3 Load-Rotation Response

The load-rotation curve for SD2M, Figure 3-34, shows that prior to yielding in tension, small rotations were experienced in the section. The initial yield rotation was 0.0022 radian. After yielding of bar 4, large rotations occurred. At the point of failure, a rotation of 0.039 radian was recorded, corresponding to a rotation ductility of 17.7, almost the same as that obtained for specimen SD1M.

3.3.4 Load-Horizontal Slip Response

Figure 3-35 shows the load-horizontal slip curve for specimen SD2M. Up to a lateral load of 5000 pounds, practically no slip has occurred between the column and the footing. Between 5000 and 10,000 pounds, slippage is starting to occur, but no major movement has developed. An initial yield slip of 0.0026 inch was measured. The slip was 0.04 inch at failure, which relates to a slip ductility of 15.4. This ratio is 1.5 times the value of 10.9 observed for SD1M, indicating that shear was more dominant in SD1M.

3.3.5 Axial Load-Deformation Response

Figure 3-36 shows the relationship between the axial force and the deformation in the lower 6.5 inches of the column. No significant deformation was noted. The relationship is nearly linear; the slight discontinuity is probably due to the noise levels of the LVDTs.

3.3.6 Load–Column Twist Response

Figure 3-37 shows the load–column twist data for specimen SD2M. The column experienced very little twist: even at the maximum load of 13,100 pounds, the measured angle of twist was only 0.0035 radian. The displacement of 0.011 inch, which results at the level and direction of horizontal load, is insignificant when compared to the 1.0 inch of deflection due to the lateral load.

3.4 Specimen SD1C

3.4.1 Load–Deflection Response

Figure 3-38 presents the lateral loading history for specimen SD1C. The specimen was subjected to nine displacement cycles at four different amplitude levels. Figure 3-39 shows the load–deflection response for the specimen. Initially, two cycles of $\pm$0.1-inch displacement were completed to capture the cracking point of the specimen. The specimen was then subjected to two cycles of $\pm$0.25-inch displacement. This displacement was the initial yield point of specimen SD1C. Three cycles were applied with a deflection of $\pm$0.50 inch, for a displacement ductility factor of 2, to monitor the effects of cyclic displacements, with a moderate degree of nonlinearity, on strength degradation of the specimen. Figure 3-39 illustrates the pinching of the hysteresis loops, indicating a reduction in the energy absorption capacity of the hinge. Finally, a displacement corresponding to a ductility level of 4.0 was applied ($\pm$1 inch lateral displacement) for two cycles; significant pinching was noted in the hysteresis loops. The sudden drop in lateral load during the last cycle was caused by the tensile failure of bar 1.

The positive load side of Figure 3-39 shows that the largest load achieved was 26,800 pounds during the fifth cycle. On the final cycle, a maximum load of 20,400 pounds was reached. The strength degradation caused by the cyclic loading was 25 percent at failure.

Figure 3-40 shows the cracking pattern during the ninth cycle at a lateral load of 17,040 pounds and a corresponding displacement of 0.89 inch. In the front of the photograph, the column has separated from the footing. At the rear of the photograph, the right corner of the column has a major crack running diagonally, starting approximately 3 inches up the side of the column and propagating to the bottom center of the column. This crack formed after the expansion joint material had been compressed and the concrete outside the hinge throat had come in contact with the footing. Horizontal ties were used in the column section, to provide confinement and enhance ductility, which significantly reduced the amount of column cracking. Figure 3-41 shows a close-up of the hinge section with bar 1 failing in tension.

3.4.2 Load-Strain Response

In specimens SD1C and SD2C, 18 strain gages were used to record strain values. Two strain gages were used on each bar, front and back, through the hinge throat region; however, only one gage was used above the hinge region to monitor the strains in the bars. Because there was negligible out-of-plane bending of the bars in specimens SD1M and SD2M, redundant gages were eliminated.

Figures 3-42 through 3-53 present the lateral load-strain data collected during the cyclic loading of specimen SD1C. In bars 1 and 6 (Figures 3-42 and 3-47, respectively), the strains change from compression to tension, as expected for the outer bars during cyclic testing. However, failure of the strain gages during testing resulted in limited strain data collection.

Figures 3-43 through 3-46 show the strain distribution for the gages located in the hinge throat on bars 2 through 5. After the lateral load was sufficiently large to overcome the effect of the axial force, the strains remained tensile. As the loading was cycled back and forth, the concrete in the hinge throat failed, and the bars were pushed and pulled in tension.

Figures 4-48 through 3-53 show the load-strain response for the gages located above the hinge throat for bars 1, 2, 5, and 6. The cyclic nature of the strain distribution is a result of lateral loading: one end of the column is subjected to tension while the other is in compression. As the load is applied toward the left, bars 1 and 2 (Figures 3-48 and 3-49) go into tension while bars 5 and 6 (Figures 3-50 and 3-51) experience compression. Just the opposite occurs when the load is reversed. The maximum strains show that yielding extended well into the column.

3.4.3 Load-Rotation Response

Figure 3-54 shows the load-rotation response of specimen SD1C. Initially, two cycles approximately equal to the cracking point of the section were completed; very small rotations of about 0.00077 radian were experienced. The initial yield displacement was applied and the corresponding rotation of 0.0079 radian was measured. Next, three cycles at a displacement ductility level of 2 ($\pm$0.50 inches), with a corresponding rotation of 0.021 radian, were completed. Finally, the last two cycles were performed at a displacement ductility level of 4 ($\pm$1.0 inch). The ultimate rotation was 0.051 radian, which correlates to a rotation ductility factor of 6.46. This is approximately 36 percent of that obtained for specimen SD1M.

A comparison of Figures 3-54 and 3-39 shows that the general shape of hysteresis curves for rotation is similar to that of displacement. This is because a major portion of horizontal displacement of the column is due to rotation at the base. However, the pinching effects in Figure 3-54 are less severe because the column horizontal slippage is not reflected in the rotations.

At large-amplitude cycles, peak rotations are larger in the positive direction than they are in the negative direction. This is because the effective axial load in the negative region was larger, thus reducing the curvature and the resulting rotation.

3.4.4 Load–Horizontal Slip Response

The load-horizontal slip curve, Figure 3-55, shows that at the cracking point ($\pm$0.08 inches), the slip between the column and the footing was negligible. At the initial yield point, a slip of 0.03 inch was recorded, twice of that of specimen SD1M. On the seventh cycle, with a displacement ductility of 2, a horizontal slip of 0.13 inch was noted, corresponding to a slip ductility of 4.3. Finally, on the ninth cycle, a maximum slip displacement of 0.25 inch was achieved, which corresponds to an ultimate horizontal slip ductility factor of 8.3.

The peak slip in the positive direction was lower than the negative slip. The trend is opposite to that observed in the rotation response. Considering that the displacements in the positive and negative directions are forced to be the same, and the horizontal displacement is dominated by a component due to the rotation at the bottom of the column and a component due to the horizontal slip, the trend is logical because rotation and slip have to compensate for each other.

3.4.5 Axial Load-Deformation Response

Figure 3-56 shows the relationship between the axial force and the deformation of the lower portion of the column. The response was elastic, as anticipated. The discontinuity between line segments at an 11,000-pound lateral load is a result of the noise level of the external LVDTs.

3.4.6 Load–Column Twist Response

Figure 3-57 shows the lateral load–column twist for specimen SD1C. Only the extreme data points were plotted. The maximum column twist angle recorded was 0.0033 radian, corresponding to a corner displacement of 0.011 inch. This is insignificant compared to the total lateral deflection of 1.0 inch.

3.4.7 Load–Base Rocking Response

Figure 3-58 shows the reduced data acquired from dial gages placed on the foundation of the specimen to monitor rocking of the base. This rotation was converted to a deflection to compare with the displacement measured during testing. Only the extreme data points were used to calculate foundation rocking. The maximum base movement contributing to the total deflection of the column was 0.016 inch; when compared to the total lateral displacement of 1.0 inch, this value is negligible.

3.5 Specimen SD2C

3.5.1 Load-Deflection Response

Figure 3-59 shows the load history response for specimen SD2C. The specimen underwent a total of ten and one-quarter cycles with five different amplitude levels.

Two small cycles of ± 0.1 inches were performed to capture the cracking point of the specimen. Next, two cycles at the initial yield displacement (± 0.25 inches) were conducted. Three cycles were then completed at a displacement ductility level of 2 (± 0.50 inch) to determine strength degradation during moderate ground motions. A ductility level of 4 (± 1.0 inch) was applied for three cycles to monitor the effects of strong earthquakes. Finally, the specimen was subjected to one-quarter cycle at a displacement of 1.33 inches (ductility factor of 5.32) to cause failure, since the column still exhibited considerable strength in the joint region.

The load-deflection response curve for SD2C is shown in Figure 3-60. A maximum load of 14,400 pounds, with a displacement of 0.93 inch, was achieved on the eighth cycle. It should be noted that there was no appreciable strength degradation in the connection, indicated by the almost perfect overlapping of the cycles. On the last cycle, the lateral load was 13,960 pounds, only a 2.9 percent drop in lateral load. Even at a ductility level of 2 (± 0.50 inch lateral displacement) some slight pinching of the hysteresis loops is present. At a ductility level of 4, significant pinching is apparent, indicating a loss of the energy-absorbing capability of the connection.

Figure 3-61 shows the cracking pattern at the two-hundredth loading increment: the lateral load was 13,500 pounds and the horizontal displacement was 1.03 inches. Very little column cracking can be seen, due to the presence of horizontal ties in the column which provided confinement for the concrete.

3.5.2 Load-Strain Response

Figures 3-62 through 3-73 show the relationship between lateral load and strain distribution in specimen SD2C. As in SD1C, gages 1 through 12 were located in the hinge throat and gages 13 through 18 above the joint interface. In bars 1 through 5 (Figures 3-62 through 3-66), the strain remained in the tension zone during most of the testing. During small amplitude cycles (approximately equal to the cracking point of the specimen), however, the strain distribution did cycle from compression to tension.

Figure 3-62 shows that bar 1, unlike other tests, remained in tension during most of the cyclic loadings. For this result to be correct, the neutral axis for negative loading would have to be to the right of bar 1. The compression area would then be unrealistically small. Furthermore, strains on bar 1 at other locations (Figures 3-68 and

3-72) show significant compression in this bar. It is, hence, concluded that the data in Figure 3-62 are erroneous.

In Figures 3-67 through 3-73 the load-strain curves are quite different: the strains cycle from positive to negative as expected for a cyclic test. During positive loading (pushing), bars 4 through 6 experience compression and bars 1 through 3 are in tension. During negative loading (pulling), just the opposite occurs.

3.5.3 Load-Rotation Response

The load-rotation curve (Figure 3-74) shows that at displacement amplitudes equal to that of the cracking point, a rotation of 0.00124 radian was recorded. At the initial yield point ($\pm$0.25 inches), the rotation was 0.00267 radian, about twice that obtained at the cracking point. At a displacement ductility of 2 ($\pm$0.5 inches) during the seventh cycle, a rotation of 0.0123 radian was measured, corresponding to a rotation ductility of 4.61. On the tenth cycle (1.0 inch deflection), the specimen had a rotation of 0.028 radian; this relates to a rotation ductility of 10.5, almost twice of that obtained for specimen SD1C. Finally, on the eleventh cycle, the rotation was 0.0384 radian, corresponding to a rotation ductility of 14.4. The lateral displacement was 1.33 inches for this cycle.

The hysteresis loops for rotation are not as narrow as those in the displacement response (Figure 3-60) because horizontal slip deformations are not included in rotations. Similar to what was observed for SD1C (Figure 3-54), the peak rotation in the positive area was larger than that in the negative direction due to differences in the axial loads in the two different directions.

3.5.4 Load-Horizontal Slip Response

Figure 3-75 shows the load-horizontal slip response for specimen SD2C. At the initial yield point, a slip of 0.0061 inch was measured, which is insignificant compared to the overall slip monitored during testing. At a displacement ductility level of 2 ($\pm$0.5 inches), the horizontal slip was 0.025 inch; this is negligible compared to the slip monitored for specimen SD1C. On the tenth cycle (ductility level of 4) a maximum slip of 0.123 inch was reached. The ultimate slip ductility was 20.2, about 25 percent higher than that obtained for SD1C. The explanation for the lack of symmetry is similar to that given for SD1C.

3.5.5 Axial Load-Deformation Response

Figure 3-76 shows the relationship between axial load and axial shorting of the lower portion of the column. The several minor discontinuities are the result of electronic noise in the LVDTs. The general shape of the diagram is nearly linear, as expected.

3.5.6 Load–Column Twist Response

Dial gages were attached to the column to monitor twisting during testing. However, soon after testing began it was apparent that the column was experiencing insignificant movement; therefore, dial gage readings were discontinued.

3.5.7 Load–Base Rocking Response

Figure 3-77 shows the rotation that was measured with dial gages located on the foundation during testing. The distance from the lateral loading point to the gage was multiplied by the rotation angle to determine the amount of lateral deflection due to rocking of the foundation. Only the envelope was plotted. A maximum lateral displacement value of 0.015 inch was obtained, which is insignificant compared with the deflectiondeflections which were applied to the column.

Chapter 4

Analysis of Specimens and Comparison to Observed Test Results

4.1 Introduction

This chapter describes the analysis of the test specimens and compares the analytical results to the behavior observed in laboratory testing. Flexural strengths, shear strengths, horizontal deflections, and column rotations relative to the foundations are discussed. Comments concerning the actual behavior versus the calculated behavior are also presented.

Flexural analyses of the hinges rotating about their strong axis were performed using a moment-curvature program called *IA1UNR*. This program calculates the moments required to cause yielding in different layers of steel, along with the corresponding column curvatures using standard techniques. The ultimate moment and curvature were determined at the crushing point of concrete, assumed at an ultimate strain of 0.004 on the extreme compression fiber of the concrete.

Several formulas from the American Concrete Institute (ACI) Building Code,[1] commonly called ACI-318, were used to calculate the shear capacity of the hinged specimens. The formulas used include the shear-axial compression formulas (ACI-318 Eqs. 11-4, 11-7, and 11-8) and the shear-friction formula (ACI-318 Eq. 11-26). In addition, the empirical dowel action formulas discussed in Ref. 18 were also employed.

Deflection calculations were performed using the moment-area method, and included plastic deformation of the hinge throat and elastic deformation of the column. Deformations due to bond slip were calculated and added to the elastic deformation to obtain the total deflection. The total hinge rotation was determined by summing the elastic and inelastic hinge rotations with the rotation caused by bond slippage.

4.2 Flexural Analysis

Results of the flexural analysis performed on each of the four test specimens are presented in Tables 4-1 through 4-4. The load required to cause yielding of the various steel layers and the load at the point where the concrete reaches a compressive strain of 0.004 were calculated and are compared to the measured loads. It can be seen that the calculated and measured results were within 15 percent of each other.

The computer program *IA1UNR* was also used to calculate moment interaction diagrams and moment-curvature diagrams for the four test specimens. The program calculates the axial load-moment data points, so that an interaction diagram can be plotted, and calculates the moments required to initiate yielding in different layers of steel, to produce a moment–curvature response. The input data consists of concrete and steel properties, section geometry, and applied axial load.

IA1UNR's concrete constitutive relationship is based on the Hognestad model.[10] Figure 4-1 shows the Hognestad model for concrete; the idealized stress–strain curve consists of a parabolic and a linear segment. For the reinforcing steel, a tri-linear stress–strain relationship with an elastic branch, yield plateau, and a strain hardening branch is used. The program assumes that plane sections remain plane before and after bending, and that the stress–strain response for the concrete and the steel are known. *IA1UNR* computes bending moments, axial loads, and corresponding curvatures based on material properties, strain compatibility and force equilibrium.

Figures 4-2 and 4-3 show the interaction diagrams for test specimens SD1M and SD2M, respectively. The 26,000 pound axial load applied to each specimen is indicated on the figures. Measured concrete and steel properties were used in the analysis. From the interaction diagram for SD1M, Figure 4-2, the moment corresponding to the 26,000 pound load was 367,000 pound-inches. The maximum moment (based on the product of the measured load and the distance to the base) achieved during testing was 405,000 pound-inches. Figure 4-3 shows a theoretical moment for specimen SD2M of 375,000 pound-inches, compared to the actual moment of 419,000 pound-inches. In both cases, the measured moment was approximately 10 percent greater than the calculated moment, indicating that the specimens were stronger than the computer model indicated.

The interaction diagrams for specimens SD1C and SD2C are shown in Figures 4-4 and 4-5, respectively. At an axial load of 26,000 pounds, specimen SD1C has a corresponding nominal moment of 366,000 pound-inches. The measured ultimate moment for specimen SD2C was 461,000 pound-inches, approximately 30 percent greater than the 364,000 pound-inch calculated moment shown in Figure 4-5. Part of the difference is due to the fact that the peak loads were reached when the column was moving towards the actuator and ther column was subjected to an effective axial load which exceeded 26,000 pounds.

Figures 4-6 through 4-9 show the moment–curvature diagrams for the four test specimens. All of these curves are similar in appearance, so Figure 4-6 will be used to describe the data. There are five distinct break points, labeled A through E. Point A is the concrete cracking point, which occurred at a moment of 124,000 pound-inches. The next three break points (B, C, and D) are the tensile yielding points for bars 1, 2, and 3, respectively. The ultimate point, E, corresponds to the crushing of concrete at a strain of 0.004 inch/inch.

In the testing of specimens SD1M and SD2M, bars 1 through 5 yielded in tension before the failure points of the specimens were reached. In order to produce tensile yielding in bars 1 through 4 in the computer model of *IA1UNR*, the ultimate strain of concrete was redefined from 0.004 to 0.10. Bar 5 would yield in tension only when the compressive strength of the concrete was raised to 10,000 psi. These results indicate that the hinge section geometry creates an "apparent" increase in the ultimate crushing strain and the compressive strength of the concrete. This is a result of concrete confinement in the hinge section.

4.3 Shear Analysis

Results from the shear strength calculations are presented in Table 4-5. The various formulas used to calculate the shear strength of the hinge section produce vastly different results.

The maximum shear applied to specimens SD1M and SD2M was 25,300 and 13,000 pounds, respectively, and 30,500 and 14,400 pounds for the cyclically-loaded specimens, SD1C and SD2C. Specimens SD1M and SD2M had lower shear capacity values because no horizontal ties were used in the column section.

The ACI-318 equations for shear-axial compression (Eqs. 11-4, 11-7, and 11-8), considerably underestimate the shear capacity of the hinge section. These low calculated values were expected, since a shear-axial compression failure was not anticipated nor present in any of the specimens. These formulas were included for completeness.

As discussed in Chapter 1, the shear-friction method (SFM) is currently used by designers to determine the ultimate shear capacity of the hinge section.[1] For the shear-friction method, shear strengths were calculated for one bar contributing, two bars contributing, and all six bars contributing. The ACI-318 Commentary Sec. 11.7.7 states that it has "been demonstrated experimentally that if a resultant compressive force acts across a shear plane, the shear-transfer strength is a function of the sum of the resultant compressive force and the force $A_{vf}f_y$ in the shear-friction reinforcement."[1] Therefore, the force due to the axial load and the weight of the column section was added to the results obtained from ACI-318 Eq. 11-26. These results are presented in Table 4-5, and are labeled SFr1, SFr2, and SFr6; the numerals indicate the number of bars contributing to the axial force. A friction coefficient of one was used.

All four test specimens failed in flexure, not in a shear slip mode. However, the shear capacities were reached at failure in specimens SD1M and SD1C, since significant horizontal slippage occurred in the column section relative to the footing. The same argument cannot be made for specimens SD2M and SD2C, since relatively little slippage was noted.

Shear forces can also be developed by dowel action across the shear plane, once significant slippage has occurred.[18] Figure 4-10 illustrates the three mechanisms for development of shear strength due to dowel action: flexure of the reinforcing steel, shear across the dowels, and "kinking" of the dowels. Kinking was not considered because kinking angles were not measured during testing. From Table 4-5, results indicate that dowel action through flexure considerably underestimated shear capacity and was most likely not the observed mode in which shear strength was developed. Dowel action from shear was a more probable mechanism; however, this also underestimated the actual shear forces developed in the test specimens.

4.4 Rotation Analysis

Calculated rotation consisted of rotation due to elastic and plastic deformation of the hinge section plus rotation due to bar slippage. The calculated load-rotation response curves are presented in Figures 4-11 through 4-14. The calculated points are superimposed on the measured response curves.

Two empirical formulas were used in determining the rotations for the test specimens.[18,23] Both Eqs. (4-2) and (4-3) attempt to compensate for the existence of so called "shear effects," or effects of "plastic spread" which develop throughout the length of a concrete member during bending.[18,24] Plastic spread begins occurring in a flexural member immediately after the concrete cracks, increasing the curvature and displacement of the member.

The first method to calculate the rotation of the column with respect to the base, caused by plastic deformation of the hinge throat, involved determining the yield curvature over the plastic hinge section. The rotation at yielding, θ_y, of each bar layer is:

$$\theta_y = \phi_y l_p, \tag{4-1}$$

where ϕ_y is the curvature at yielding of each particular bar layer, calculated by the computer program *IA1UNR*, and l_p is the equivalent length of the plastic hinge. The plastic hinge length can be determined using Baker's equation:[18]

$$l_p = k_1\, k_2\, k_3\, d \left(\frac{z}{d}\right)^{0.25}, \tag{4-2}$$

where k_1 is equal to 0.7 for mild steel and 0.9 for cold-rolled reinforcing steel; k_2 is equal to $1+0.5(P_u/P_o)$, where P_u is the axial compressive force applied to the member and P_o is the member's axial compressive strength; k_3 is a factor which ranges from 0.9 for a concrete compressive strength, f'_c, of 1700 psi to 0.6 for an f'_c of 5100 psi; z is the distance from the critical section to the point of contraflexure; and d is the effective depth of the section.

The additional curvature area developed from the plastic hinge length is added to the existing curvature diagram, shown in Figure 4-15, improving the accuracy of the calculated rotations.

The second method used was a formula developed by S. Sugano.[23] This empirically-derived method determines a new yield curvature value for the member, based on certain geometric and material properties. The equation also considers the effects of diagonal tension on the member's yield displacement. With this new curvature, the corresponding yield rotations are computed using the moment-area method of Eq. (4-1). Sugano's formula for yield curvature, ϕ_y, is:

$$\phi_y = \frac{M_y}{a_y\, E_c\, I_g}, \tag{4-3}$$

where

$$M_y = d''\, A_{st} f_y,$$

$$a_y = \left[0.043 + 1.64\left(\frac{E_s}{E_c}\right)\left(\frac{A_{st}}{bh}\right) + 0.043\left(\frac{a}{h}\right)\right]\left(\frac{d}{h}\right)^2.$$

In these equations, M_y is the yield moment, a_y is the stiffness reduction factor at yielding, a is the depth of the rectangular compressive stress block, A_{st} is the area of tensile steel, b is the cross-sectional width, d is the effective depth of the section, d'' is the distance between tension and compression steel, E_c is the concrete modulus of elasticity, E_s is the steel modulus of elasticity, f_y is the yield strength of the tensile steel, and h is the total depth of the section.

The bond-slip rotation was calculated with respect to the location of the neutral axis using the following relationship:

$$\theta_s = \frac{e}{d - kd}, \tag{4-4}$$

where d is the distance from the extreme compressive fiber to the centroid of the rebar and e is the steel elongation due to bar slippage. kd is the distance from the extreme compressive fiber to the neutral axis, and is calculated as:

$$kd = \frac{\epsilon_c}{\phi_y}.$$

The strain in the concrete at the extreme compressive fiber, ϵ_c, is computed from strain compatibility for each layer of steel that is yielding. An ultimate concrete strain of 0.004 was used as the crushing point of concrete. Bar elongation due to bond slip, e, is computed using:

$$e = \frac{f_s \, l_d}{2E_s},$$

where f_s is the steel yield stress, l_d is the development length of the reinforcement from ACI-318 Sec. 12.3.2,[1] and E_s is the steel's modulus of elasticity.

Bar slippage in an ordinary reinforced concrete connection exists primarily in the column anchorage system, as shown in Figure 4-16.[16,22] Bar slippage in a typical reinforced concrete beam section is very small due to the flexibility and cracking distribution of the element. However, in hinged specimens, there are two rigid concrete blocks that are rotating relative to each other with no crack development in either section; thus, bar slippage can take place in both portions, as shown in Figure 4-17. Bond-slip due to rotation can, therefore, be twice that of what would be anticipated in a normal reinforced concrete member.

4.4.1 Specimen SD1M

Figure 4-11 shows that the calculated load–rotation values for both Baker's and Sugano's methods overestimate the rotations until yielding of bar 1. At yielding of bars 2 and 3 the calculated values underestimate the actual rotation, most likely due to a reduction in stiffness, for which the calculation methods do not account. The ultimate rotations determined from Baker's and Sugano's formulas greatly underestimate the actual rotations. However, Sugano's formula approximates the actual rotations more closely than does Baker's.

4.4.2 Specimen SD2M

Figure 4-12 shows the load–rotation diagram for specimen SD2M. During small displacements, the measured curve shows a much higher hinge stiffness than the calculated curves. This stiffness retention is likely due to the aspect ratio of 2, in which the shearing effect on the hinge was not yet apparent. At yielding of bars 2 and 3, both Baker's and Sugano's formulas give good approximations of the measured response curve. In both of the monotonically loaded test specimens (SD1M and SD2M) the calculated ultimate rotations greatly underestimate the actual failure rotation.

4.4.3 Specimen SD1C

Figure 4-13 shows only the positive portion of the load-response curve envelope of Figure 3-54. In general, the load-response curves for Baker's and Sugano's methods fit the trend of the measured curve well. For the yielding of bars 1 and 3, the calculated results are very close to the cyclic response envelope; however, at yielding of bar 2 the calculated values do not as closely match the envelope. Both calculation methods underestimate the stiffness of the hinge envelope.

4.4.4 Specimen SD2C

Figure 4-14 shows the relationship between the calculated and measured load–rotation curves. As with specimen SD1C, the measured response curve is only the positive envelope of the load-rotation curve of Figure 3-75. The two methods overestimate the column rotation at yielding of bars 1 and 2. However, even though at yielding of bar 3 the methods again overestimate the rotation, the calculated values and the measured response are fairly close.

4.4.5 General Comments

All of the theoretical load–rotation response diagrams initially overestimate the column rotation, but overall correlation between the curves is good. In the early stages of loading there is only concentrated hinge rotation, with very little plastic rotation contributing to the overall column rotation. As loading proceeds, plastic rotation and bond-slippage effects are induced and very large rotations are experienced. This accounts for the calculated ultimate rotations greatly underestimating the actual failure rotations. In the theoretical calculations, crushing of concrete was assumed to occur at a strain of 0.004; however, all four test specimens exhibited a much higher ultimate strain. This appears to be the major reason for the differences between the measured and the calculated curves at ultimate rotation. It should also be noted that neither of the calculation methods were based on hinged specimens; they were used in this study to explore their applicability.

4.5 Deflection Analysis

The deflection components that contribute to column displacement are: deflection due to plastic deformation of the hinge throat, elastic deformation of the column, and deflection due to bond slip of reinforcing bars crossing the hinge throat. Calculated load–deflection curves are presented in Figures 4-18 through 4-21, and are superimposed on the measured load–deflection curves to examine the applicability of the analytical procedure.

To determine the yield displacements for each bar, Baker's equation, Eq. (4-2), was used to determine the plastic hinge length, l_p. The results from the computer program *IA1UNR* were then used, in conjunction with l_p, to calculate the yield displacements for bars 1 through 3 and the ultimate deflection at concrete crushing.

The model used in the moment-area calculations was a cantilever beam representing the column, with a fixed end as the foundation.[4] The cantilever section consisted of a 6.5-inch by 16-inch element connected to the fixed base by a 2.5-inch by 16-inch by ½-inch hinge section, as shown in Figure 4-22. The curvature varied linearly along the length of the element, from zero at the unsupported end to M_y/EI at the fixed end. The moment of inertia, I, was based on the uncracked section and the modulus of elasticity, E_c, was calculated from:[1]

$$E_c = 57{,}000 \sqrt{f_c'}.$$

The curvature over the plastic hinge length was calculated using the computer program *IA1UNR*. This curvature, combined with Baker's equation, produced the deflection caused by inelastic deformation. The idealized curvature distribution for the test specimen is shown in Figure 4-15. Deflections were calculated at yielding of the different layers of steel, with the value of M_y determined from *IA1UNR*.

Deflection due to bond slip was calculated from the following equation:

$$\delta_s = \theta_s L,$$

where θ_s is the rotation due to bond slip determined from Eq. (4-4), and L is the length measured from the support to the intersection of the hinge throat.

4.5.1 Specimen SD1M

Figure 4-18 shows the relationship between the measured and the calculated load-deflection diagrams. The calculated displacements at the different steel yielding locations underestimate the actual deformations, but Sugano's formula appears to approximate the curvature and the displacement response better than Baker's. The disparity between the calculated data and the observed results is partly a result of the horizontal slippage experienced during testing. (See Figure 3-17.) The horizontal slip causes a reduction in column stiffness, as indicated by the change in slope of the load–deflection diagram.

4.5.2 Specimen SD2M

Figure 4-19 shows the relationship between the calculated response and the measured deflection for this specimen. The calculated curves approximate the actual displacements fairly well up to the yielding of bars 1 through 3. At the concrete crushing point the calculated curves are much lower than the measured point, most likely because no horizontal ties were used in the column. The correlation between calculated and measured curves is much better for SD2M than for SD1M, probably due to SD2M's aspect ratio of 2.

4.5.3 Specimen SD1C

The load–deflection curve, Figure 4-20, shows the measured and calculated response for specimen SD1C. Only the cyclic deflection envelope has been plotted, not the hysteresis loops. The calculated curve underestimates the displacement envelope, a result of the stiffness reduction caused by the large horizontal slippage and subsequent large lateral deformation. SD1C did have horizontal ties located in the pier section, which reduced the amount of stiffness loss in the specimen; this is apparent when Figure 4-18 and 4-20 are compared.

4.5.4 Specimen SD2C

Figure 4-21 shows the load-deflection envelope for specimen SD2C. The calculated deformation response using Baker's method overestimates the deflection slightly; just the opposite from the first three test specimens.

4.5.5 General Comments

The Baker and Sugano procedures used to calculate the deformations underestimate the actual deflections. Agreement between the calculated and measured deflections is generally acceptable up to the yield point for bar 3, and is actually better than indicated by the load-deflection diagrams: a 0.10-inch gap between the hydraulic ram collar and the specimen resulted in measured displacements slightly larger than actual. Beyond this point, the specimens were able to sustain large strains which were well above the assumed ultimate concrete strain of 0.004; this is attributed to concrete confinement in the hinge throat.

Chapter 5

Comparison with Previous Testing

5.1 Introduction

The study presented in this report is part of a continuing study at the University of Nevada, Reno. The pilot study for this project, conducted in 1988, also considered four specimens.[16] The variables in that study were the same as in the present study; however, there are several differences between the two projects. This chapter highlights those differences, and discusses how the new results relate to the conclusions of the first study.

5.2 Comparison of Test Specimens

The research performed in 1988 was a pilot study of reinforced concrete hinges subject to shear and flexure in the strong direction.[16] Four one-eighth scale specimens were fabricated and tested in the laboratory. The reinforcing steel used in each specimen was Grade 40 plain No. 2 bars. Shear keyways measured 2 inches by 12 inches and had a roughness amplitude of approximately ¼ inch. Two test variables were considered in the preliminary study: cyclic versus monotonic loading, and shear-span to depth ratio. Only one specimen was tested cyclically, CH4; this specimen had an aspect ratio of 3. The remaining specimens, CH1, CH2 and CH3, were loaded monotonically. CH1, CH2 and CH3 had shear-span to depth ratios of 3, 2, and 1, respectively, to simulate the Rose Creek Interchange, which has effective shear-span to depth ratios ranging from 1.2, for double-curvature column deformation, to 3, for single curvature deformation.

The objective of the current study was to construct and test four one-sixth scale model bridge pier specimens. All specimens were subjected to the simultaneous effects of axial load, shear, and flexure. The reinforcing steel used in each specimen was Grade 60 deformed No. 3 bars. The shear keys incorporated in the models measured 2.5 inches by 16 inches and had a roughness amplitude of ½ inch.

The same test variables were considered as in the previous study: cyclic versus monotonic loading, and shear-span to depth ratio. Only two aspect ratio were considered in this study, 1 and 2, because aspect ratios of 2 and 3 gave nearly the same results in the pilot study.[16] These two ratios still provided the ability to monitor the behavior of a short, stiff column and a taller, more flexible column. For each shear-span to depth ratio, one specimen was subjected to monotonic loading and another subjected to cyclic loading.

Specifically, the differences between the previous study and the current research are the following:[20]

1. One-sixth scale models were used in the present SD (*S*tandard *D*etail) specimen series as opposed to one-eighth scale used in the original CH (*C*oncrete *H*inge) specimens. In the SD series, specimen size was increased to better represent an actual bridge pier. This increase in size, however, is not expected to significantly alter the behavior of the column.

2. Deformed (ribbed) reinforcing bars were used in the SD specimens, whereas plain bars were used in the original CH series. Deformed bars were used to enhance the bond between concrete and steel, and minimize crack widths at the hinge throat. Plain bars were used in the original specimens because deformed No. 2 bars were not available.

3. The original CH specimens consisted of two "column" elements joined together with a large "footing" block. The specimens were treated as beams for testing, with the columns simply-supported and the lateral load applied vertically to the footing section. The SD specimens were tested in an upright position with the lateral load applied horizontally to the column.

4. An axial load was applied to each of the SD specimens to simulate the effects of dead load from the bridge deck. The CH specimens had no applied axial load. An axial load will tend to enhance the shear resistance of a column, and creates a more realistic model.

5.3 Failure Modes

5.3.1 Original Concrete Hinge Series

Specimen CH1 had a shear-span to depth ratio of 3 and was loaded monotonically. An ultimate lateral load of 4200 pounds was obtained. Failure was caused by flexure and not by shear slip.

Specimen CH2, which had an aspect ratio of 2, was also loaded monotonically until failure. CH2 withstood a peak lateral load of 6000 pounds. CH2 also failed in flexure, as expected for a large shear-span to depth ratio. Neither CH1 nor CH2 showed any sign of cracking in the column, outside of the hinge area.

The last specimen loaded monotonically was CH3, which had an aspect ratio of 1. The ultimate load was 12,500 pounds, approximately twice that of CH2. CH3 exhibited a rapid strength deterioration after the peak load was reached, indicating a shear-slip failure immediately after the steel reinforcement yielded.

Specimen CH4 was loaded cyclically. This specimen had an aspect ratio of 3, as did CH1. The ultimate load for CH4 was 3605 pounds, after being subjected to five cycles of increasing lateral displacement. The maximum displacement ductility level achieved was 5. Failure was dominated by flexure.

5.3.2 Standard Detail Series

Test specimen SD1M was loaded monotonically until failure. The ultimate load was 25,300 pounds. Failure was caused by shear, as indicated by the rapid decrease in lateral load resistance. This was preceded by yielding of five of the bars in tension.

SD2M had an aspect ratio of 2, and was also loaded monotonically. The peak load achieved during testing was 13,100 pounds. A gradual decline in lateral load was observed, indicating a flexural failure.

Test specimens SD1C and SD2C were both loaded cyclically. SD1C withstood nine complete cycles, with a maximum ductility factor of 4.0. The ultimate load was 28,200 pounds, achieved on the fifth cycle. At the higher amplitude levels there was considerable pinching of the hysteresis loops, indicating rapid stiffness deterioration. The failure of specimen SD1C was caused by excessive flexural deformation.

Specimen SD2C was subjected to ten and one-quarter cycles of increasing amplitude displacements. SD2C achieved a maximum ductility level of 5.32 on the last quarter-cycle of testing. The peak load occurred on the eighth cycle and was 14,400 pounds. SD2C also failed in flexure. At higher levels of displacement amplitudes, pinching was present in the hysteresis loops, indicating a reduction in the energy absorbing capability of the hinge.

5.4 Scale Effect

The scale difference between the previous study (CH group) and this study created minimal performance differences. With the increase in size, SD specimens were able to withstand larger lateral loads before failure. Comparison of the test results, however, indicates that the scale had an insignificant influence on the performance of the specimens. The size contributed only to the ability to sustain larger loads.

5.5 Effects of the use of Deformed Bars

In the original CH series the steel reinforcement consisted of six No. 2 Grade 40 plain bars placed in a single row in the direction of bending. In the SD group, the steel crossing the hinge throat consisted of a single row of six No. 3 Grade 60 deformed bars.

The use of deformed bars in the SD specimens enhanced the bond between concrete and steel. Additionally, deformed bars helped reduce the crack widths across the hinge throat.

Chapter 6

Summary and Conclusions

6.1 Summary

This report presents the results of a study conducted on one-way reinforced concrete pier hinges subjected to a combination of axial load and uniaxial moment and shear in the strong direction. This type of hinge is typically used as the connecting link between the foundation and the columns of highway bridges. This "pinned" connection detail is typically known as a Freyssinet-type reinforced concrete hinge, and allows rotation in the weak direction while providing resistance to bending in the strong direction. The scope of this study was to construct and test four one-sixth scale hinge models. There were two primary variables in the testing sequence: shear-span to depth ratio (aspect ratio), and monotonic versus cyclic loading.

The first two specimens, with shear-span to depth ratios of 1 and 2, respectfully, were loaded monotonically to failure. The last two specimens, also with aspect ratios of 1 and 2, were subjected to cyclic loading until failure. The purpose of the cyclic loading was to determine the effects on shear stiffness of the hinge. The use of various aspect ratios was to determine a limiting shear-span to depth ratio that would produce a shear failure. By reducing the shear span, the effect of shear failure was significantly increased.

Analysis of the hinged specimens involved determining flexural and shear strengths, concentrated hinge rotations, and displacement of the column elements. Flexural analysis was performed using a moment-curvature program called *IA1UNR*. A comparison between the measured and the calculated yield and failure loads were presented for each specimen. The various shear equations that were used to determine shear capacities, and their relative accuracies, were presented. Shear strengths of the hinges due to dowel action, in both flexure and shear, were also examined.

Concentrated hinge rotation and column deflection consisted of two components: reinforcement bond slippage and column flexure. Flexural displacements were determined from the curvature distribution along the column and include elastic deformation of the column and plastic deformation of the hinge. Empirical formulas used to estimate the rotational and deformation effects were also discussed.

6.2 Observations

During testing and analysis, the following observations were made:

1. Cyclic loading of specimen SD1C and SD2C showed that slow load reversals reduce the stiffness of the hinge region, until closure of the crack on the compression side of the column is achieved.

2. The absence of horizontal ties in the column section of SD1M and SD2M reduced the shear and flexural strength of the specimens after some of the bars yielded.

3. Shear resistance is controlled mainly by friction forces within the compression zone of the hinge throat, and not along the entire length of the hinge as the shear-friction method assumes.

4. Significant flexural deformations occurred in all four specimens during testing. Even in specimens SD1M and SD1C, which had aspect ratios of 1, appreciable ductility was apparent.

5. The maximum applied shear was developed in specimen SD1C, which had a shear-span to depth ratio of 1 and was cyclically loaded until failure. This, however, did not determine the limiting shear-span to depth ratio of the specimens tested, since the maximum shear was obtained after the specimen had yielded in flexure. The shear span must be further reduced to obtain shear slip failure.

6. The moment-curvature program *IA1UNR* produced a good correlation between the theoretical flexural capacities of the specimens and the actual measured values.

7. In all four specimens, the engagement of the shear key provided extra shear strength and ductility at large displacements.

8. The presence of a constant axial load applied to the specimens reduced the crack width and increased the apparent shear strength.

9. The use of deformed bars reduced bond slip and reduced crack width at the hinge throat.

10. A gap of approximately 0.10 inch between the hydraulic ram collar and the test specimen led to larger displacements in the load–deflection curves than actually existed. The correlation between the actual and calculated yield displacements improves when this gap is taken into account.

6.3 Conclusions

The shear-friction method did not produce reasonable estimates of shear capacity in the hinged sections. From the test results, primary shear resistance was developed only in the compression zone of the hinge interface. Further research should be conducted to develop an accurate method for determining the shear capacity of hinges.

The effects of dowel action (primarily developed from flexure and/or shear) appeared only after noticeable deformations had occurred. The primary resistance to shear in the hinge for small deflections was the friction force created by aggregate interlock. As the deflections became significantly greater, crack propagation became increasingly larger, and primary shear resistance was generated from reinforcing steel dowel action.

As the shear-span to depth ratio (aspect ratio) was decreased, the energy dissipation capacity of the hinge also decreased. The ductility levels for specimens SD1C and SD2C were 4.0 and 5.3, respectively. Both specimens exhibited considerable hysteresis pinching. Hinge detail modifications to increase both the ductility and the energy absorbing capability of the connection during cyclic loading need to be explored.

References

1. ACI Committee 318. 1989. *Building code requirements for reinforced concrete (ACI 318-83) and commentary—ACI 318R-89*. Detroit: American Concrete Institute.

2. ACI-ASCE Committee 426. 1973. "The shear strength of reinforced concrete members." *[ASCE] Journal of the Structural Division*, 99(ST6): 1091-1187.

3. Base, G. D. *Tests on four prototype reinforced concrete hinges*, Research Report 17. London: Cement and Concrete Association.

4. Beer, F. P., and R. E. Johnson, Jr. 1981. *Mechanics of materials*. New York: McGraw-Hill.

5. Cheok, G. S., and W. C. Stone. 1986. *Behavior of 1/6-scale model bridge column subjected to cyclic inelastic loading*, NBSIR Report 86-3494. Washington, D.C.: U. S. Department of Commerce, National Bureau of Standards.

6. Gosain, N. K., R. H. Brown, and J .O. Jirsa. 1977. "Shear requirements for load reversals on RC members," *[ASCE] Journal of the Structural Division*, 103(ST7): 1461-1475.

7. Hewlett-Packard. 1985. *Basic 4.0 programming techniques for HP 9000 series 200/300 computers*. Corvallis, Oreg.: Hewett-Packard Company.

8. Hewett-Packard. 1982. *3054A (series 200 Basic) data acquisition control system library: Operating and programming manual*. Corvallis, Oreg.: Hewett-Packard Company.

9. Hoedajanto, D. 1983. *A model to simulate lateral force response of reinforced concrete structures with cylindrical and box sections*, Doctoral dissertation. Urbana: University of Illinois.

10. Hognestad, E. 1951. "A study of combined bending and axial load in reinforced concrete members." *Bulletin Series No. 399*. Urbana: University of Illinois Experimental Station.

11. Lew, H. S., E. V. Leyendecker, and R. D. Dikkers. 1971. "Engineering aspects of the 1971 San Fernando earthquake." *NBS Building Science Series No. 40*. Washington, D.C.: National Bureau of Standards.

12. Maruyama, K., H. Ramirez, and J. O. Jirsa. 1984. "Short RC columns under bilateral load histories." *[ASCE] Journal of Structural Engineering*, 110(1): 120-137.

13. Mattock, A. H. 1981. "Cyclic shear transfer and type of interface." *[ASCE] Journal of the Structural Division*, 107(10): 1945-1963.

14. Mattock, A. H., and N. M. Hawkins. 1972. "Shear transfer in reinforced concrete: Recent research." *PCI Journal*, 17(2): 55-75.

15. McLean, D. I., K.Y. Lim, E. H. Henley, and U. Vasishth. 1989. "Plastic hinge details for the bases of architecturally oversized bridge columns." *Proceedings*, First Workshop on Bridge Engineering Research in Progress, 251-254. Des Moines: Iowa State University.

16. Orie, J. L. 1987. *Behavior of bridge column-to-foundation hinge connections with uniaxial moment transfer*. Master's thesis. Reno: University of Nevada.

17. Paulay, T., R. Park. and M. H. Phillips. 1974. "Horizontal construction joints in cast in place reinforced concrete." *Shear in Reinforced Concrete*, SP-42, 599-616. Detroit: American Concrete Institute.

18. Paulay, T., and R. Park. 1975. *Reinforced Concrete Structures*. New York: John Wiley & Sons.

19. Kosmatka, S. H., and W. C. Panarese. 1988. *Design and control of concrete mixtures*, 13th ed. Skokie, Ill.: Portland Cement Association.

20. Saiidi, M., D. Bergman, and D. Straw. 1989. "Scaled model testing of bridge hinged piers subjection to a lateral loads." *Proceedings*, First Workshop on Bridge Engineering Research in Progress, 305-308. Washington, D.C.: National Science Foundation.

21. Saiidi, M., J. L. Orie, and B. Douglas. 1988. "Lateral load response of reinforced concrete bridge columns with a one-way pinned end." *ACI Structural Journal*, 85(6): 609-616.

22. Sozen, M. A. 1974. "Hysteresis in structural elements." *Applied Mechanics in Earthquake Engineering*, Proceedings of the 1974 Winter Annual Meeting of the Applied Mechanics Division, vol. 8, 63-98. New York: American Society of Mechanical Engineers.

23. Sugano, S. 1970. *Experimental study on restoring force characteristics on reinforced concrete members*. Doctoral dissertation. Tokyo: University of Tokyo.

24. Thomas, K., and M. A. Sozen. 1965. *A study of the inelastic rotation mechanism of reinforced concrete connections*. Urbana: University of Illinois, Department of Civil Engineering.

25. Umehara, H., and J. O. Jirsa. 1984. "Short rectangular RC columns under bidirectional loadings." *[ASCE] Journal of the Structural Division*, 110(3): 605-618.

26. Wang, C. K., and C. G. Salmon. 1985. *Reinforced concrete design*, 4th ed. New York: Harper & Row.

27. Woodward, K. A., and J. O. Jirsa. 1984. "Influence of reinforcement on RC short column lateral resistance." *[ASCE] Journal of the Structural Division*, 110(1): 90-104.

28. Wright, J. K., and M. A. Sozen. 1975. "Strength decay of RC columns under shear reversals" *[ASCE] Journal of the Structural Division*, 101(5): 1053-1065.

Table 4-1. Measured and Computed Yield Loads for Specimen SD1M.

Layer of Steel	Measured Load (lbs.)	Calculated Load (lbs.)	Measured / Calculated
1	18,300	20,200	0.91
2	20,000	22,600	0.88
3	20,800	24,500	0.85
Ultimate	25,300	26,600	0.95

Table 4-2. Measured and Computed Yield Loads for Specimen SD2M.

Layer of Steel	Measured Load (lbs.)	Calculated Load (lbs.)	Measured / Calculated
1	9,100	10,200	0.89
2	9,800	11,400	0.86
3	11,000	12,400	0.89
Ultimate	13,100	13,700	0.96

Table 4-3. Measured and Computed Yield Loads for Specimen SD1C.

Layer of Steel	Measured Load (lbs.)	Calculated Load (lbs.)	Measured / Calculated
1	17,100	20,100	0.85
2	19,900	22,400	0.89
3	22,100	24,400	0.91
Ultimate	30,500	26,600	1.15

Table 4-4. Measured and Computed Yield Loads for Specimen SD2C.

Layer of Steel	Measured Load (lbs.)	Calculated Load (lbs.)	Measured / Calculated
1	9,600	10,000	0.96
2	10,100	11,200	0.90
3	11,000	12,100	0.91
Ultimate	14,400	13,200	1.09

Table 4-5. Shear Strength Analysis based on Different Methods.

Method	Shear Capacity, lbs. SD1M	SD2M	SD1C	SD2C
SF1A Shear Axial Compression (ACI-318 Eq. 11-4)	7,470	7,820	7,270	7,260
SF2A Shear Axial Compression (ACI-318 Eqs. 11-7, 11-8)	7,270	6,280	6,900	5,850
SFr1 Shear Friction Method, 1 bar (ACI-318 Eq. 11-26)	32,600	32,700	32,500	32,600
SFr2 ShearFriction Method, 2 bars	39,000	39,100	38,700	38,900
SFr6 ShearFriction Method, 6 bars	64,500	64,600	63,800	64,000
Dowel Action, Shear (Ref 18)	22,100	22,100	21,700	21,700
Dowel Action, Flexure (Ref 18)	9,140	9,140	8,990	8,990
Maximum Applied Shear, Measured in Laboratory	25,300	13,000	30,500	14,400

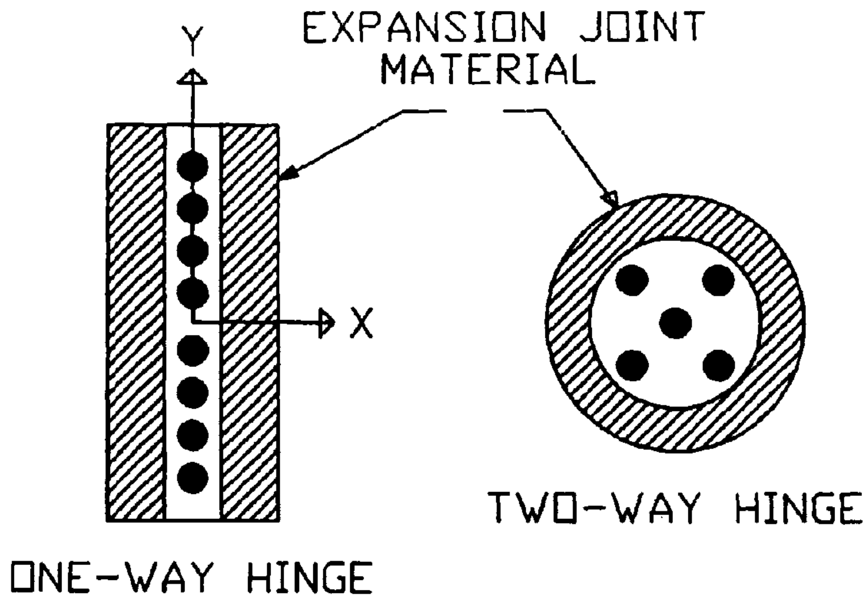

Figure 1-1. Typical Reinforced Concrete Hinge.

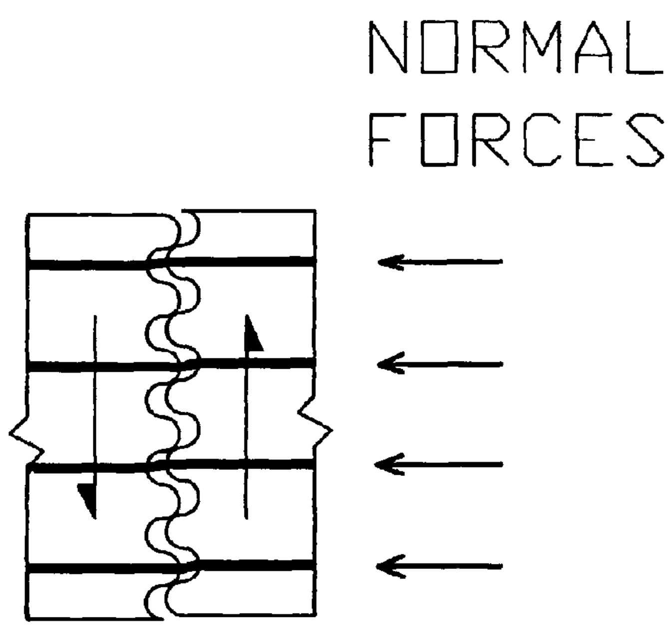

Figure 1-2. Shear Friction Mechanism.

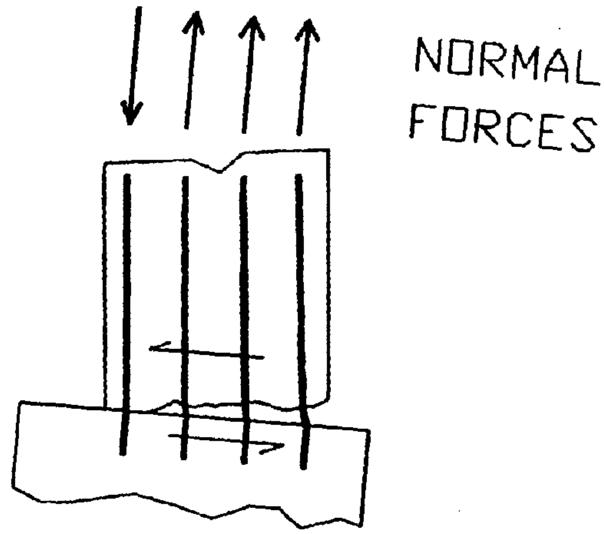

Figure 1-3. One-Way Hinge Failure Mechanism.

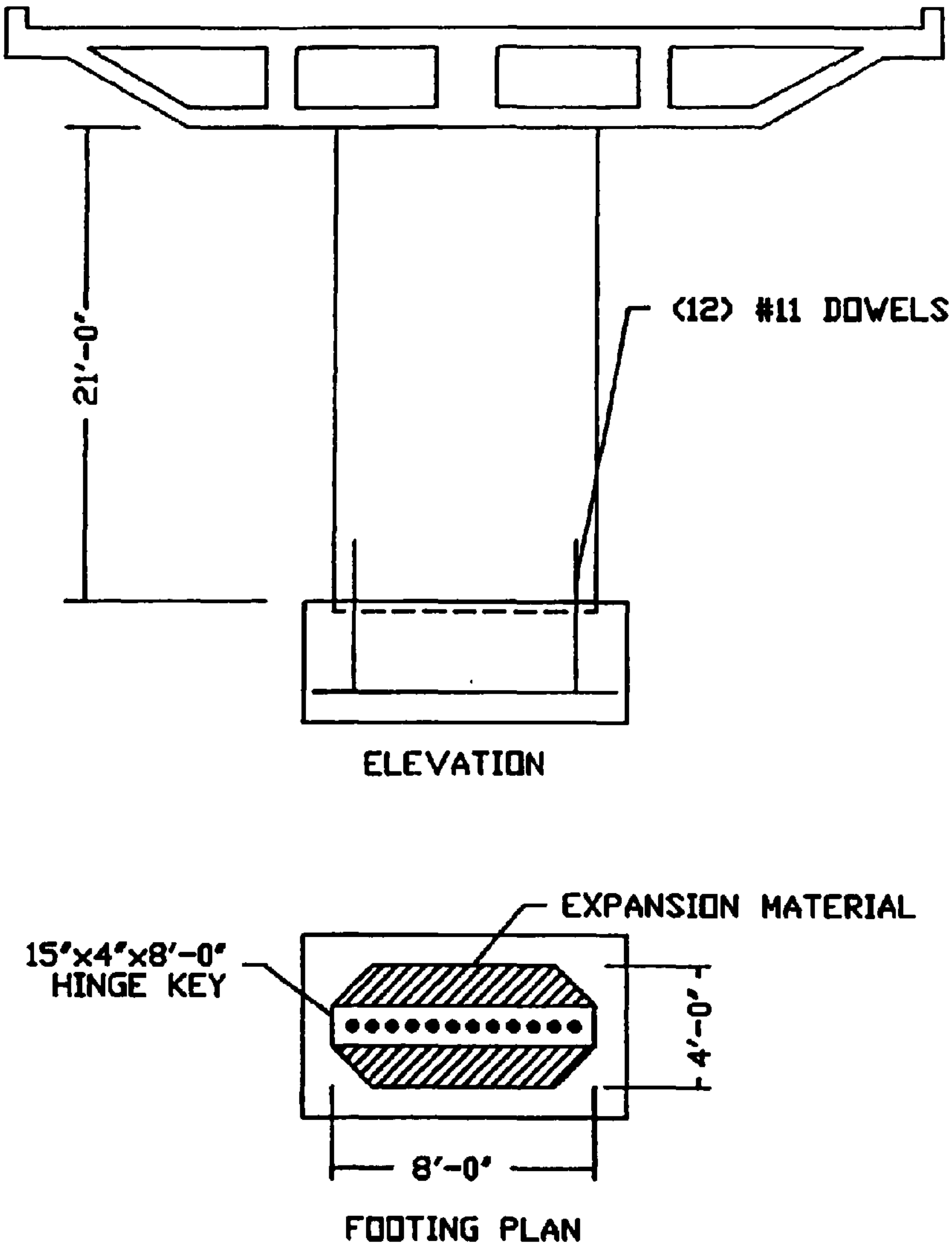

Figure 2-1. Cross-Sections of the Rose Creek Interchange.

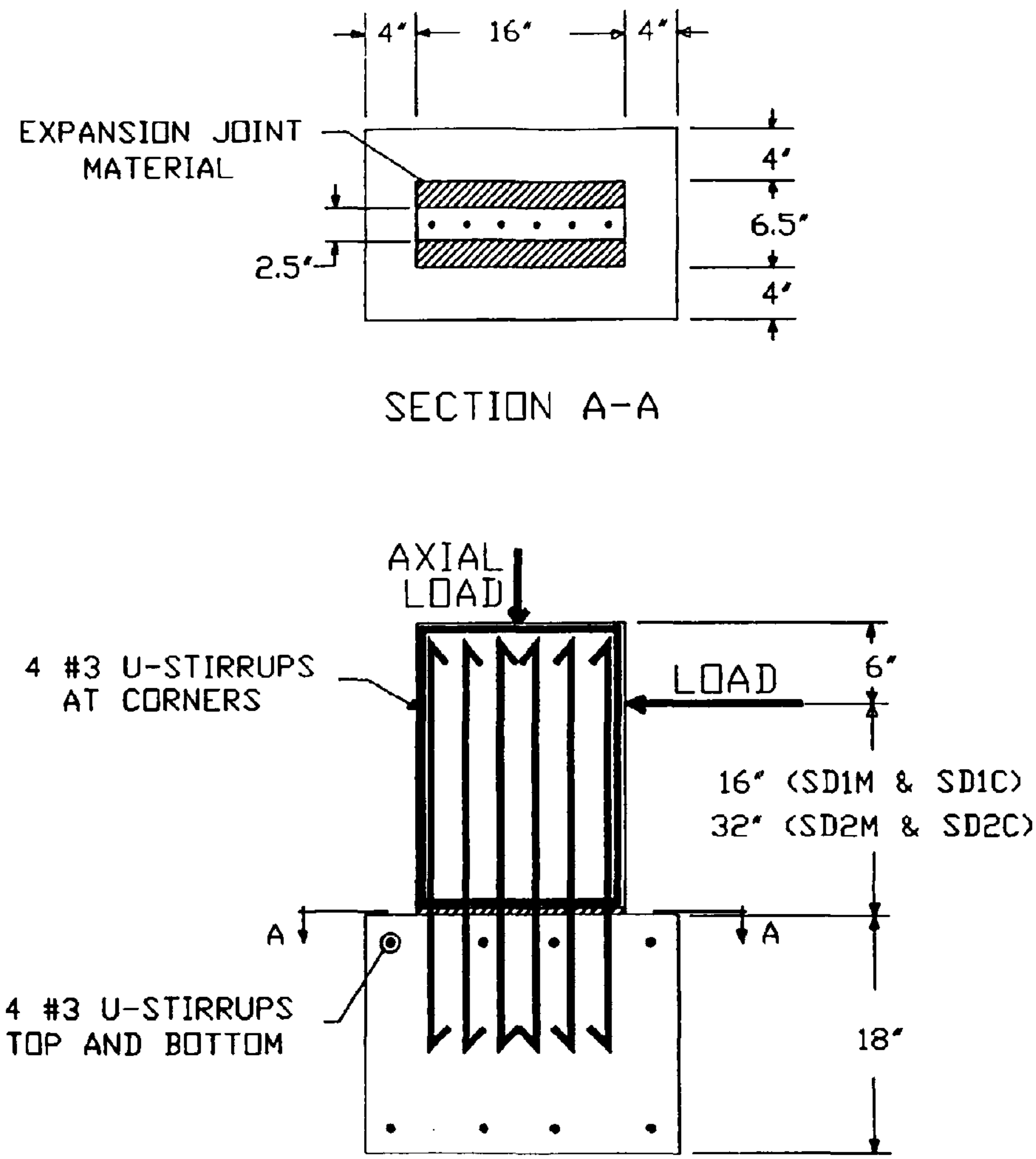

Figure 2-2. Typical Hinge Cross-Section and Elevation of SD-Series Test Specimens.

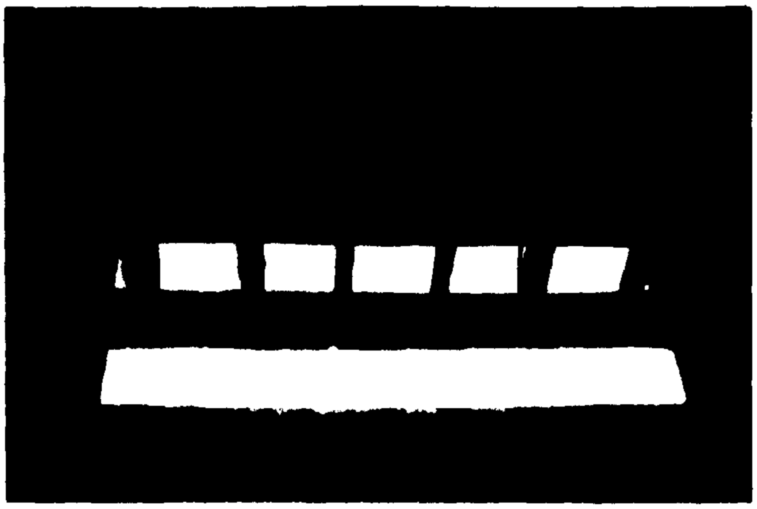

Figure 2-3. Typical Foundation Segment after Curing.

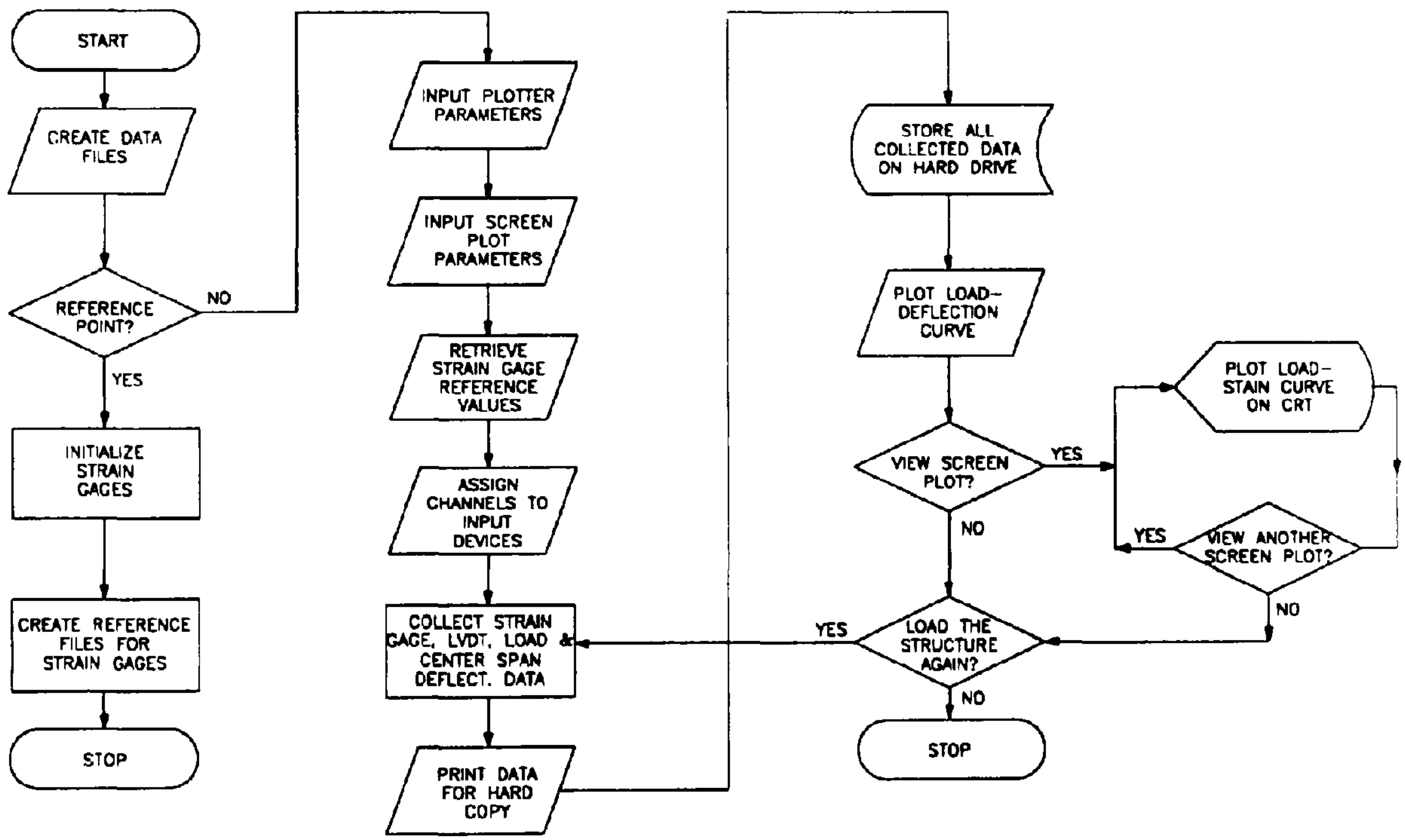

Figure 2-4. Flowchart for Data Acquisition Software Program *PIERHINGE*.

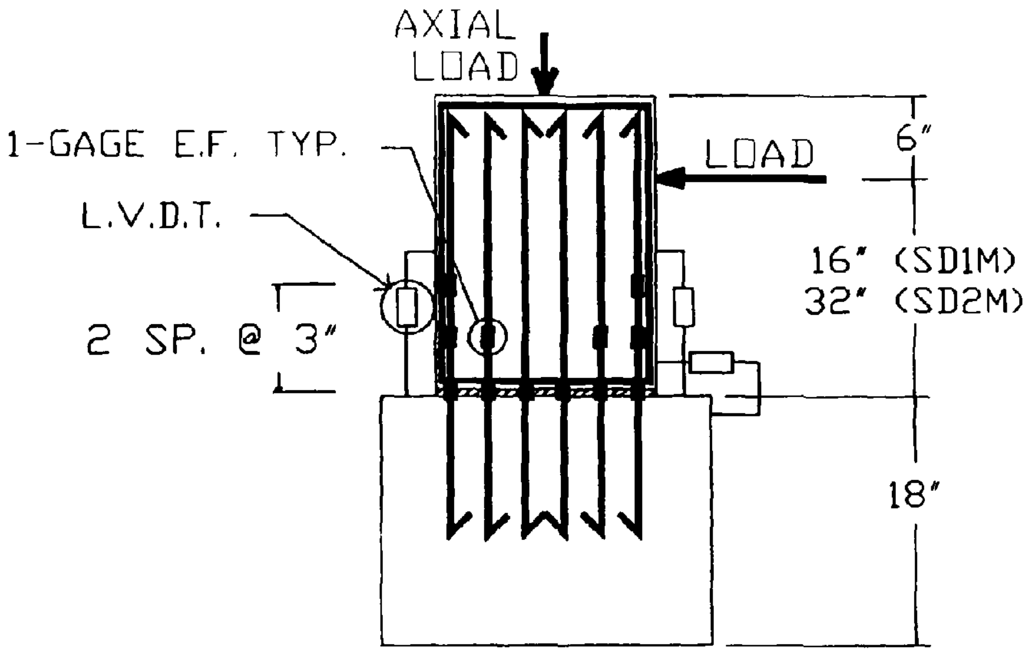

Figure 2-5. Instrumentation Detail for Specimens SD1M and SD2M.

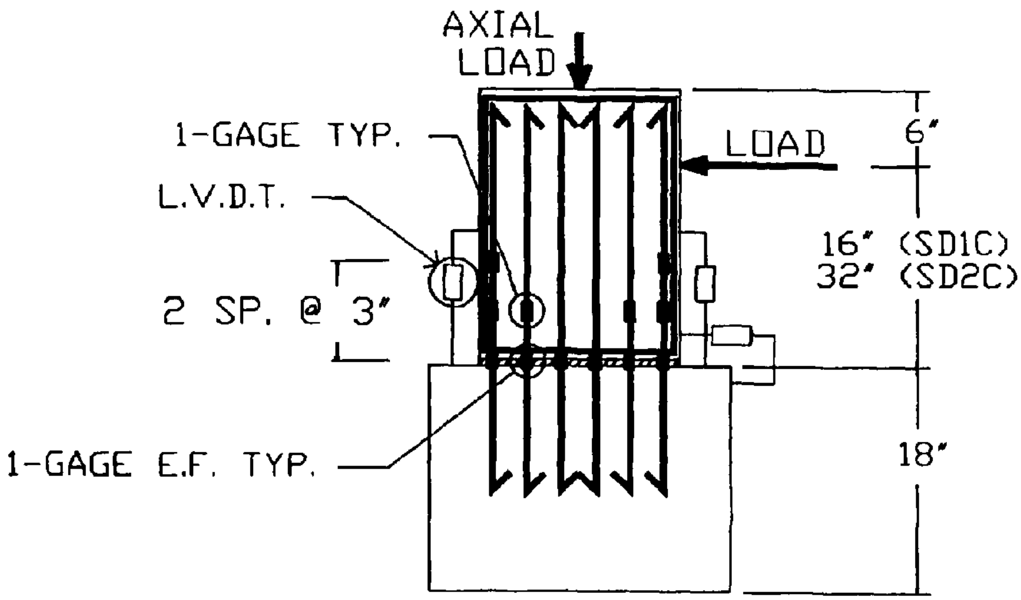

Figure 2-6. Instrumentation Detail for Specimens SD1C and SD2C.

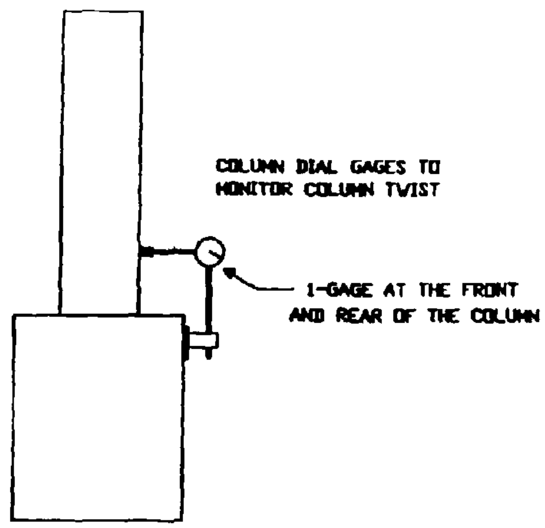

Figure 2-7. Instrumentation Detail for Measuring Column Twist.

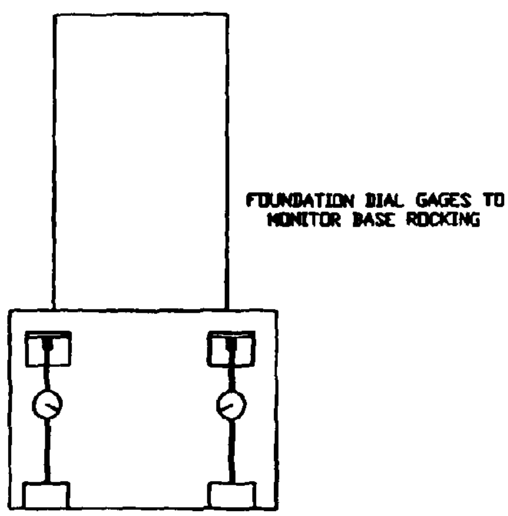

Figure 2-8. Instrumentation Detail for Measuring Base Rocking.

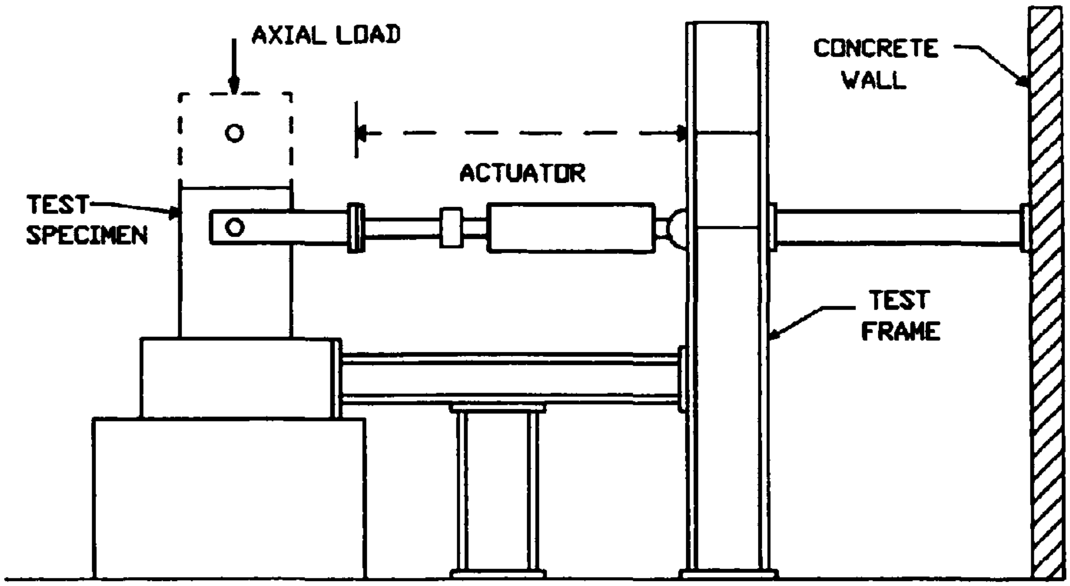

Figure 2-9. Test Frame Setup.

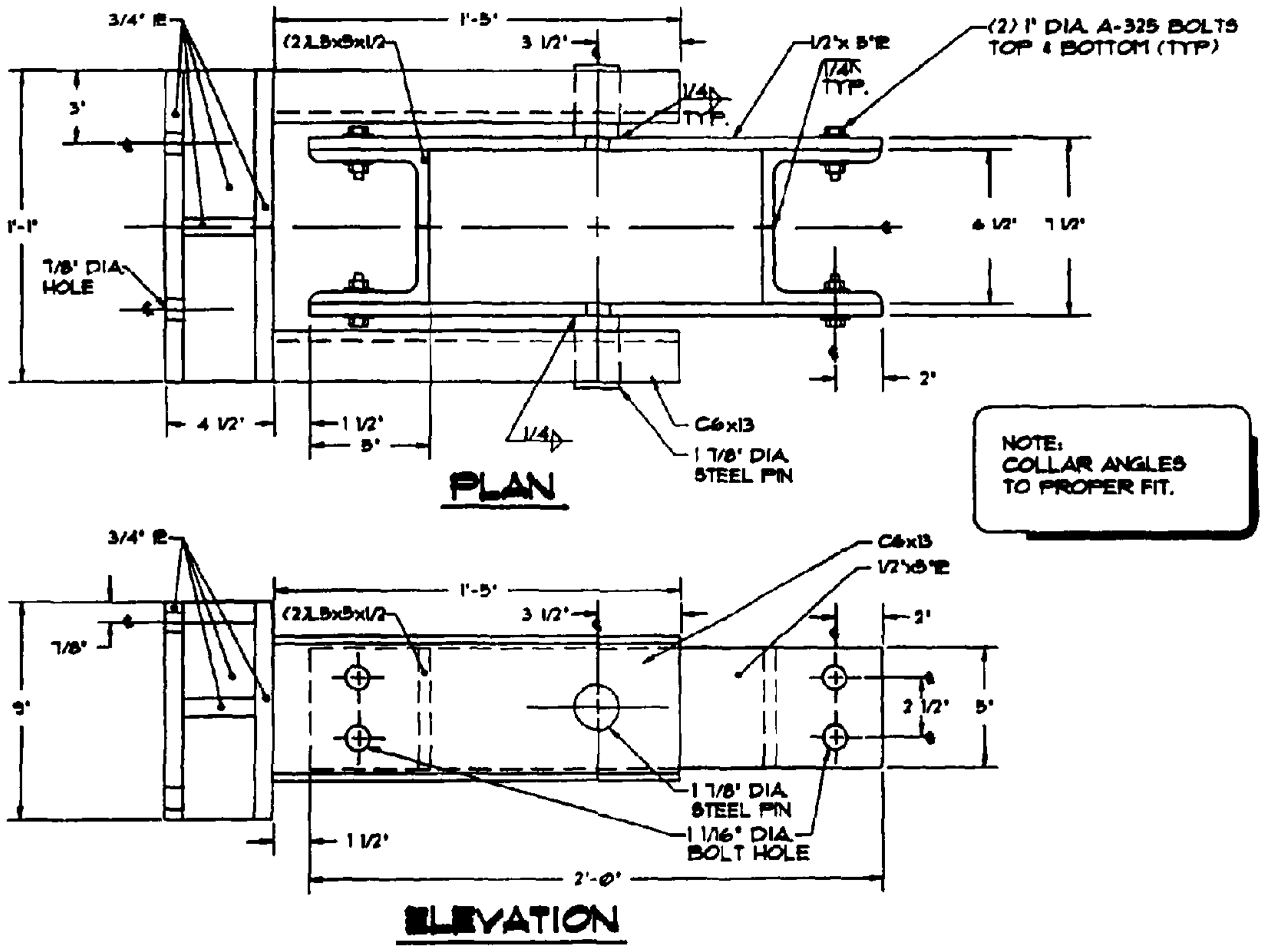

Figure 2-10. Hydraulic Ram Collar.

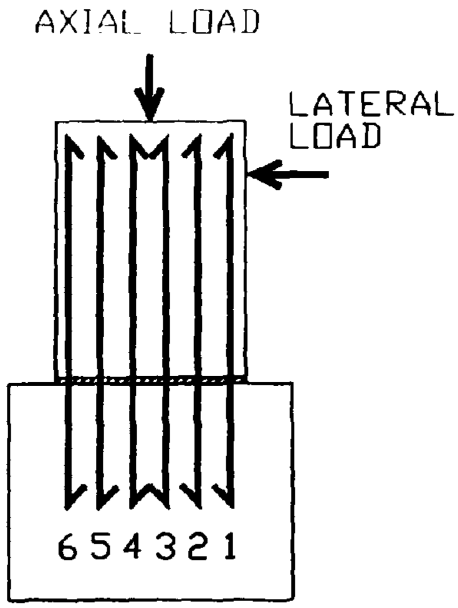

Figure 3-1. Dowel Numbering for Test Specimens.

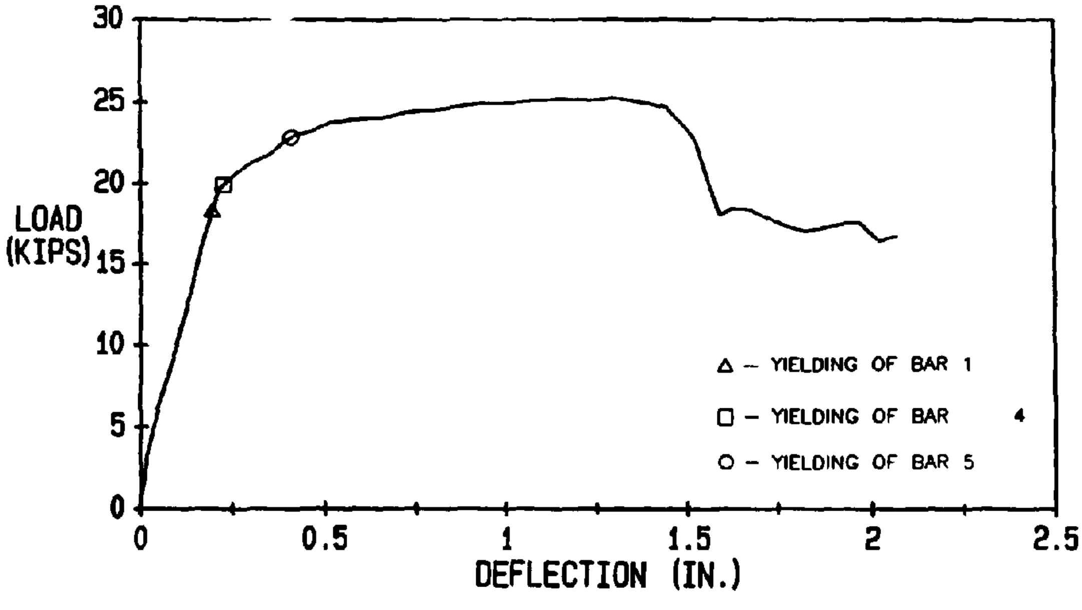

Figure 3-2. Measured Load-Deflection Diagram for Specimen SD1M.

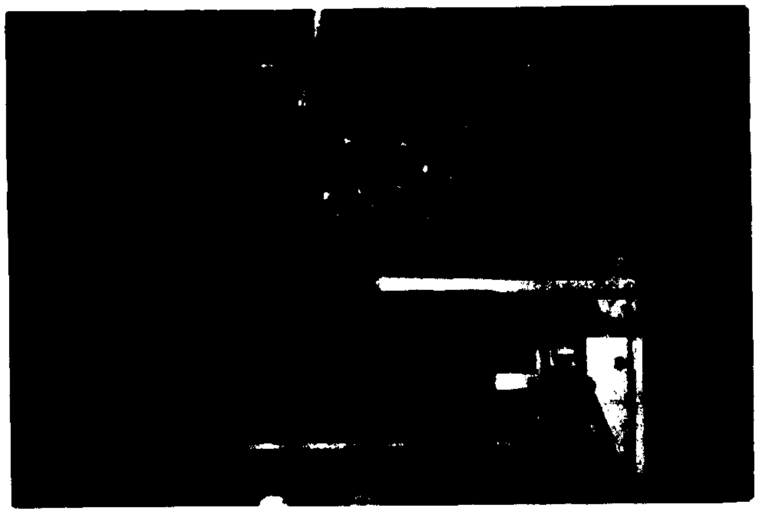

Figure 3-3. Cracking Pattern of Specimen SD1M.

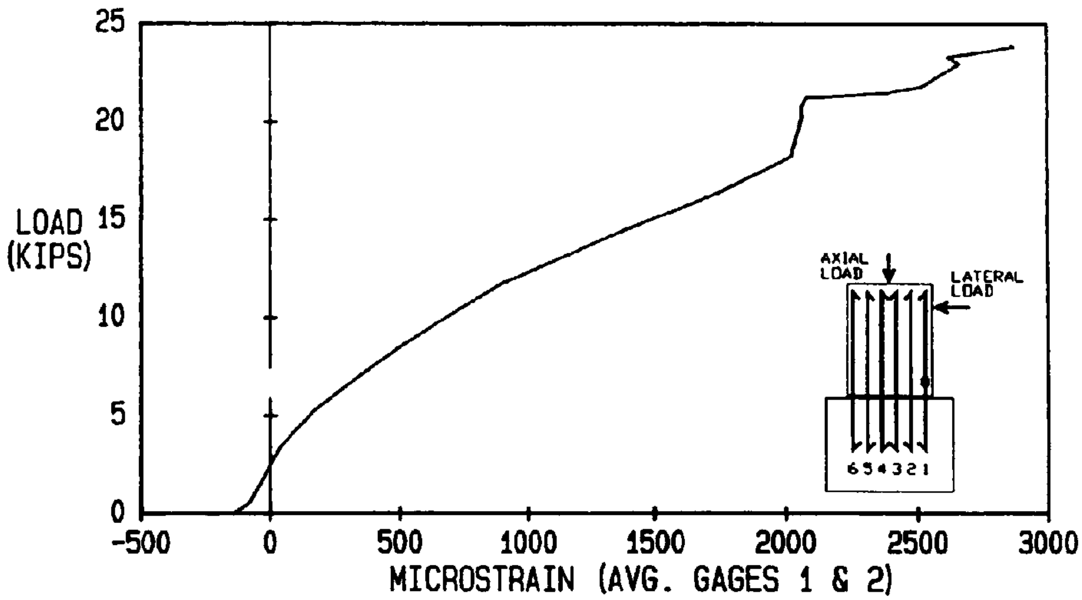

Figure 3-4. Load-Strain Diagram for SD1M, Bar 1 (Avg. of Gages 1 and 2).

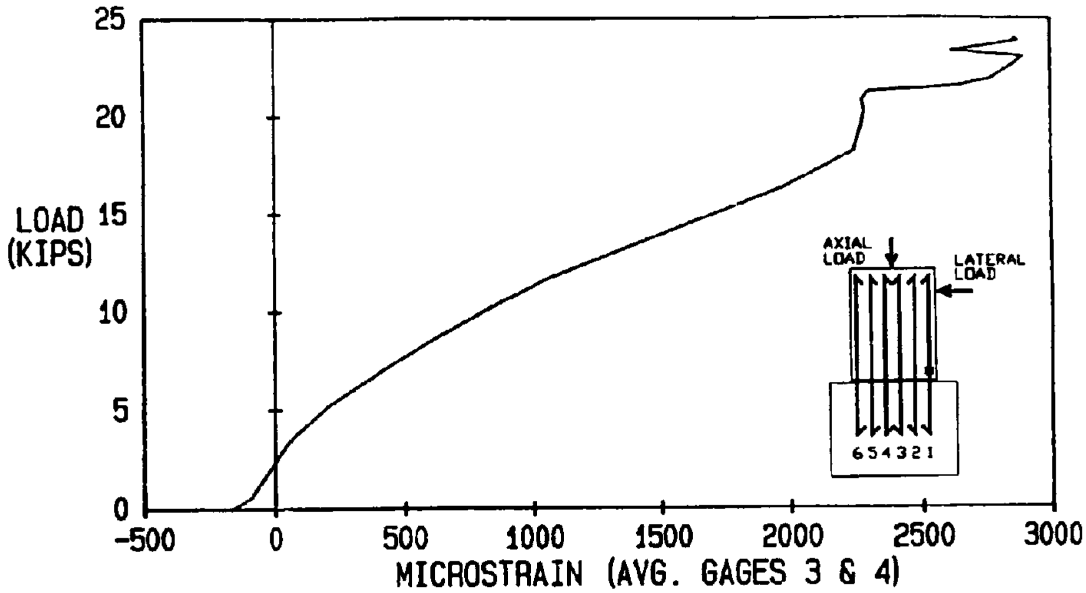

Figure 3-5. Load-Strain Diagram for SD1M, Bar 1 (Avg. of Gages 3 and 4).

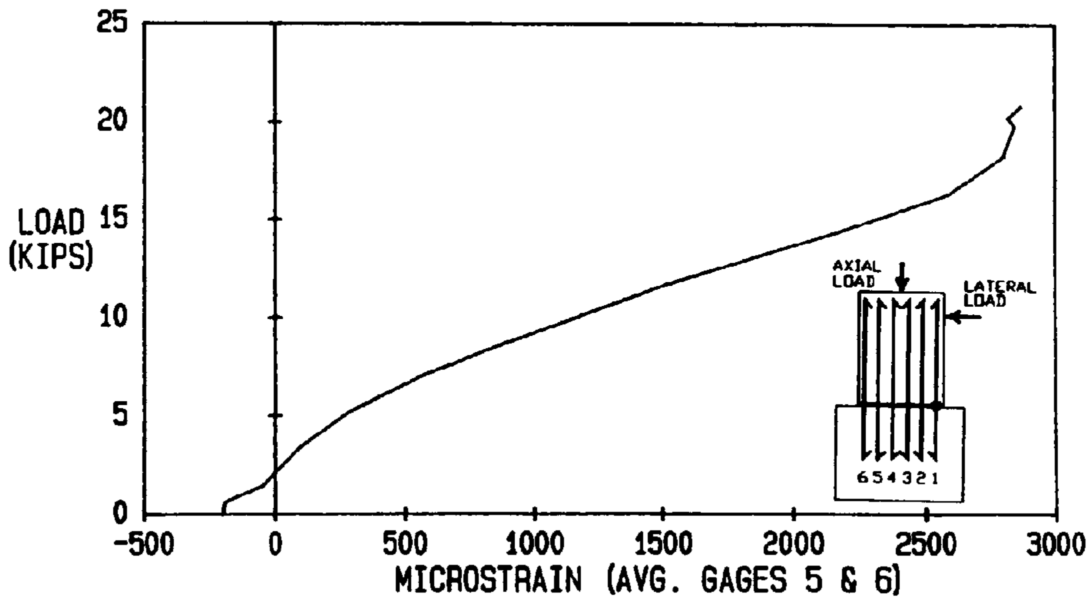

Figure 3-6. Load-Strain Diagram for SD1M, Bar 1 (Avg. of Gages 5 and 6).

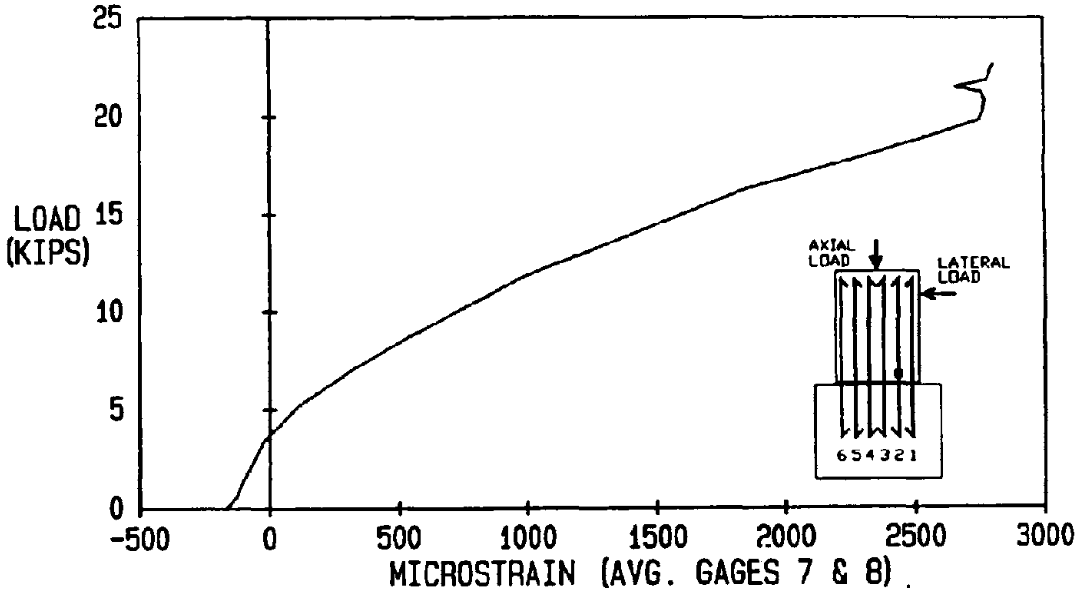

Figure 3-7. Load-Strain Diagram for SD1M, Bar 2 (Avg. of Gages 7 and 8).

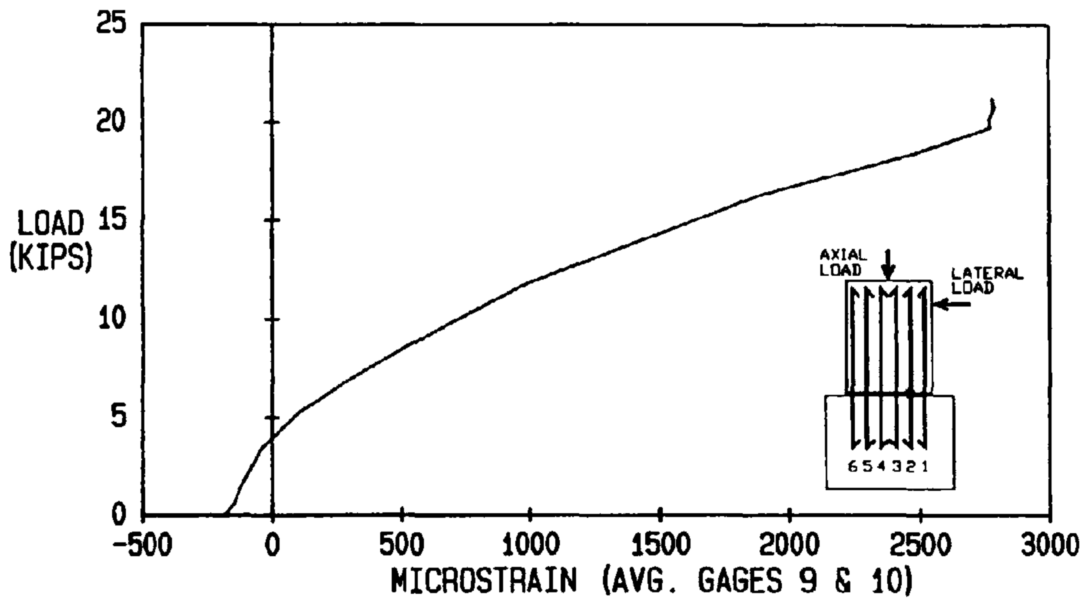

Figure 3-8. Load-Strain Diagram for SD1M, Bar 2 (Avg. of Gages 9 and 10).

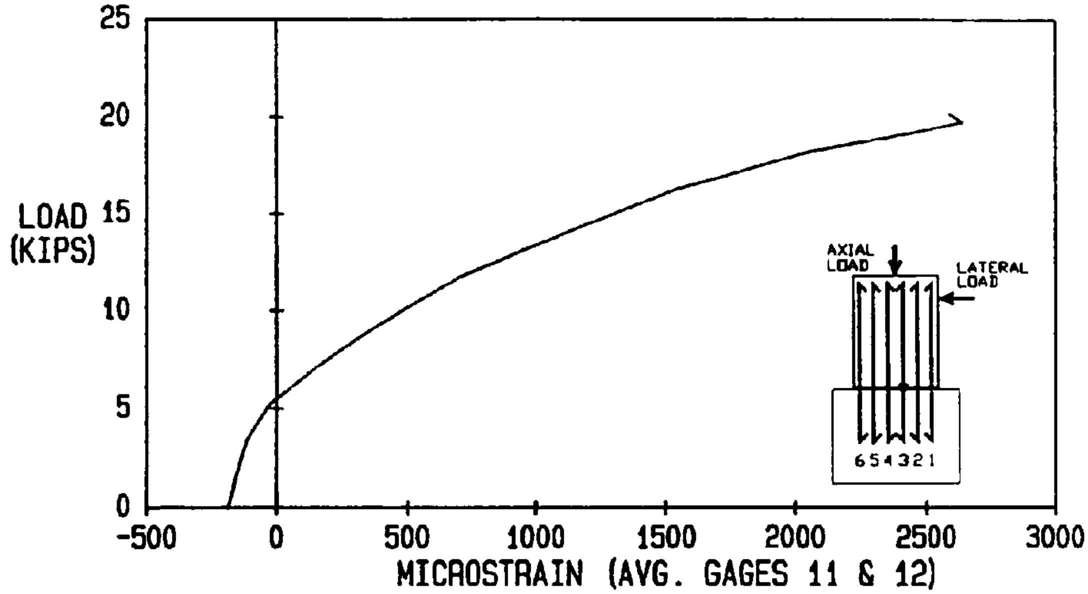

Figure 3-9. Load-Strain Diagram for SD1M, Bar 3 (Avg. of Gages 11 and 12).

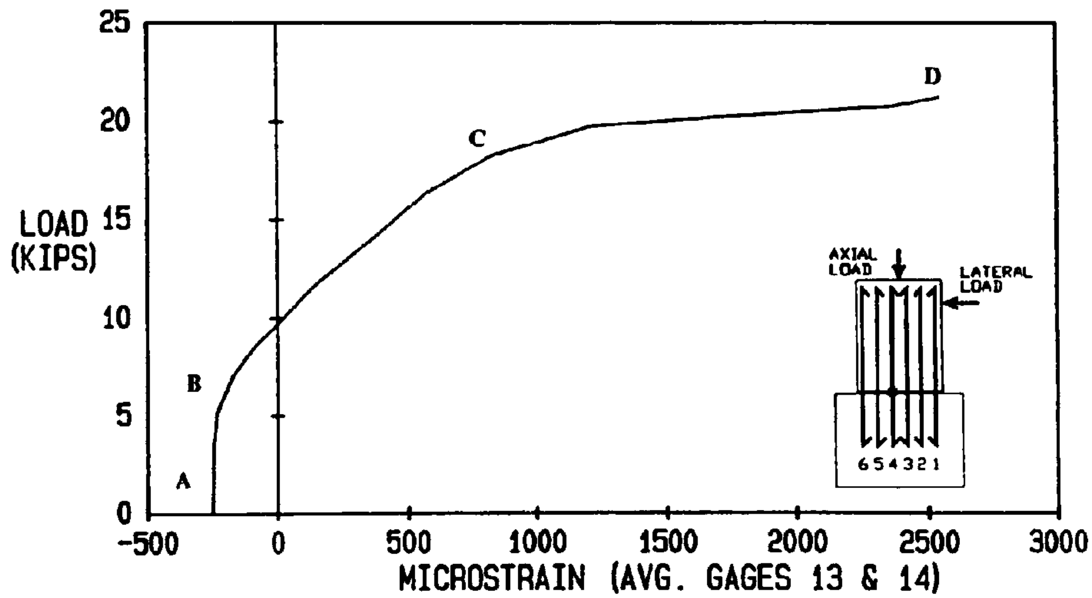

Figure 3-10. Load-Strain Diagram for SD1M, Bar 4 (Avg. of Gages 13 and 14).

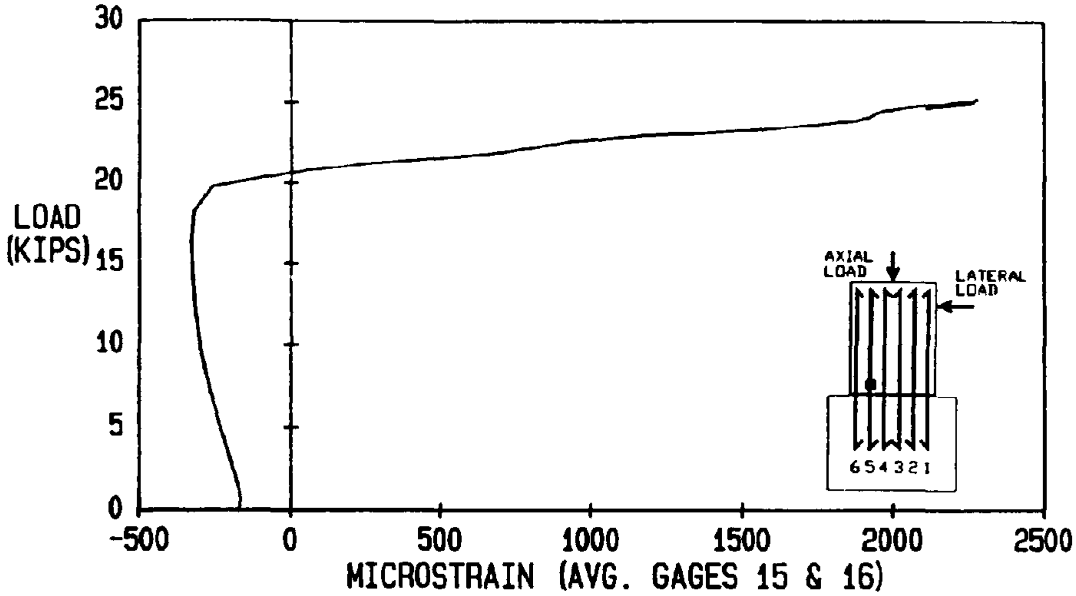

Figure 3-11. Load-Strain Diagram for SD1M, Bar 5 (Avg. of Gages 15 and 16).

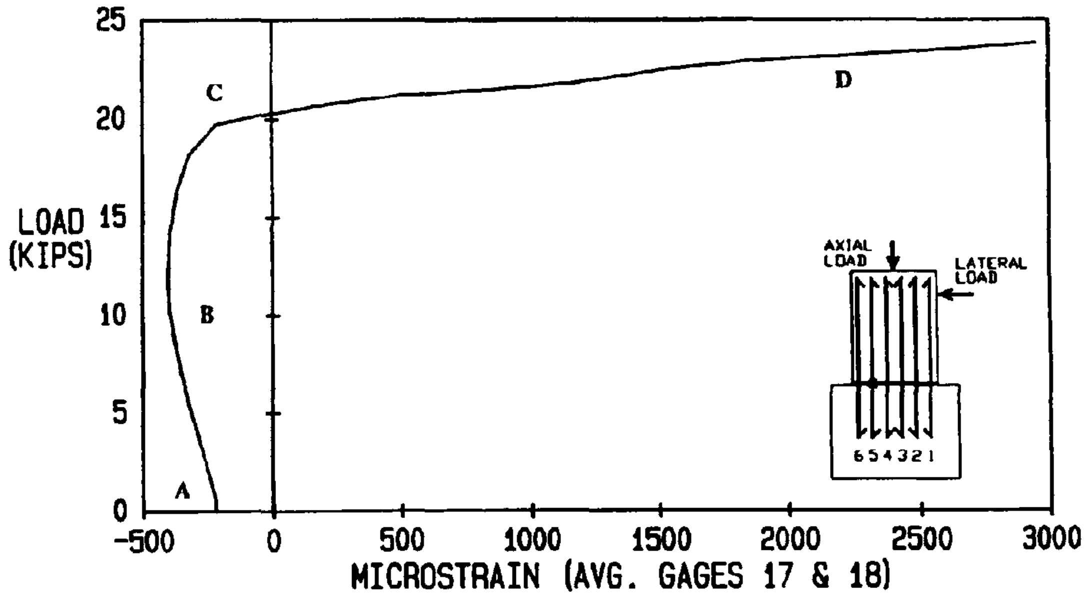

Figure 3-12. Load-Strain Diagram for SD1M, Bar 5 (Avg. of Gages 17 and 18).

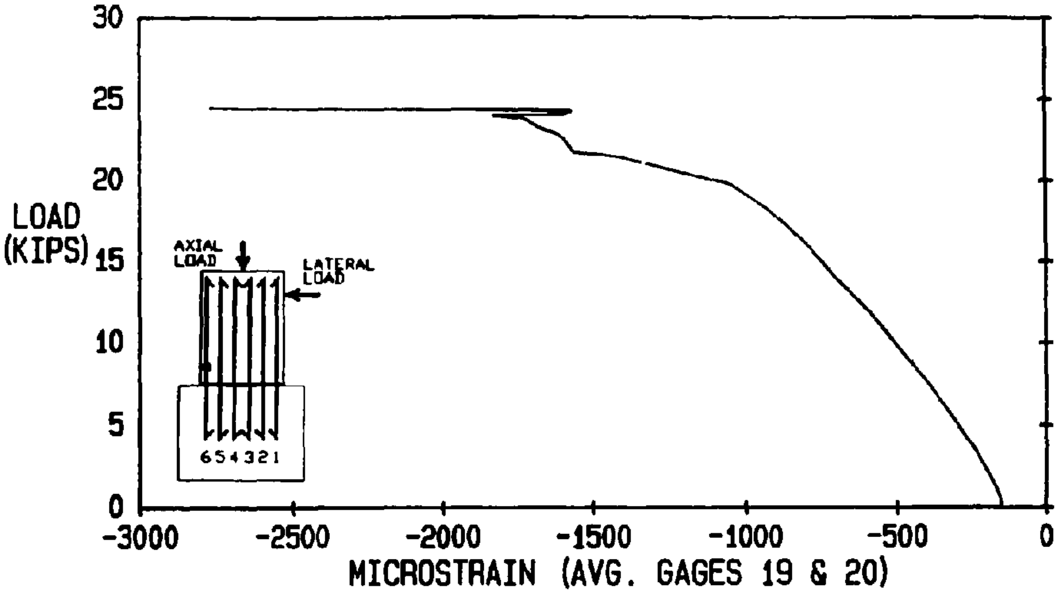

Figure 3-13. Load-Strain Diagram for SD1M, Bar 6 (Avg. of Gages 19 and 20).

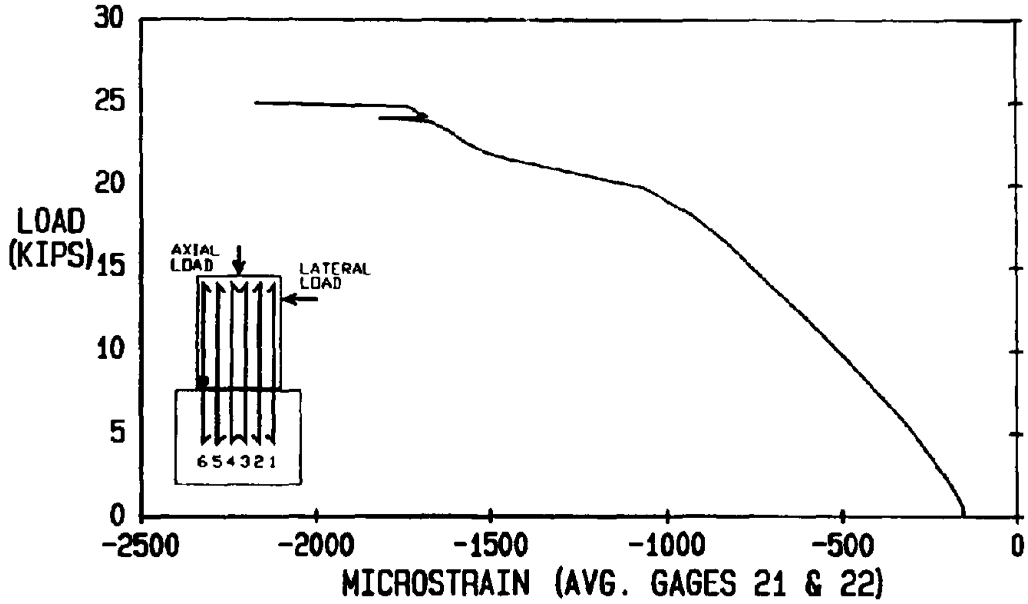

Figure 3-14. Load-Strain Diagram for SD1M, Bar 6 (Avg. of Gages 21 and 22).

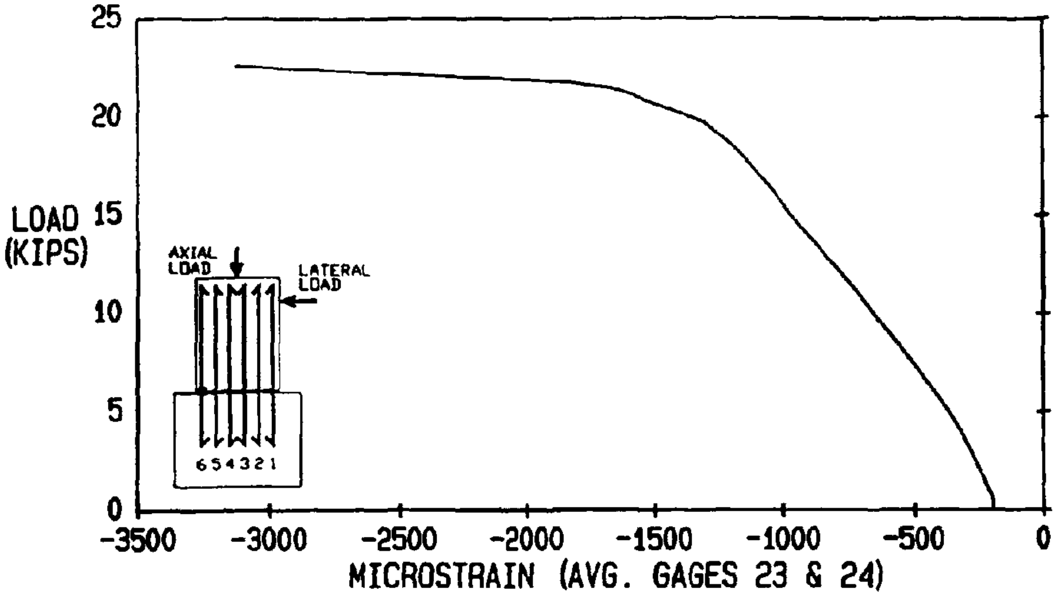

Figure 3-15. Load-Strain Diagram for SD1M, Bar 6 (Avg. of Gages 23 and 24).

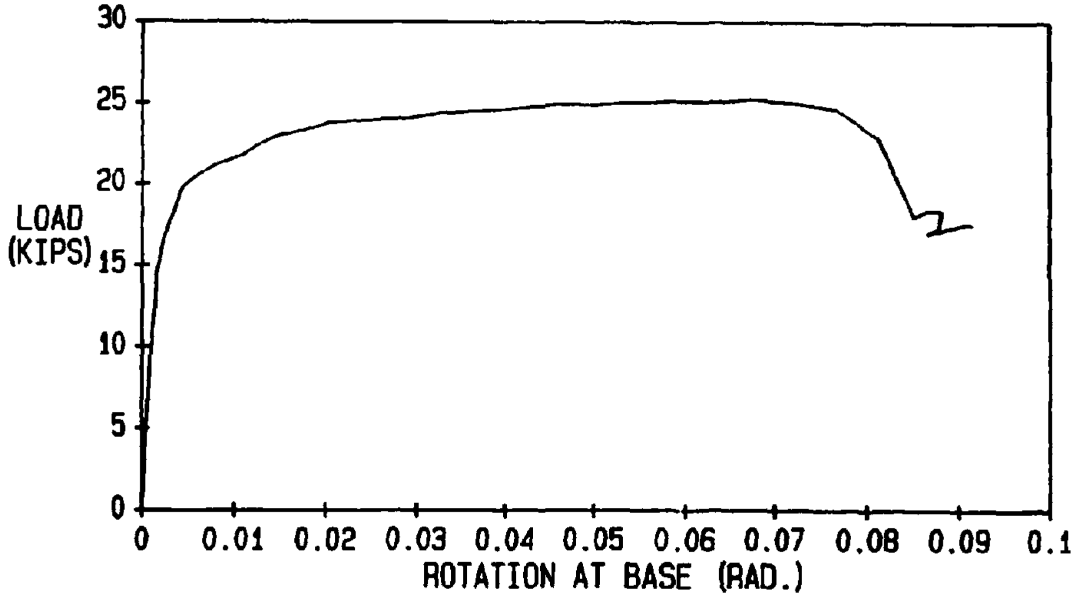

Figure 3-16. Load-Rotation Diagram for Specimen SD1M.

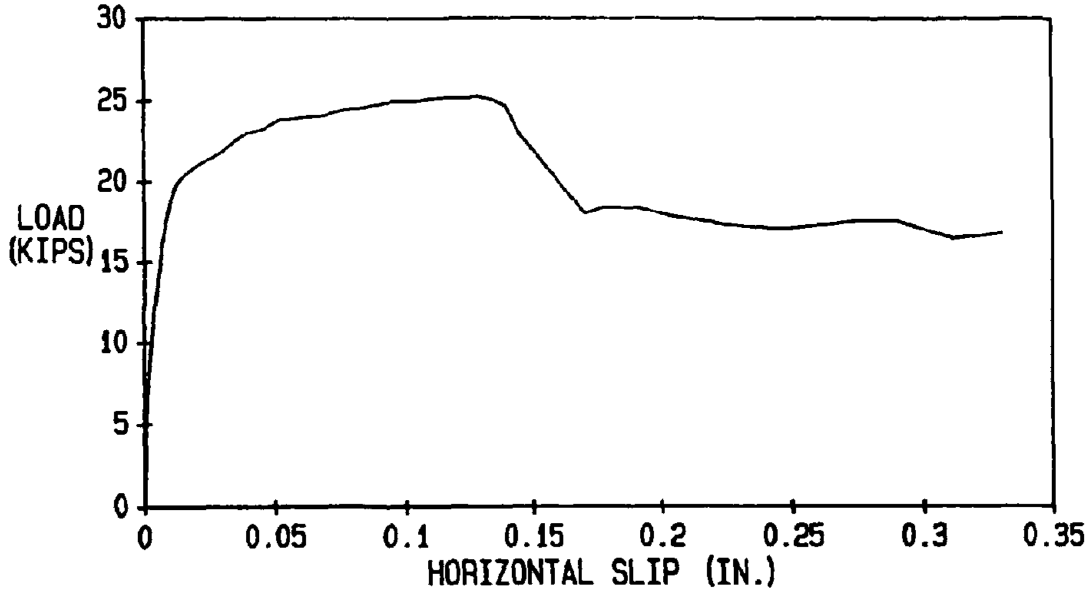

Figure 3-17. Load-Horizontal Slip Diagram for Specimen SD1M.

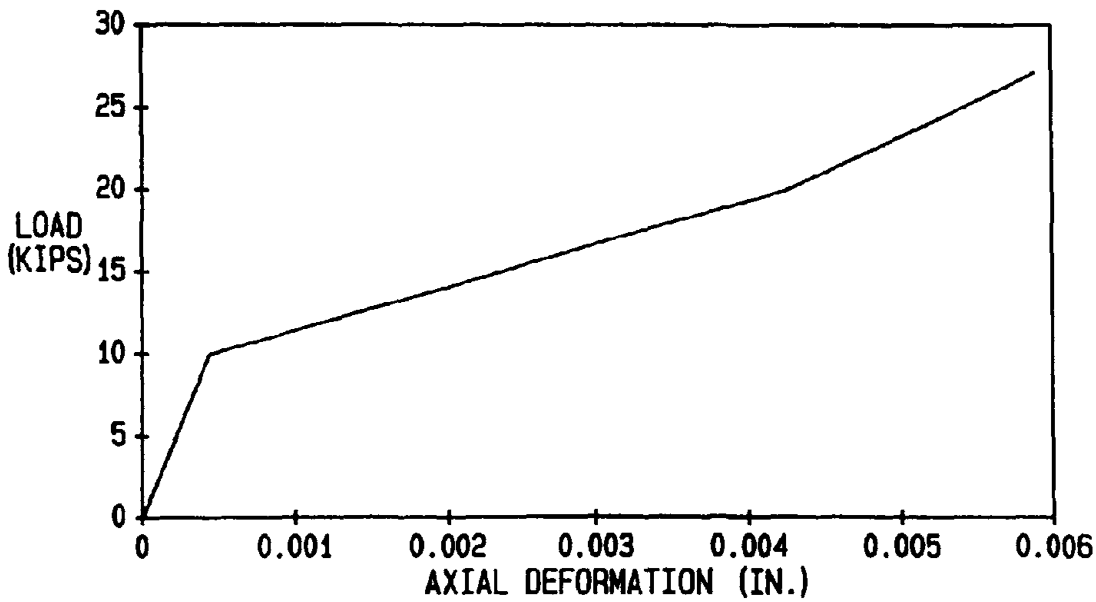

Figure 3-18. Axial Load-Deformation Diagram for Specimen SD1M.

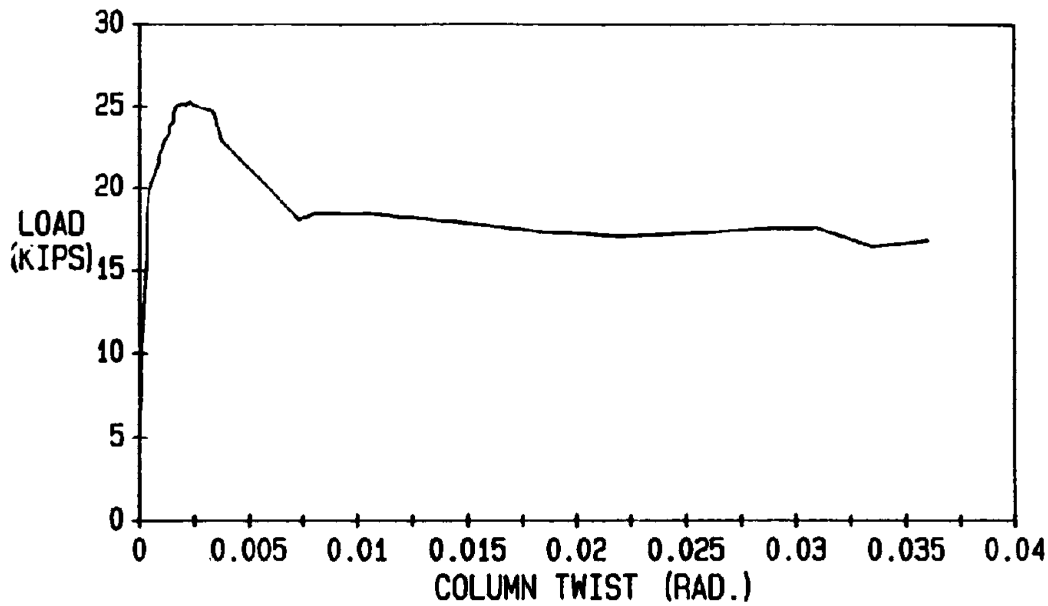

Figure 3-19. Load–Column Twist Diagram for Specimen SD1M.

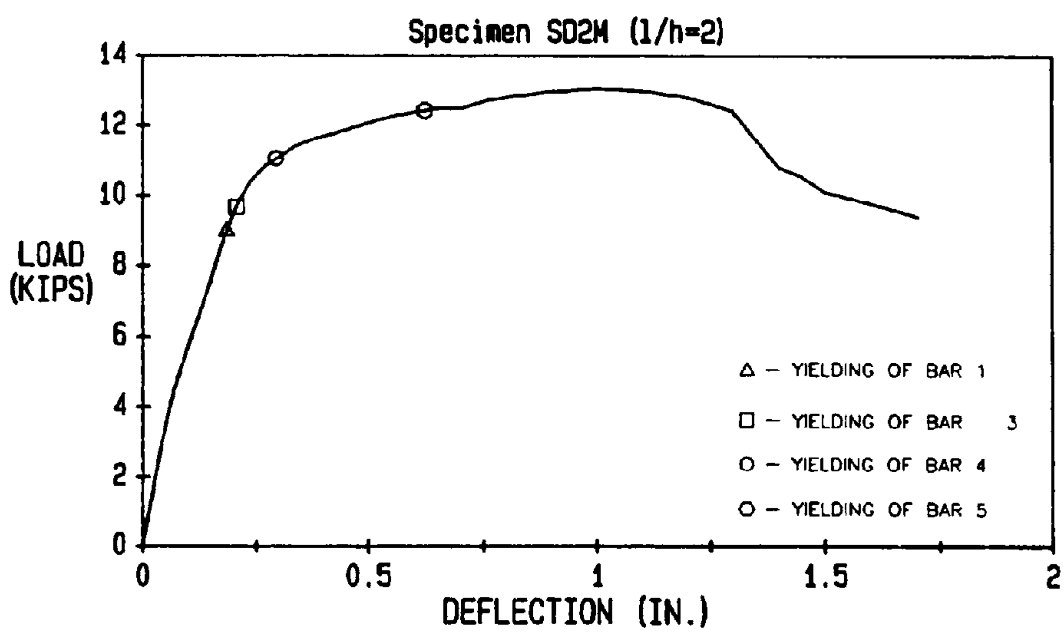

Figure 3-20. Load–Deflection Diagram for Specimen SD2M.

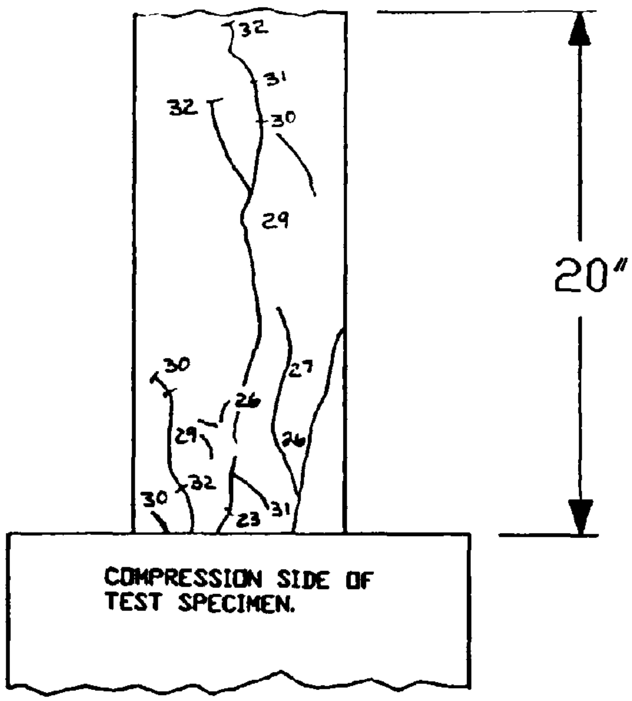

Figure 3-21. Cracking Pattern of Specimen SD2M.

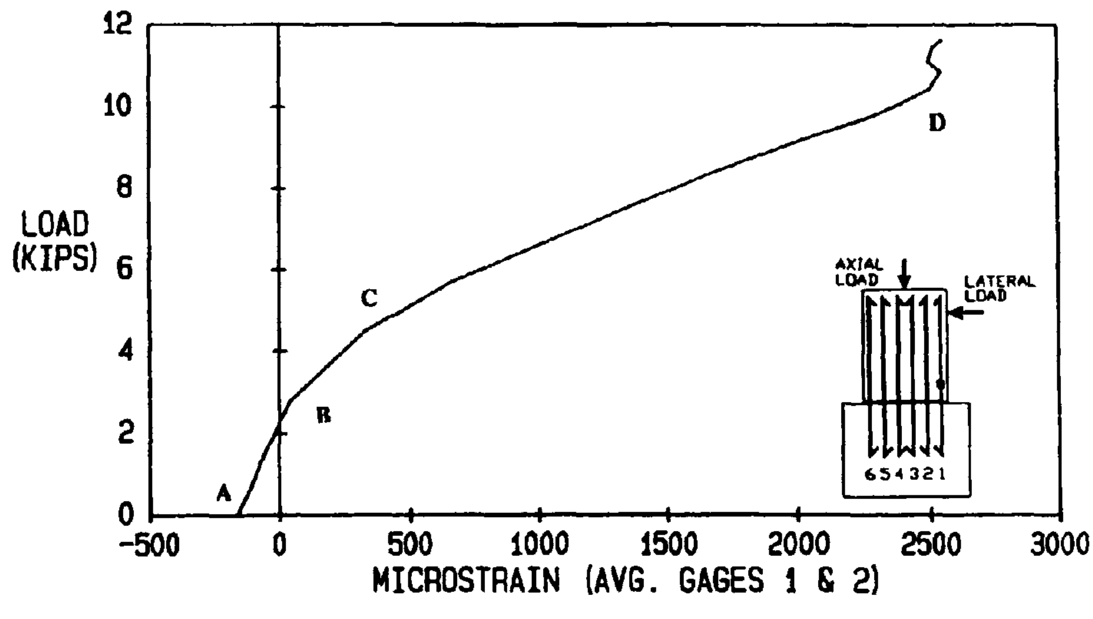

Figure 3-22. Load-Strain Diagram for SD2M, Bar 1 (Avg. of Gages 1 and 2).

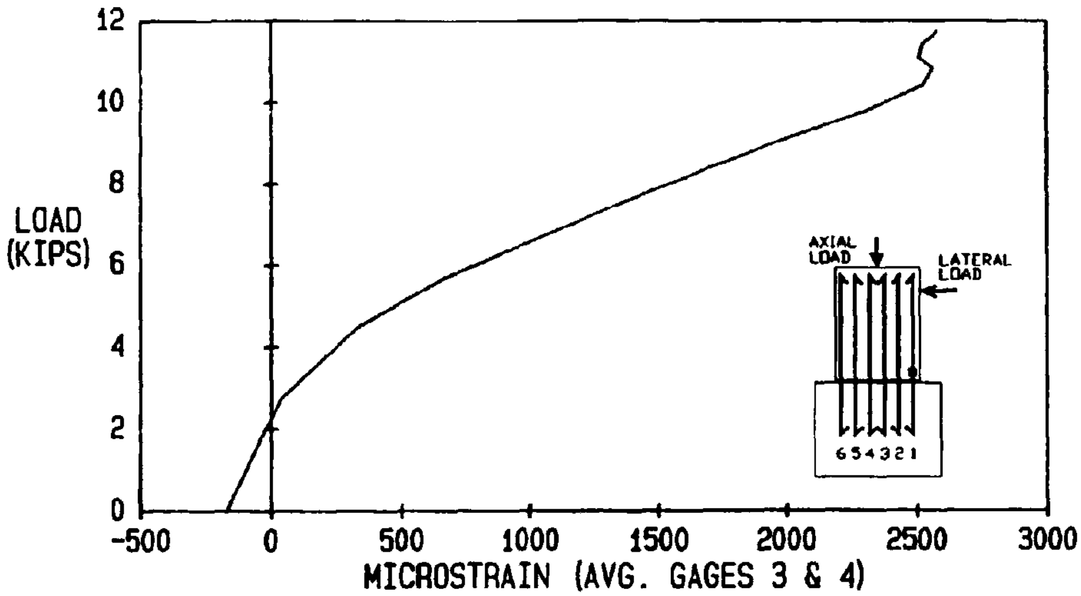

Figure 3-23. Load-Strain Diagram for SD2M, Bar 1 (Avg. of Gages 3 and 4).

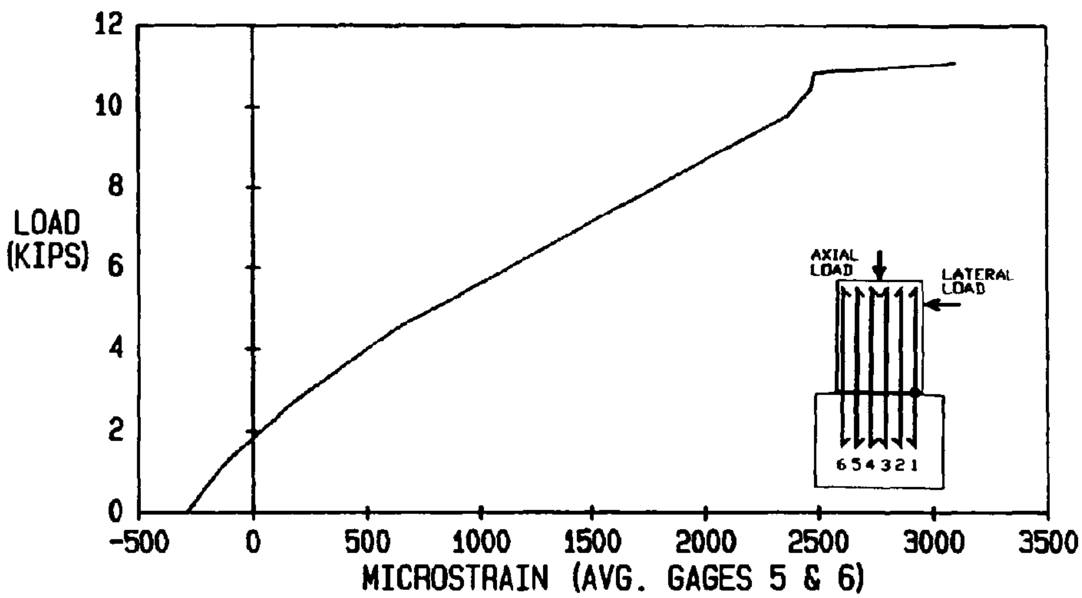

Figure 3-24. Load-Strain Diagram for SD2M, Bar 1 (Avg. of Gages 5 and 6).

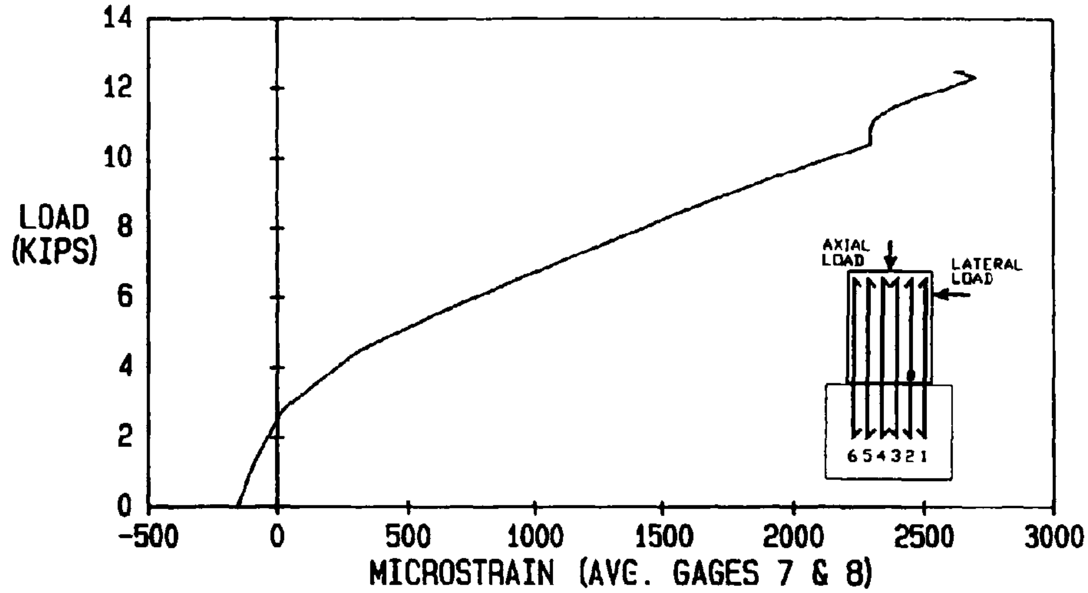

Figure 3-25. Load-Strain Diagram for SD2M, Bar 2 (Avg. of Gages 7 and 8).

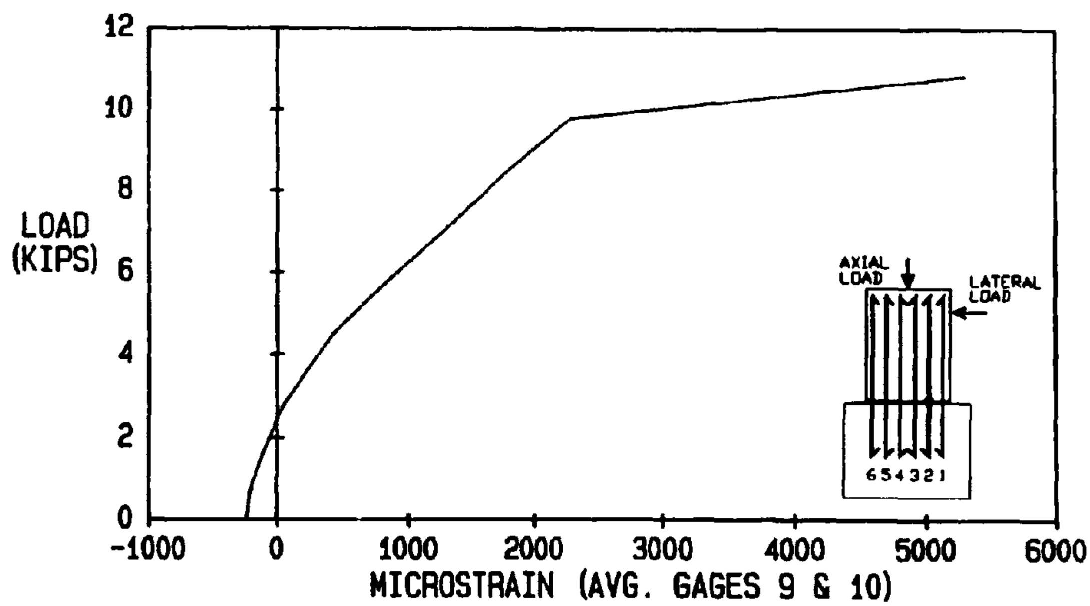

Figure 3-26. Load-Strain Diagram for SD2M, Bar 2 (Avg. of Gages 9 and 10).

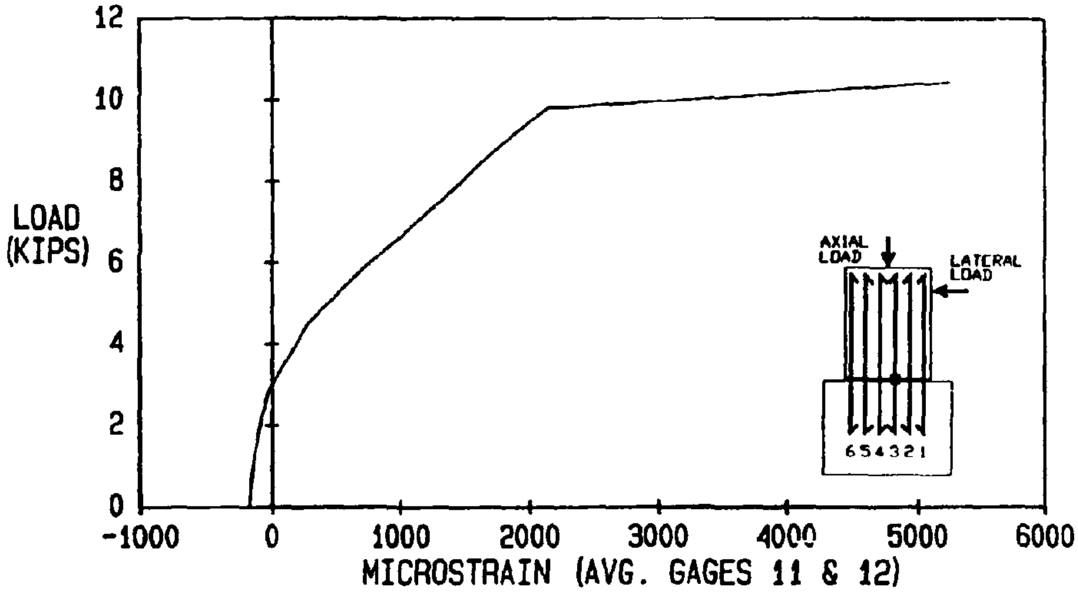

Figure 3-27. Load-Strain Diagram for SD2M, Bar 3 (Avg. of Gages 11 and 12).

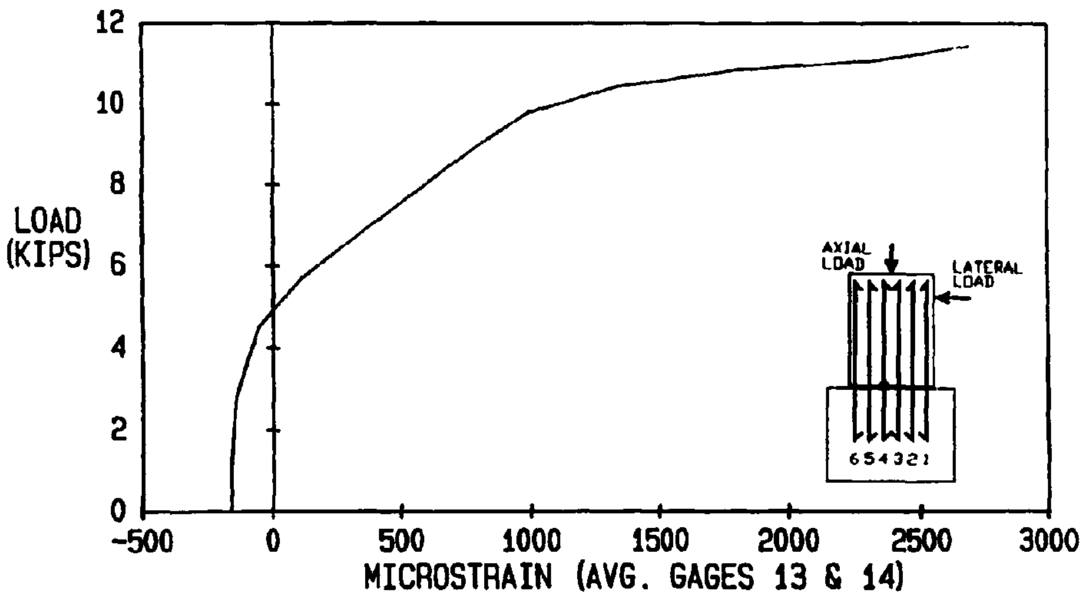

Figure 3-28. Load-Strain Diagram for SD2M, Bar 4 (Avg. of Gages 13 and 14).

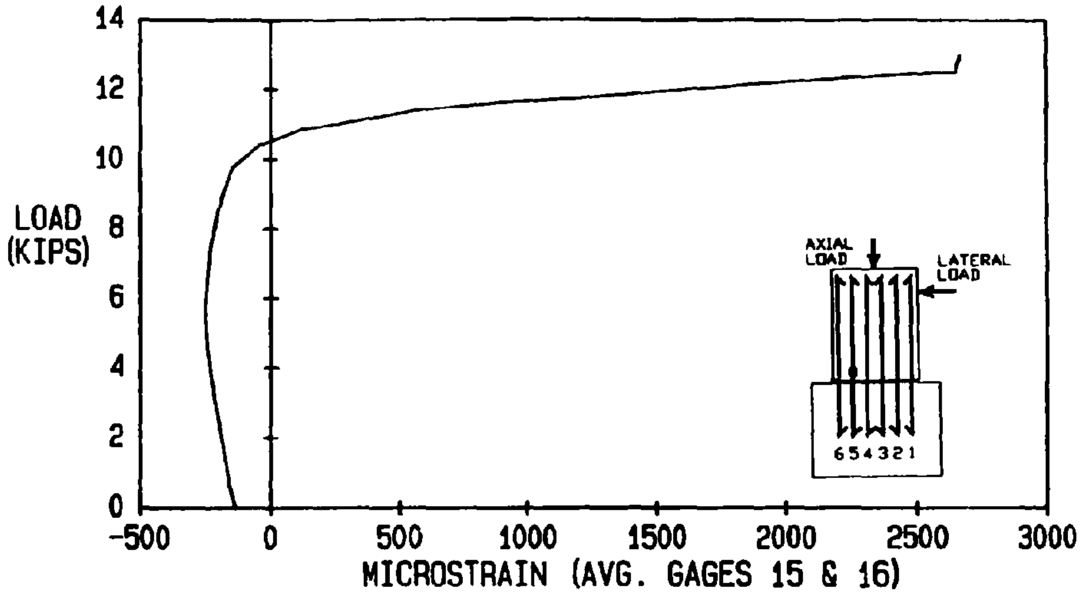

Figure 3-29. Load-Strain Diagram for SD2M, Bar 5 (Avg. of Gages 15 and 16).

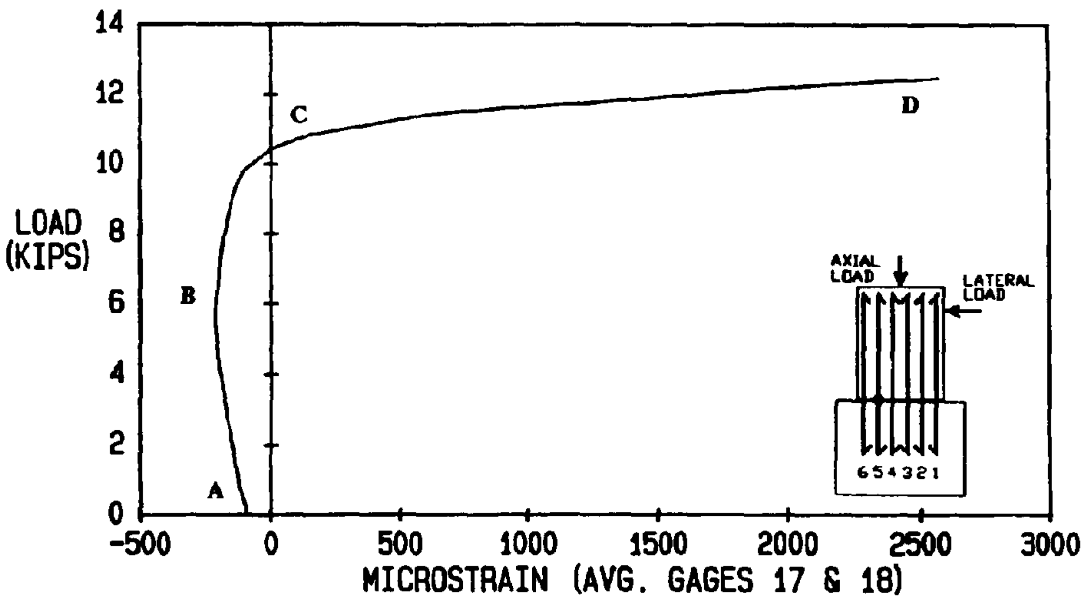

Figure 3-30. Load-Strain Diagram for SD2M, Bar 5 (Avg. of Gages 17 and 18).

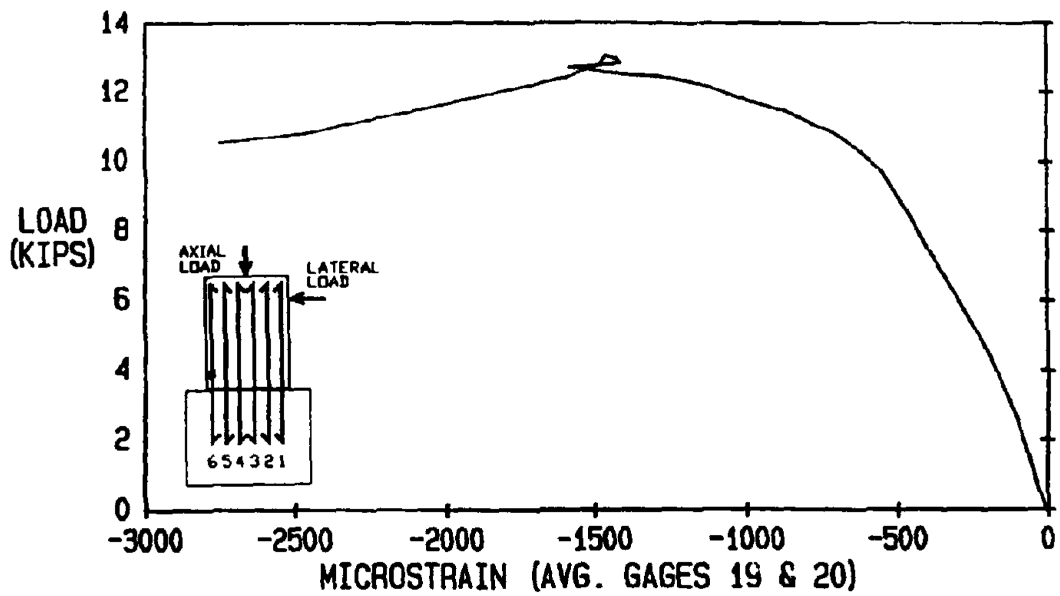

Figure 3-31. Load-Strain Diagram for SD2M, Bar 6 (Avg. of Gages 19 and 20).

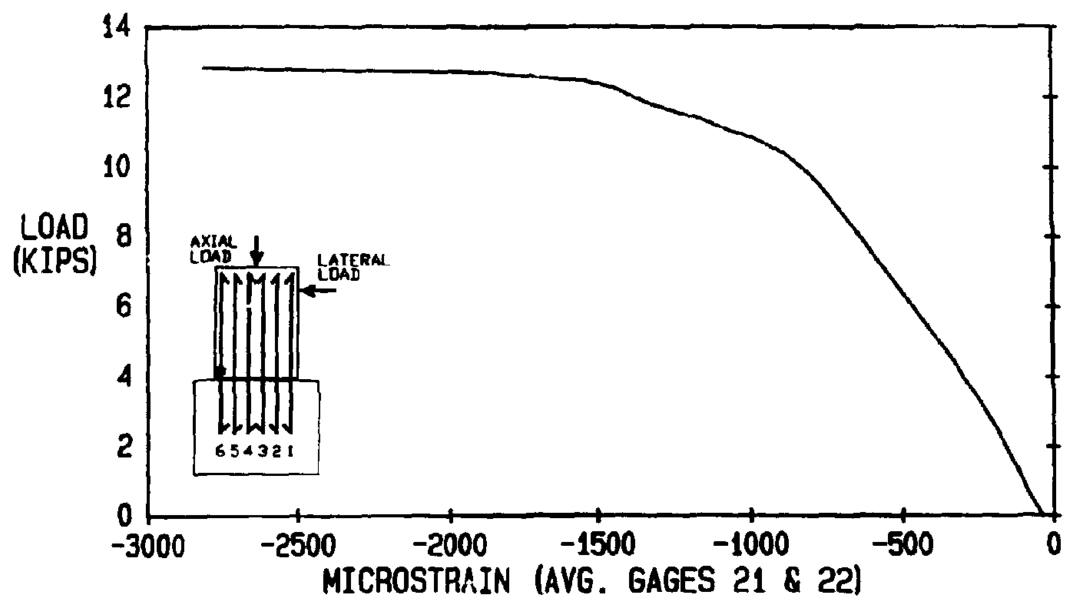

Figure 3-32. Load-Strain Diagram for SD2M, Bar 6 (Avg. of Gages 21 and 22).

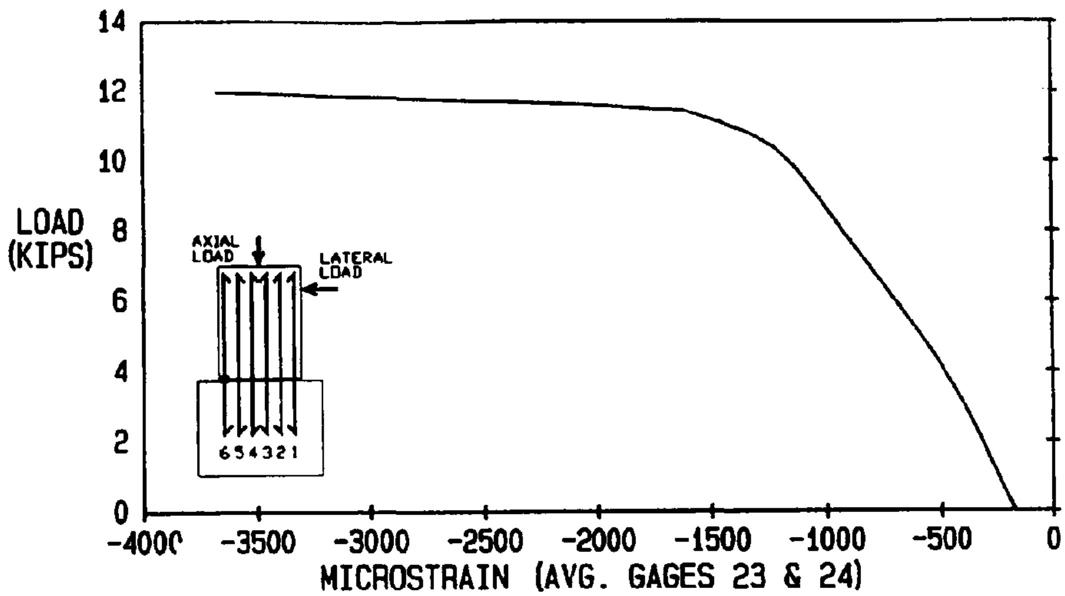

Figure 3-33. Load–Strain Diagram for SD2M, Bar 6 (Avg. of Gages 23 and 24).

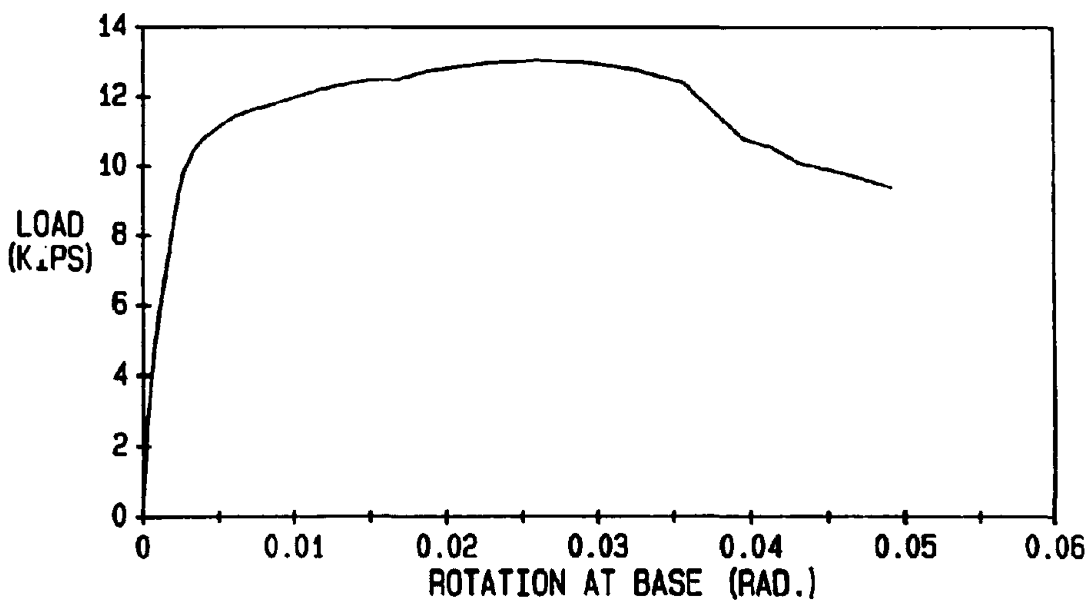

Figure 3-34. Load–Rotation Diagram for Specimen SD2M.

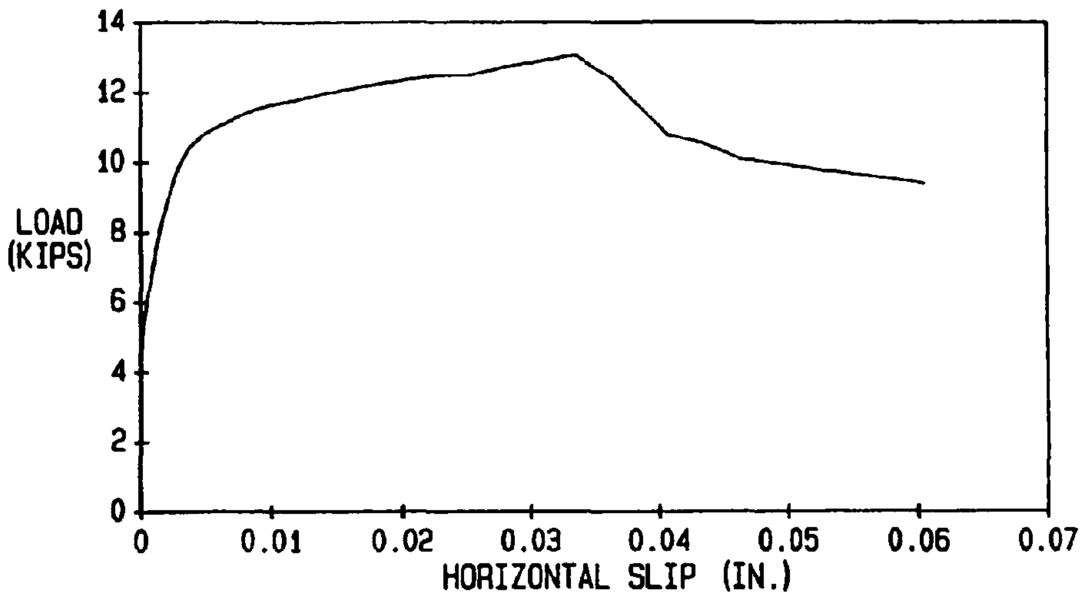

Figure 3-35. Load-Horizontal Slip Diagram for Specimen SD2M.

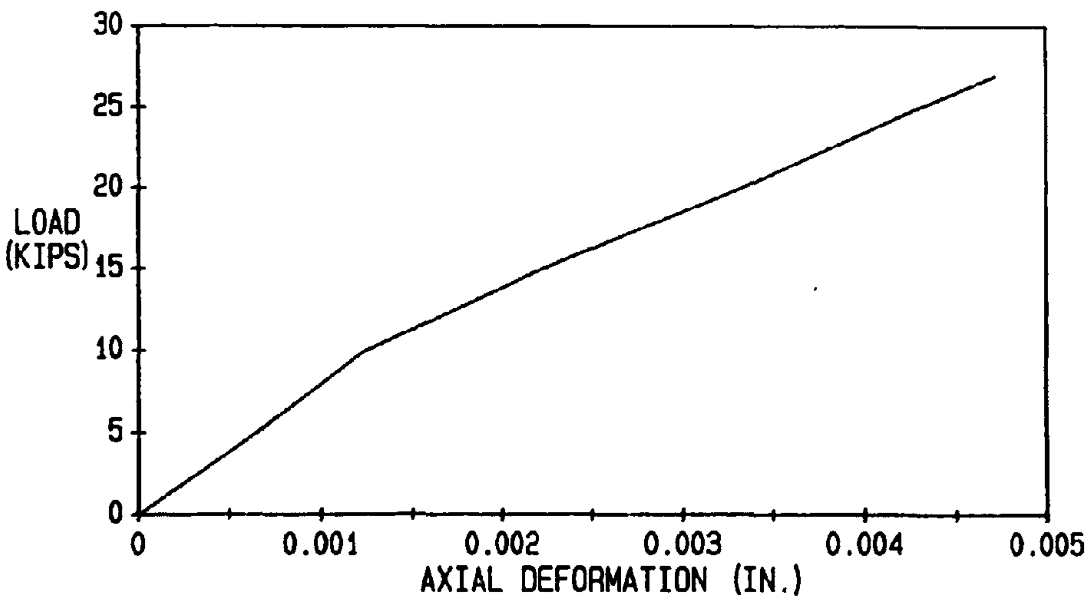

Figure 3-36. Axial Load-Deformation Diagram for Specimen SD2M.

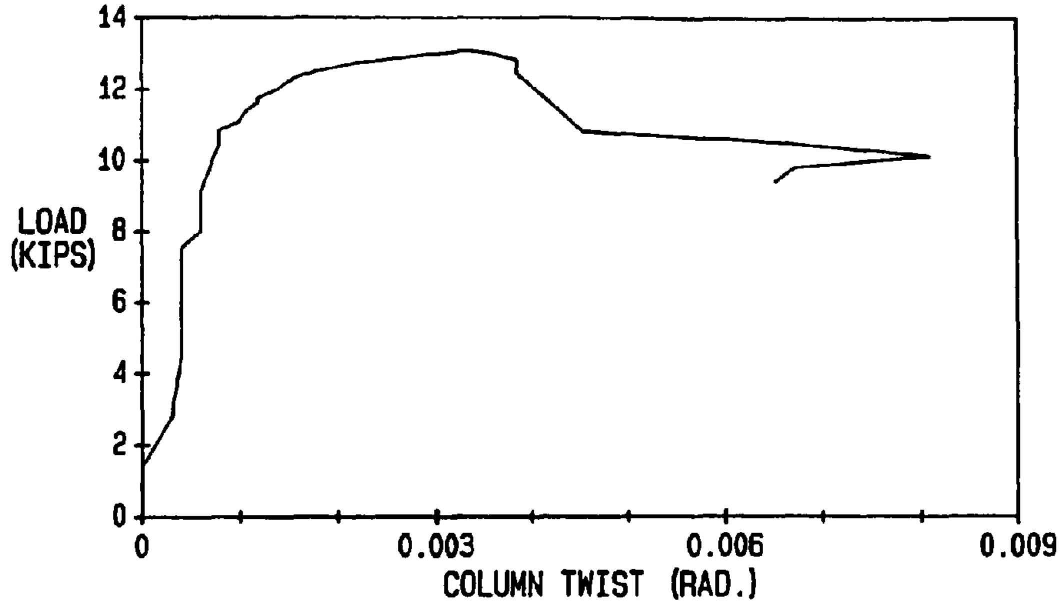

Figure 3-37. Load-Column Twist Diagram for Specimen SD2M.

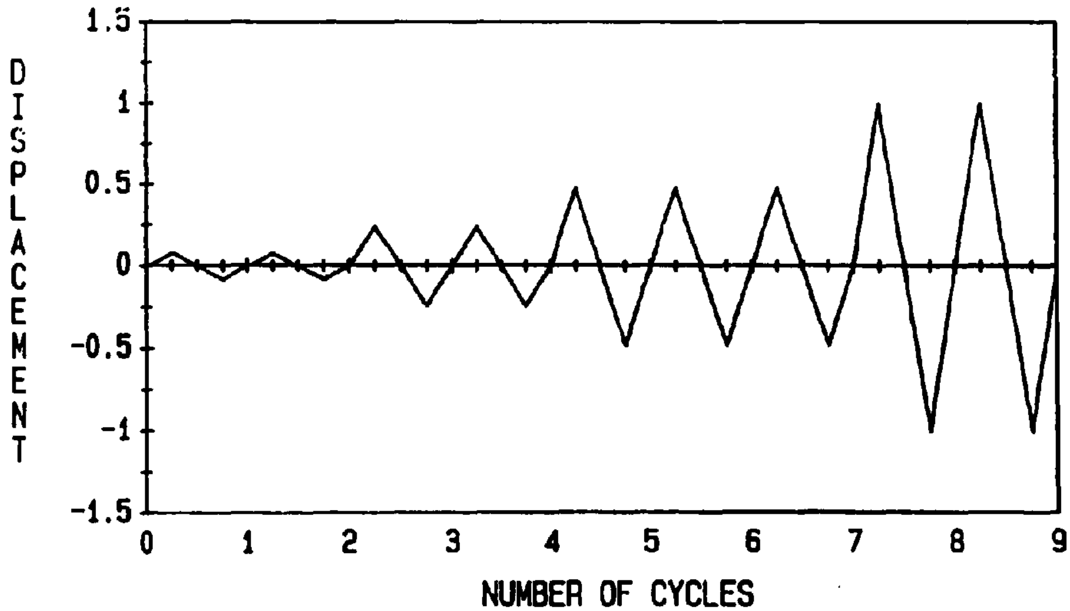

Figure 3-38. Cyclic Loading for Test Specimen SD1C.

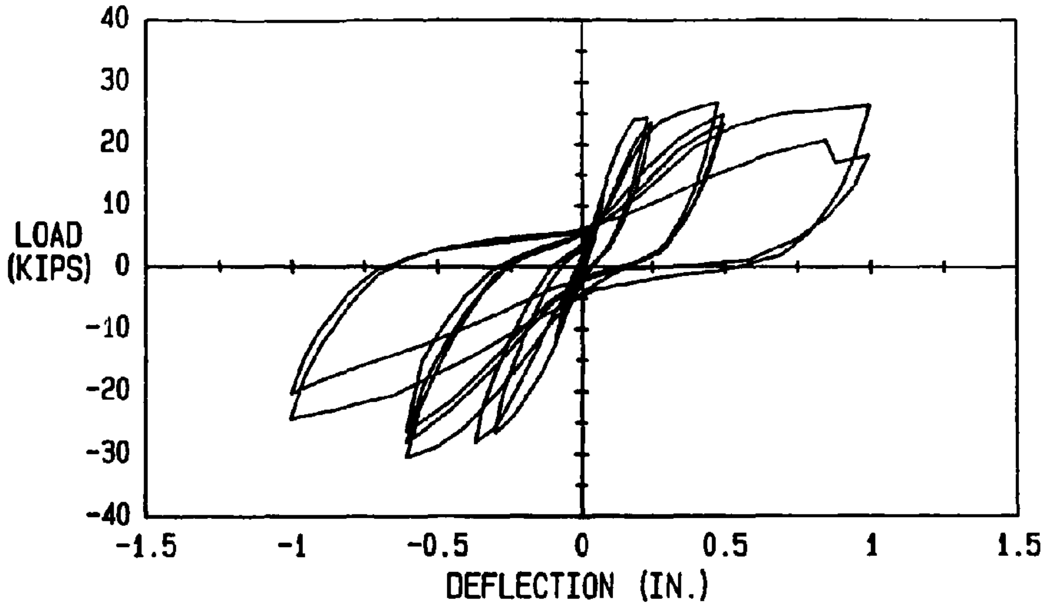

Figure 3-39. Load-Deflection Diagram for Specimen SD1C.

Figure 3-40. Cracking Pattern of Specimen SD1C.

Figure 3-41. Failure of SD1C Bar Number 1 in Tension.

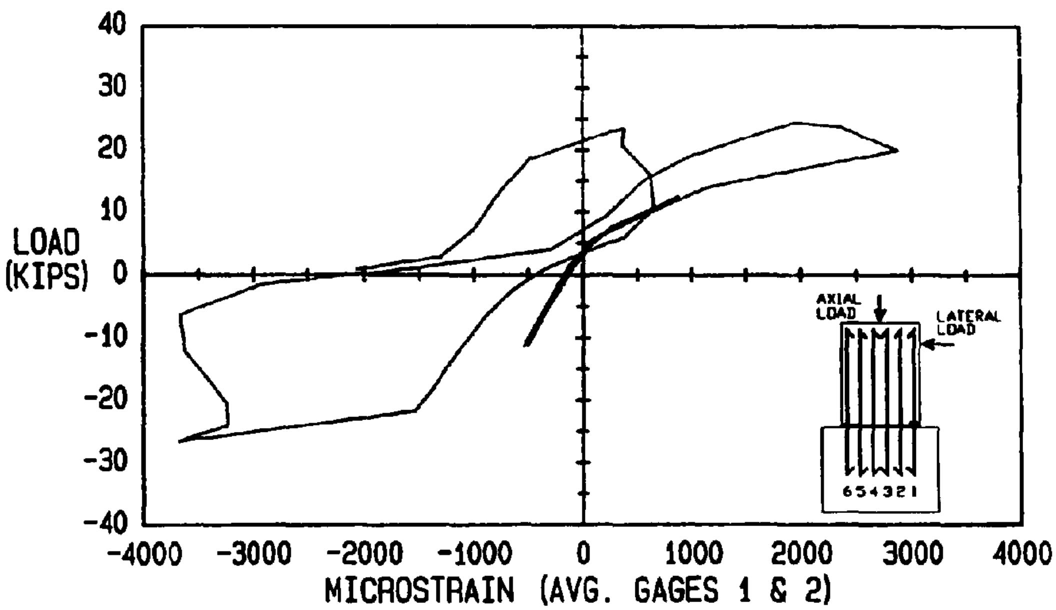

Figure 3-42. Load-Strain Diagram for SD1C, Bar 1 (Avg. of Gages 1 and 2).

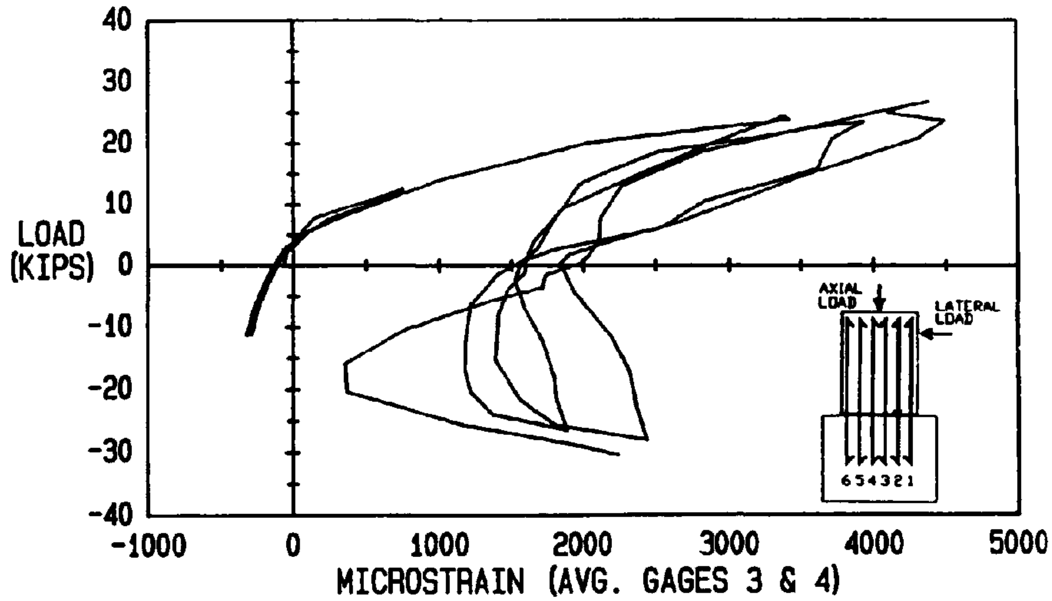

Figure 3-43. Load-Strain Diagram for SD1C, Bar 2 (Avg. of Gages 3 and 4).

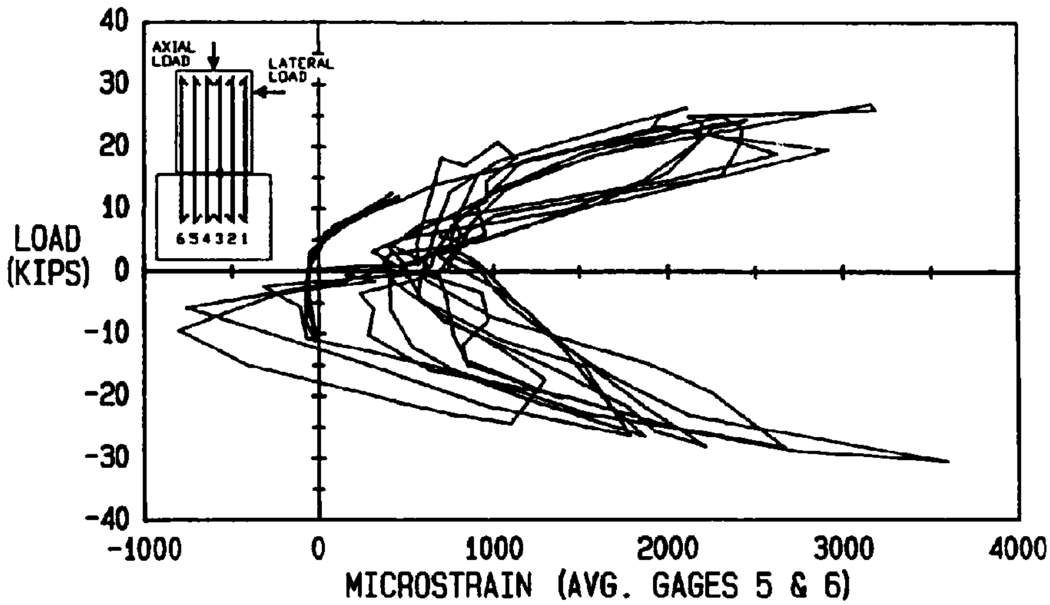

Figure 3-44. Load-Strain Diagram for SD1C, Bar 3 (Avg. of Gages 5 and 6).

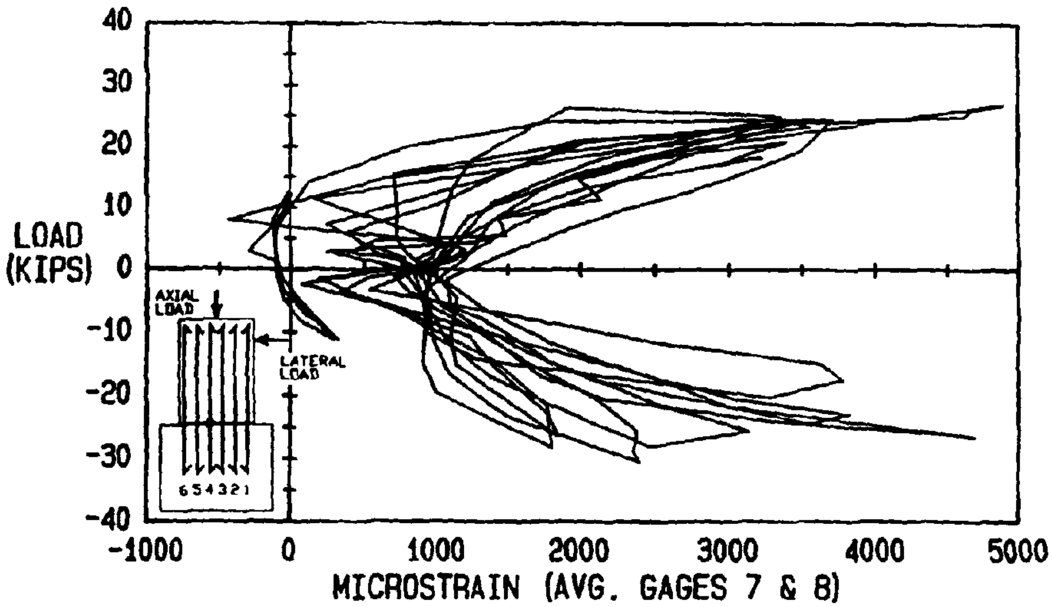

Figure 3-45. Load-Strain Diagram for SD1C, Bar 4 (Avg. of Gages 7 and 8).

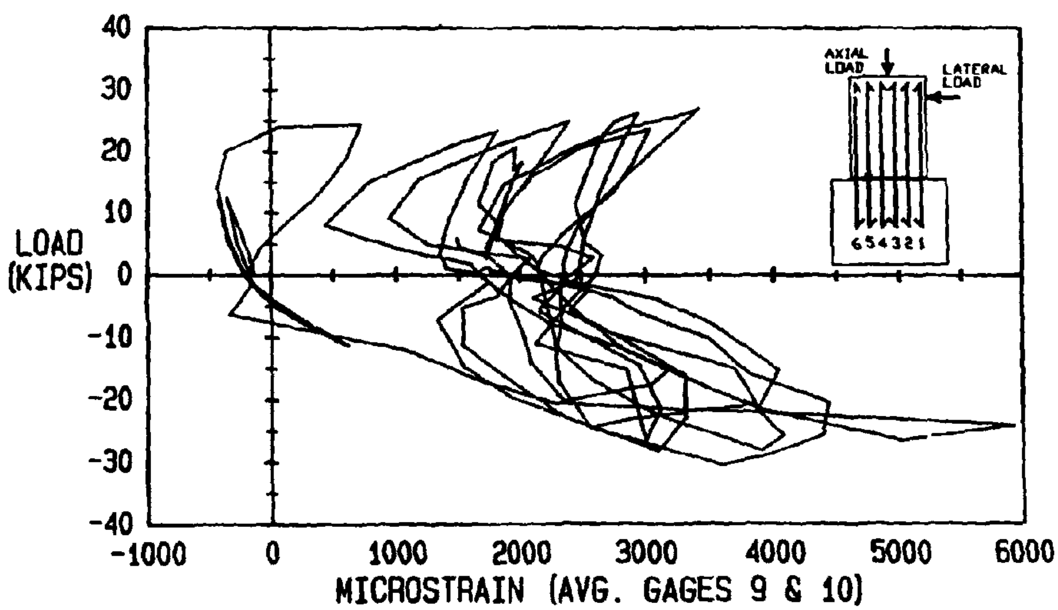

Figure 3-46. Load-Strain Diagram for SD1C, Bar 5 (Avg. of Gages 9 and 10).

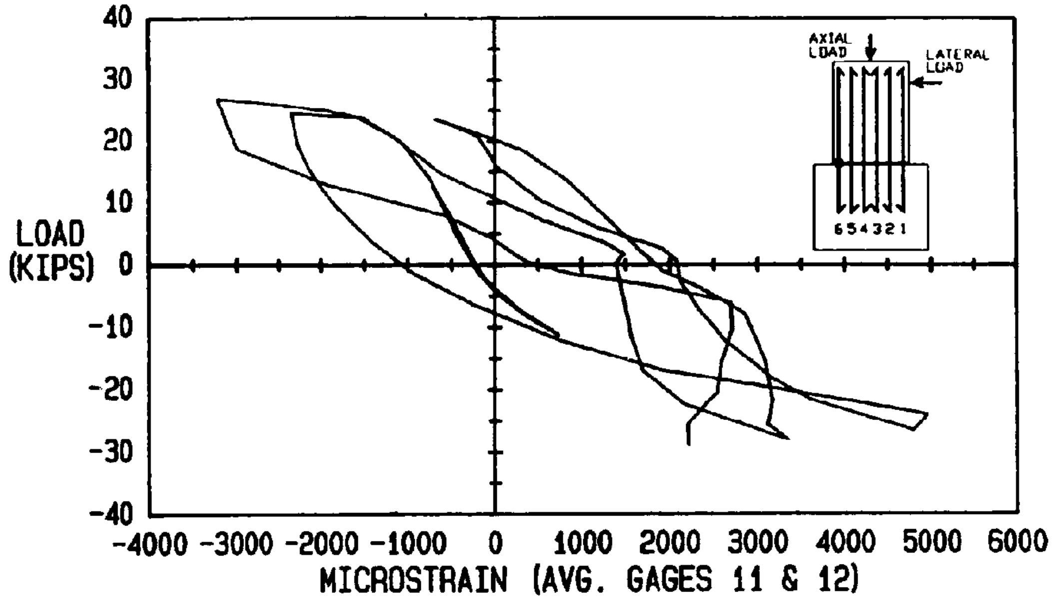

Figure 3-47. Load-Strain Diagram for SD1C, Bar 6 (Avg. of Gages 11 and 12).

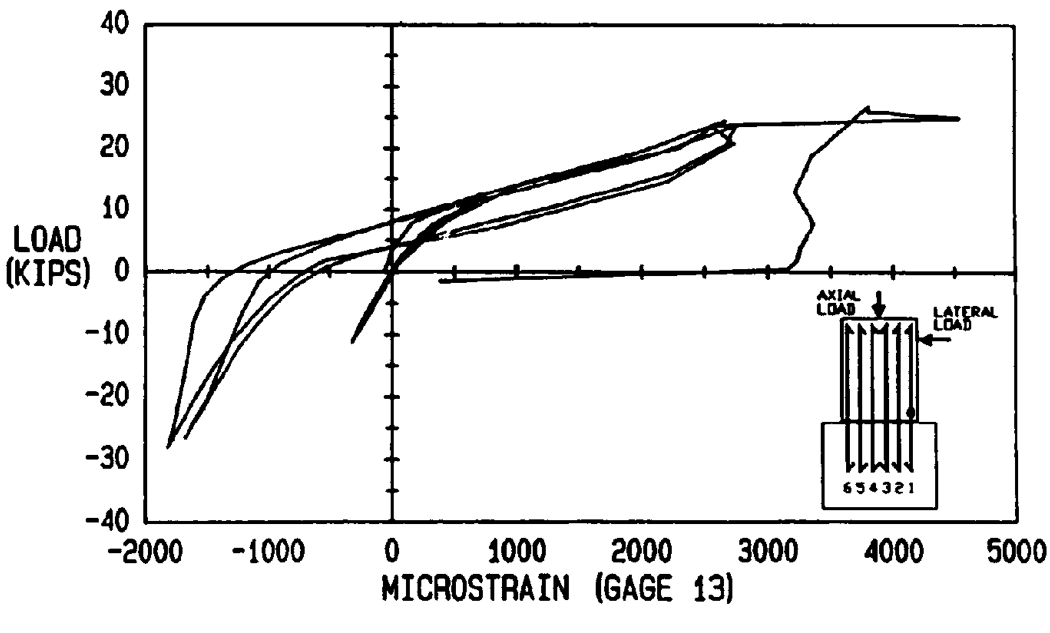

Figure 3-48. Load-Strain Diagram for SD1C, Bar 1 (Gage 13).

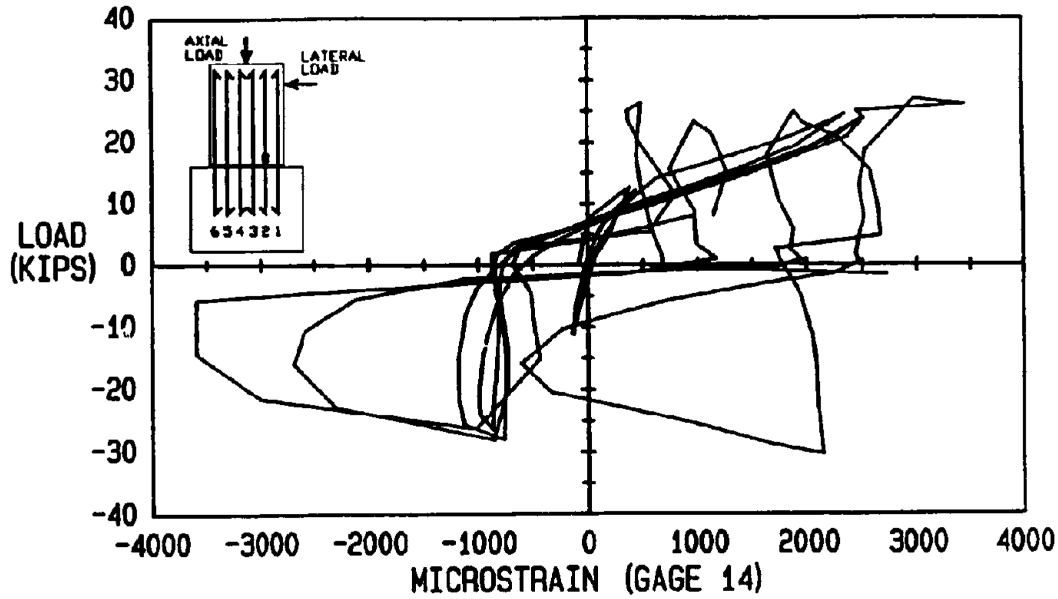

Figure 3-49. Load-Strain Diagram for SD1C, Bar 2 (Gage 14).

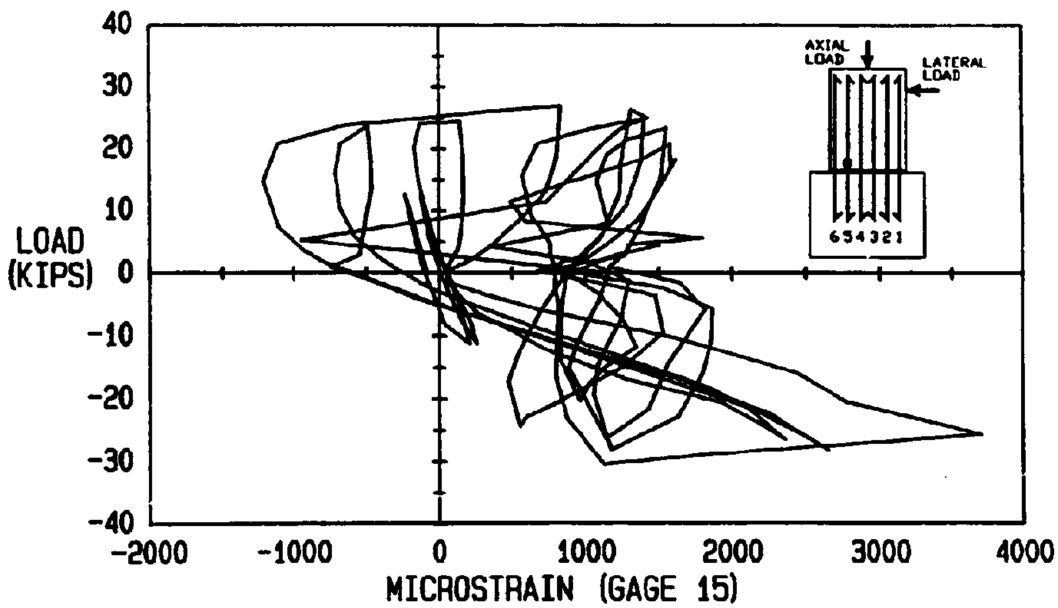

Figure 3-50. Load-Strain Diagram for SD1C, Bar 3 (Gage 15).

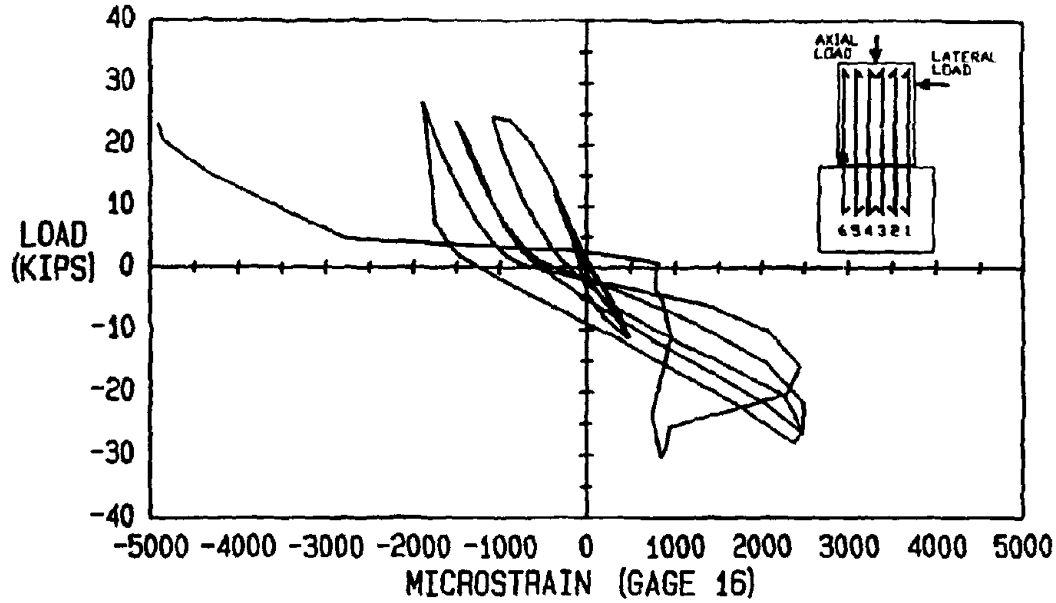

Figure 3-51. Load-Strain Diagram for SD1C, Bar 4 (Gage 16).

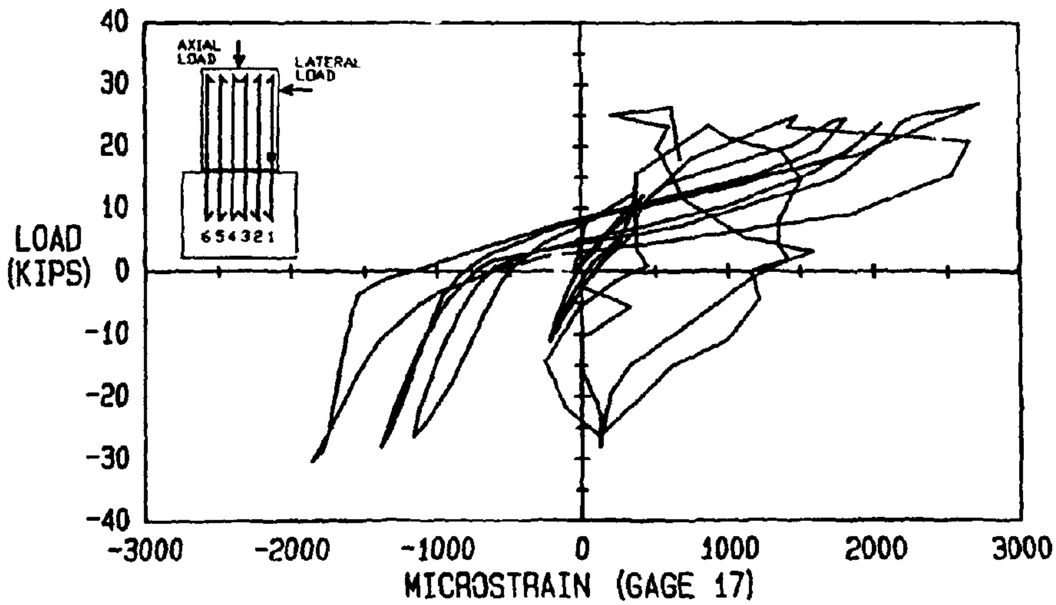

Figure 3-52. Load-Strain Diagram for SD1C, Bar 5 (Gage 17).

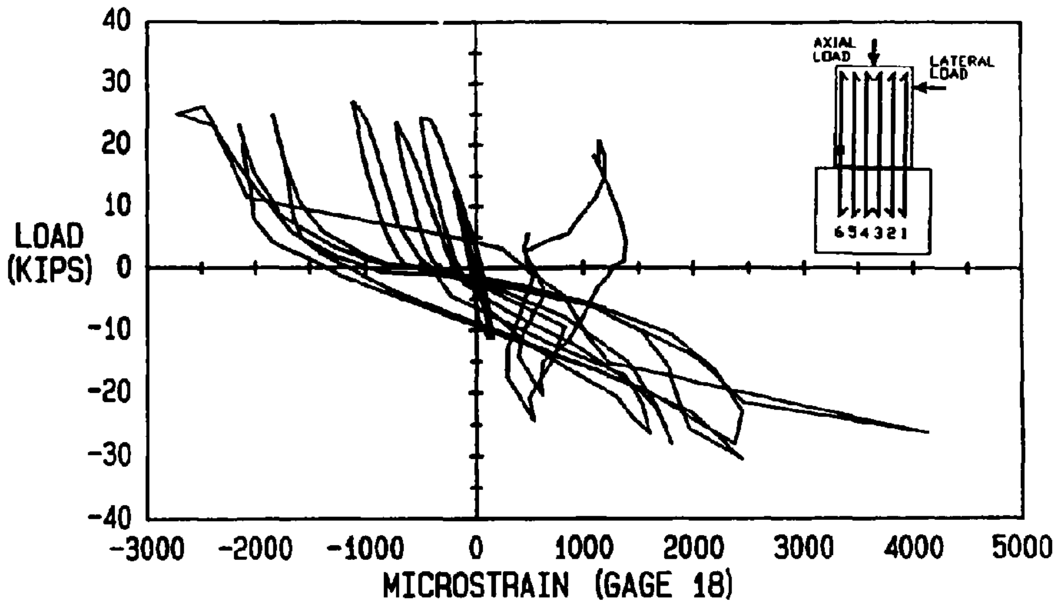

Figure 3-53. Load-Strain Diagram for SD1C, Bar 6 (Gage 18).

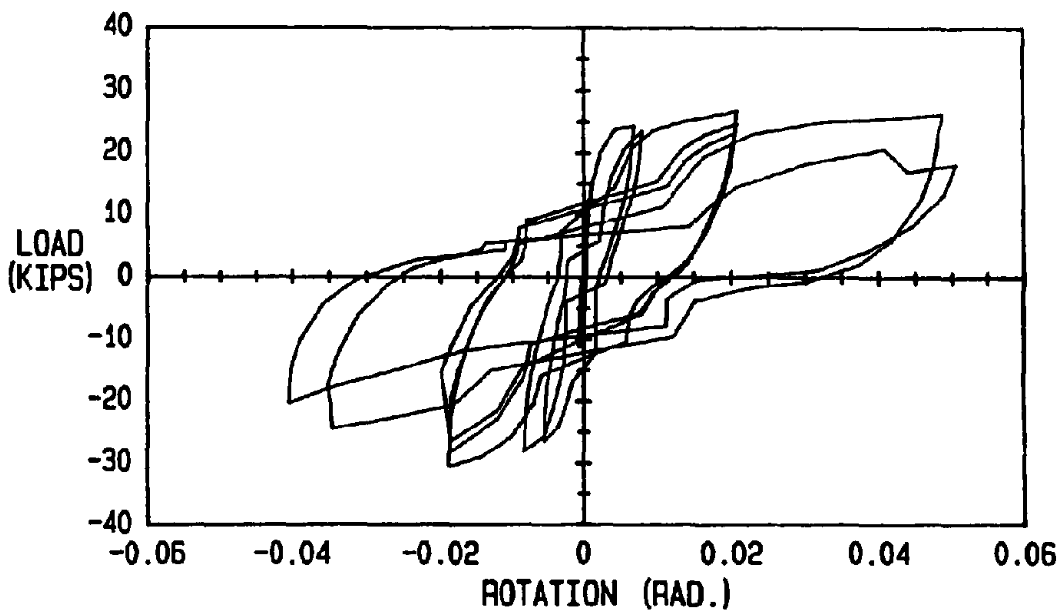

Figure 3-54. Load-Rotation Diagram for Specimen SD1C.

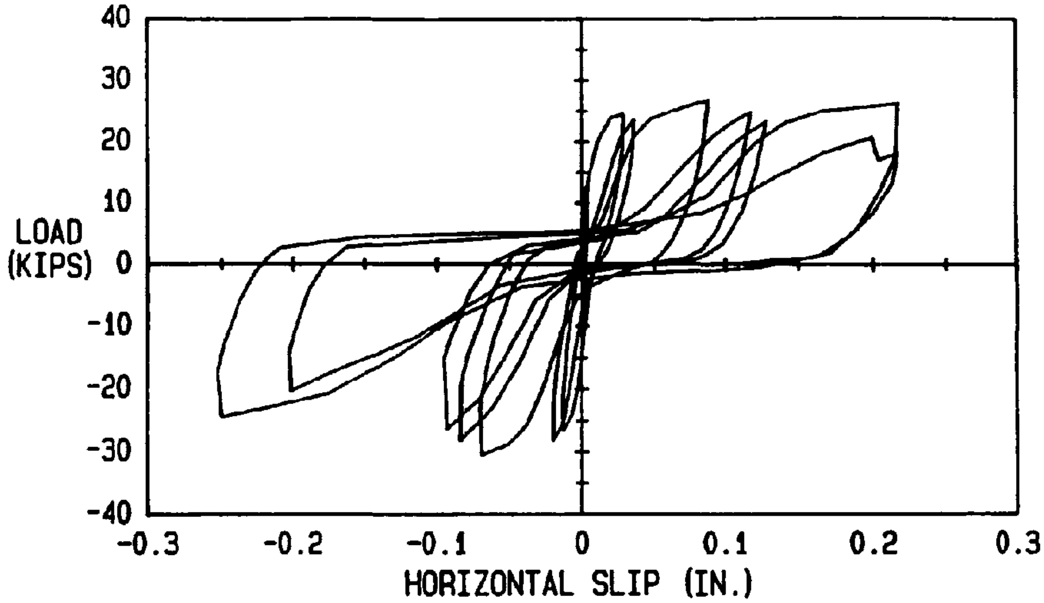

Figure 3-55. Load-Horizontal Slip Diagram for Specimen SD1C.

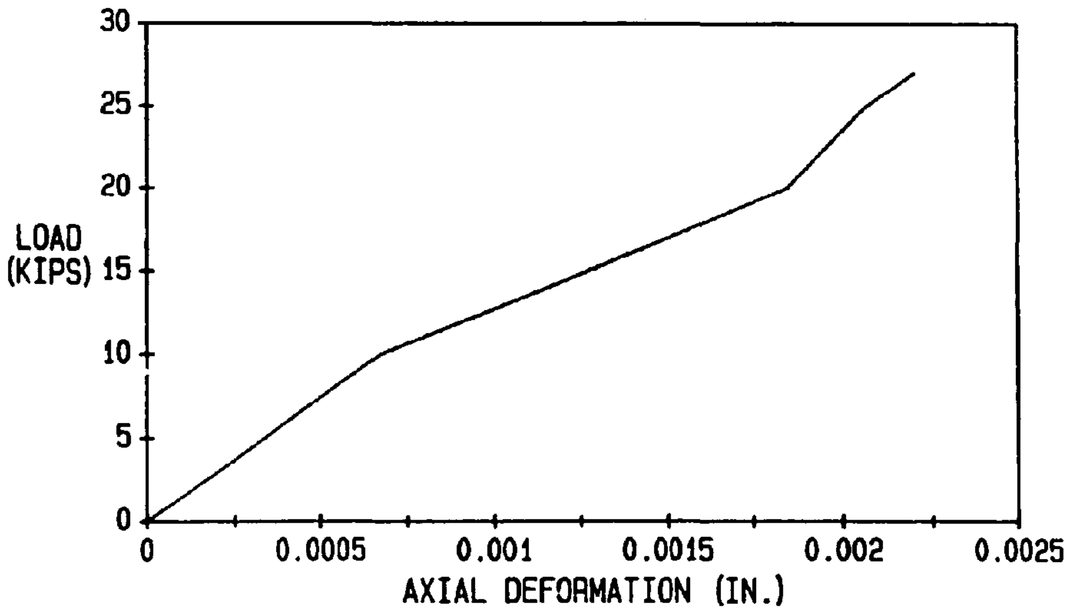

Figure 3-56. Axial Load-Deformation Diagram for Specimen SD1C.

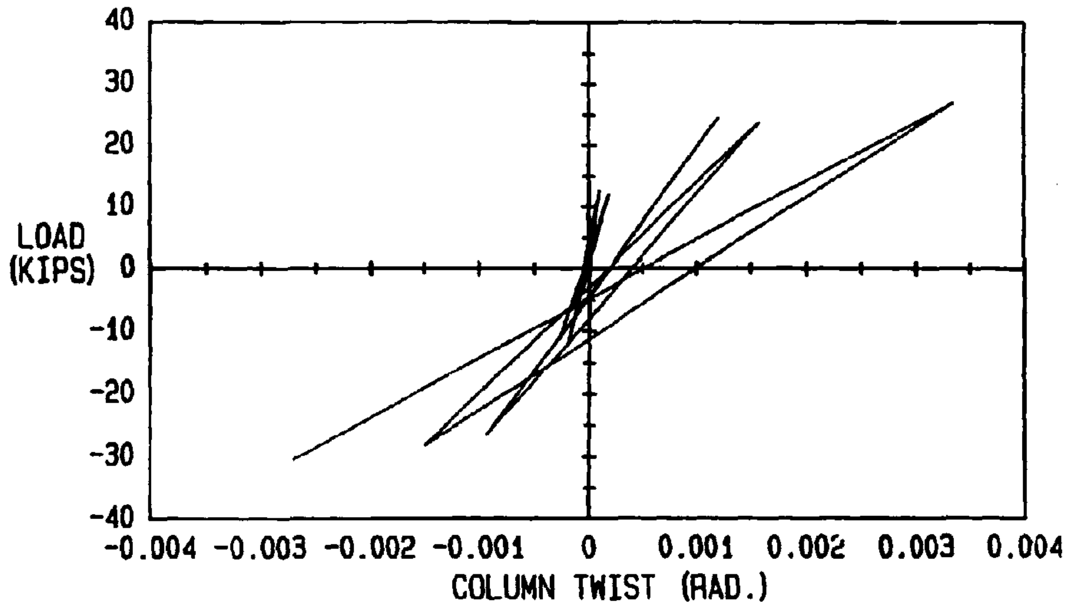

Figure 3-57. Load-Column Twist Diagram for Specimen SD1C.

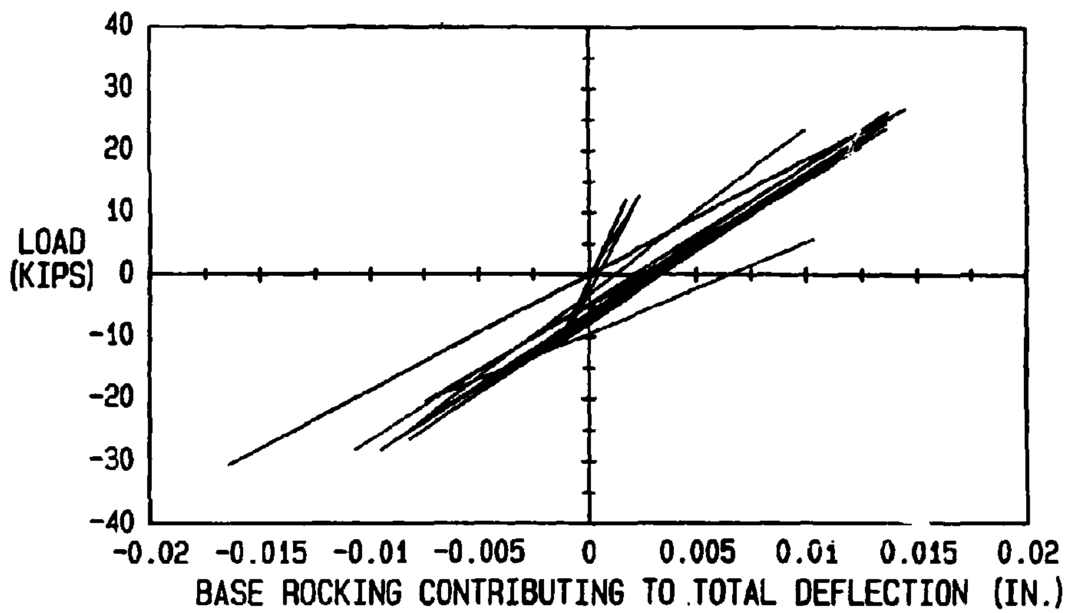

Figure 3-58. Load-Base Rotation Contributing to Total Deflection for SD1C.

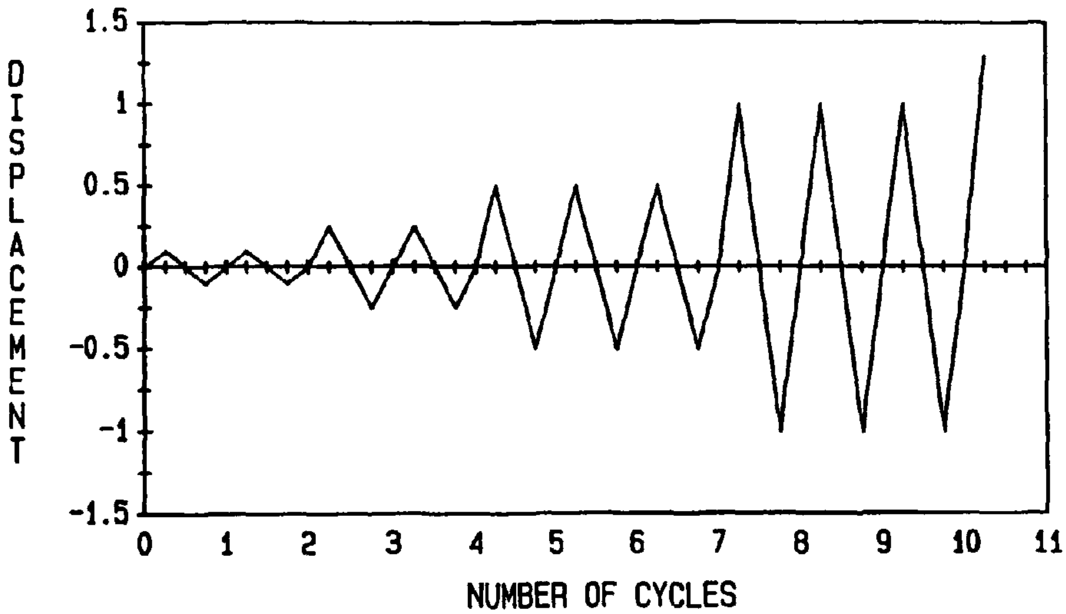

Figure 3-59. Cyclic Loading for Test Specimen SD2C.

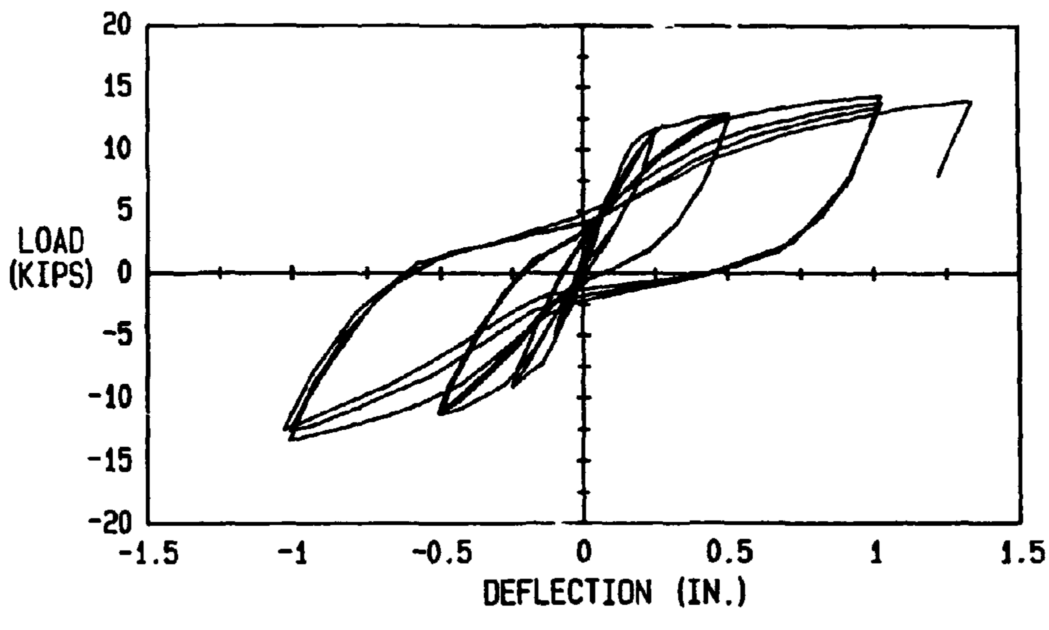

Figure 3-60. Load-Deflection Diagram for Specimen SD2C.

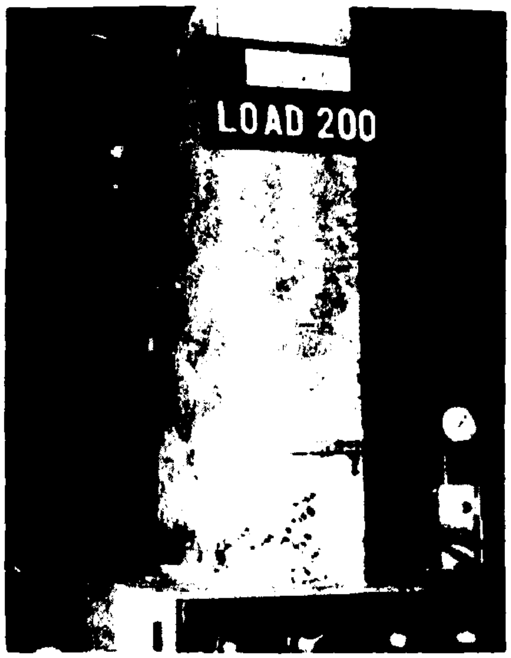

Figure 3-61. Cracking Pattern of Specimen SD2C.

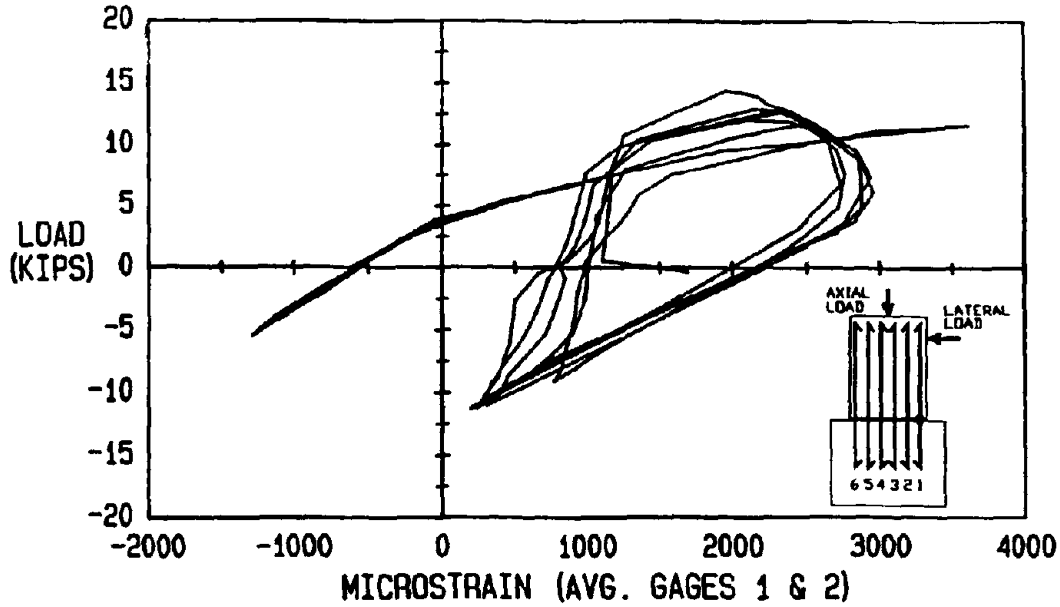

Figure 3-62. Load-Strain Diagram for SD2C, Bar 1 (Avg. of Gages 1 and 2).

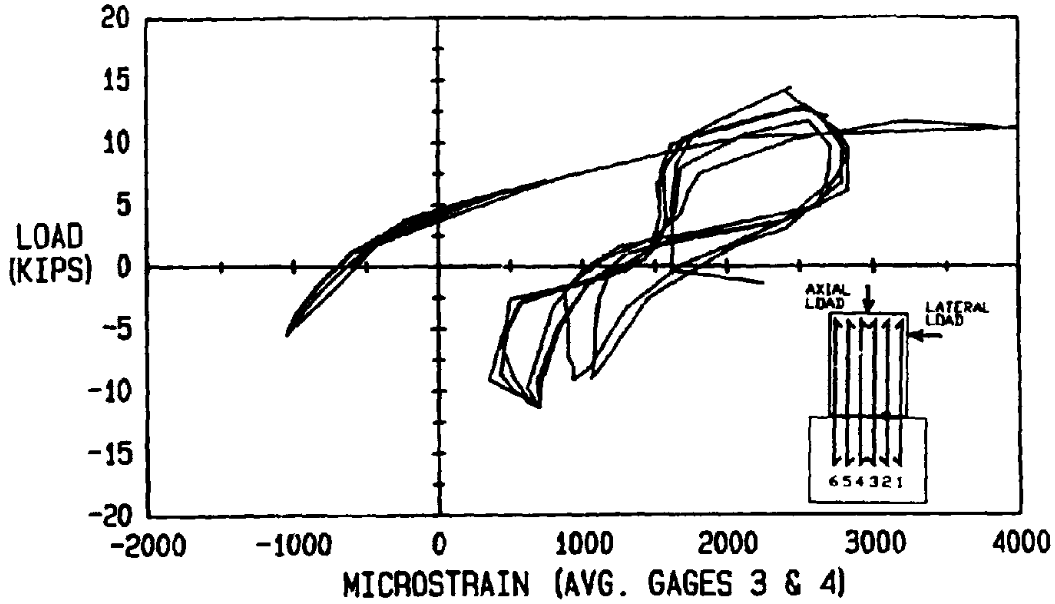

Figure 3-63. Load-Strain Diagram for SD2C, Bar 2 (Avg. of Gages 3 and 4).

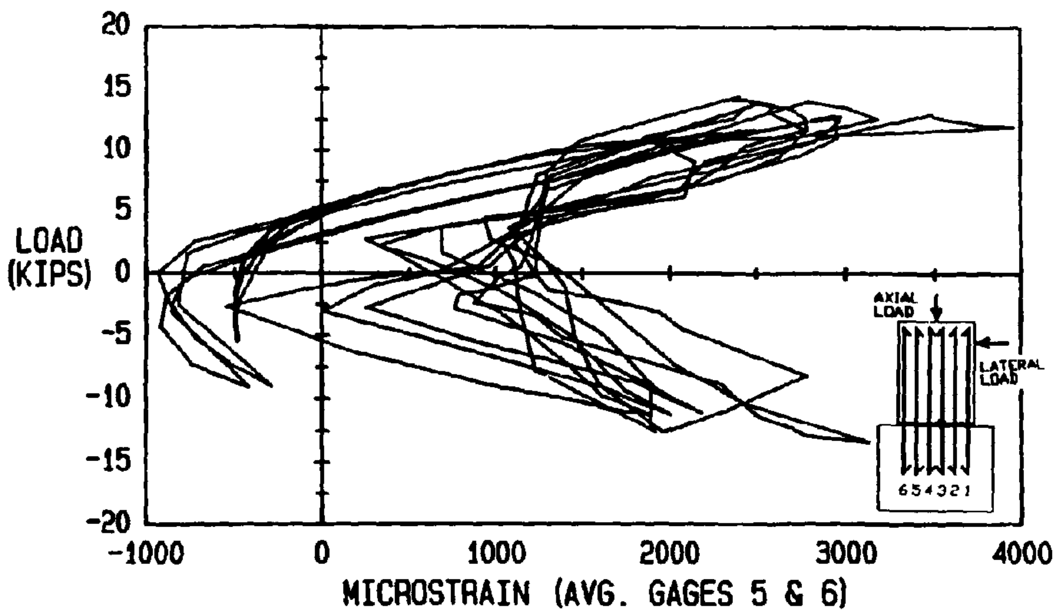

Figure 3-64. Load-Strain Diagram for SD2C, Bar 3 (Avg. of Gages 5 and 6).

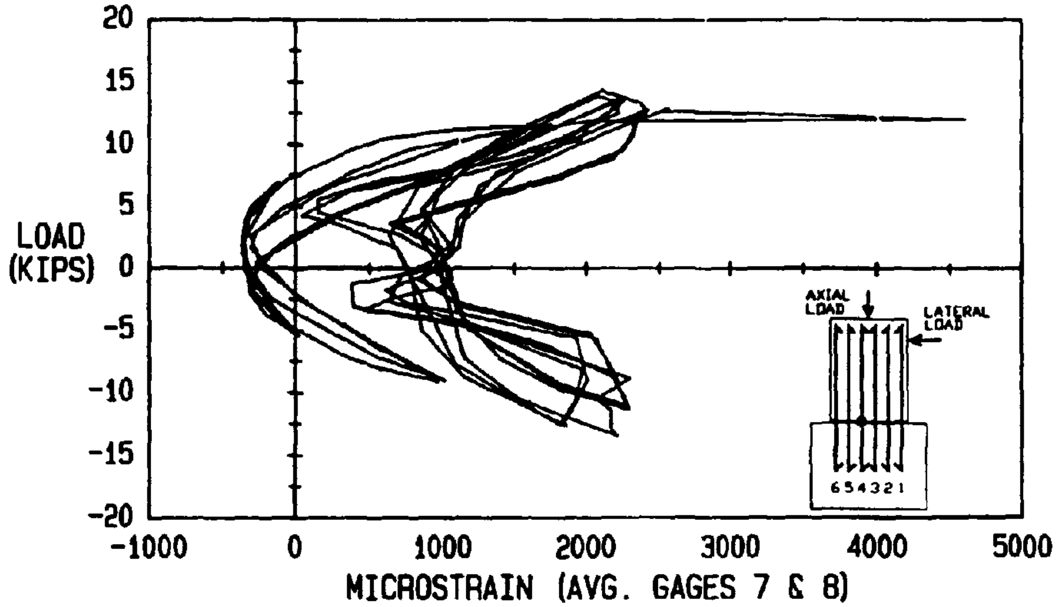

Figure 3-65. Load-Strain Diagram for SD2C, Bar 4 (Avg. of Gages 7 and 8).

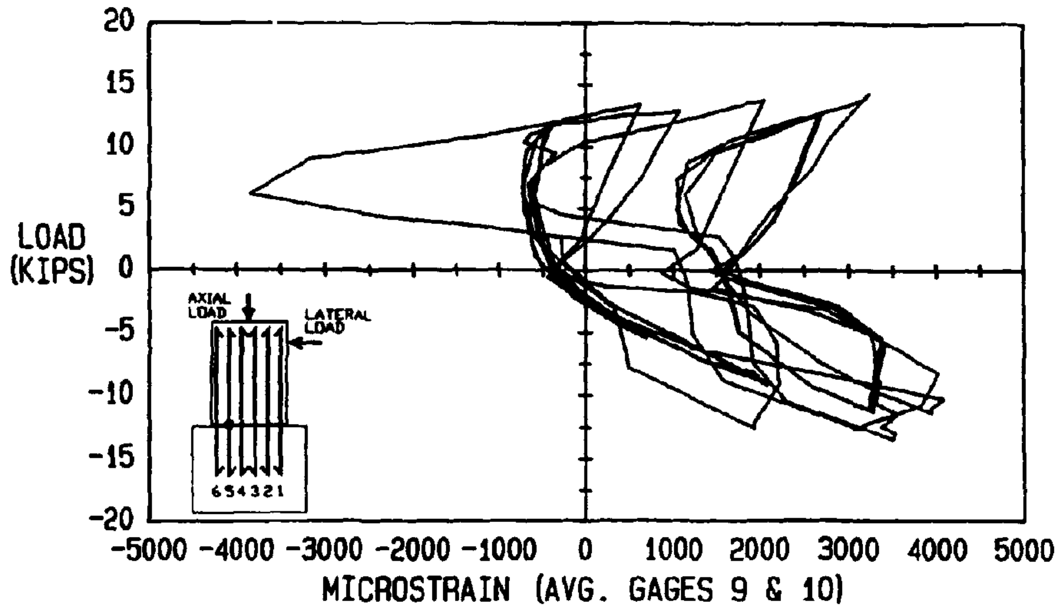

Figure 3-66. Load-Strain Diagram for SD2C, Bar 5 (Avg. of Gages 9 and 10).

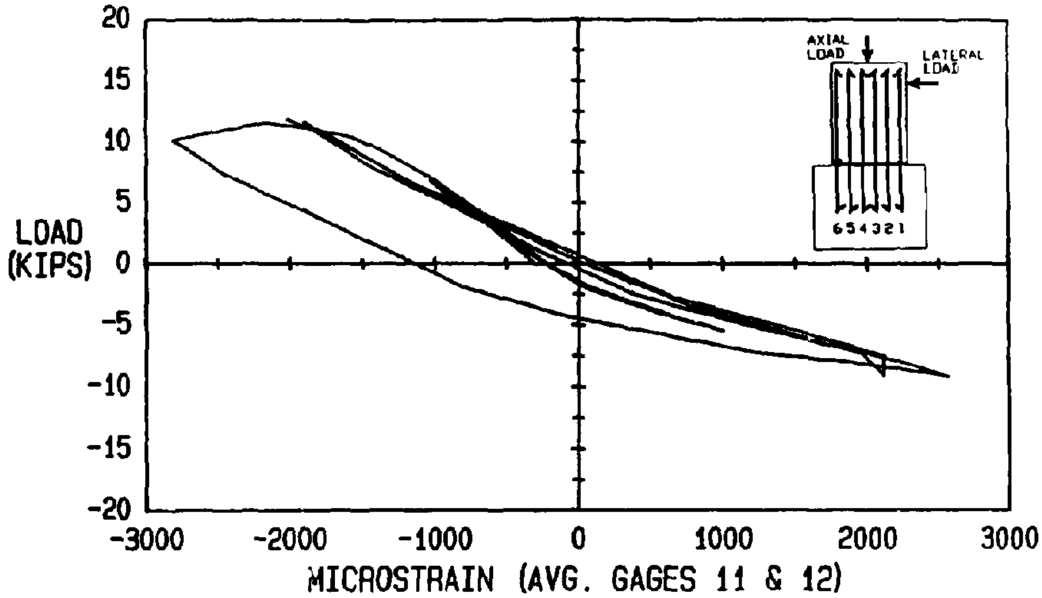

Figure 3-67. Load-Strain Diagram for SD2C, Bar 6 (Avg. of Gages 11 and 12).

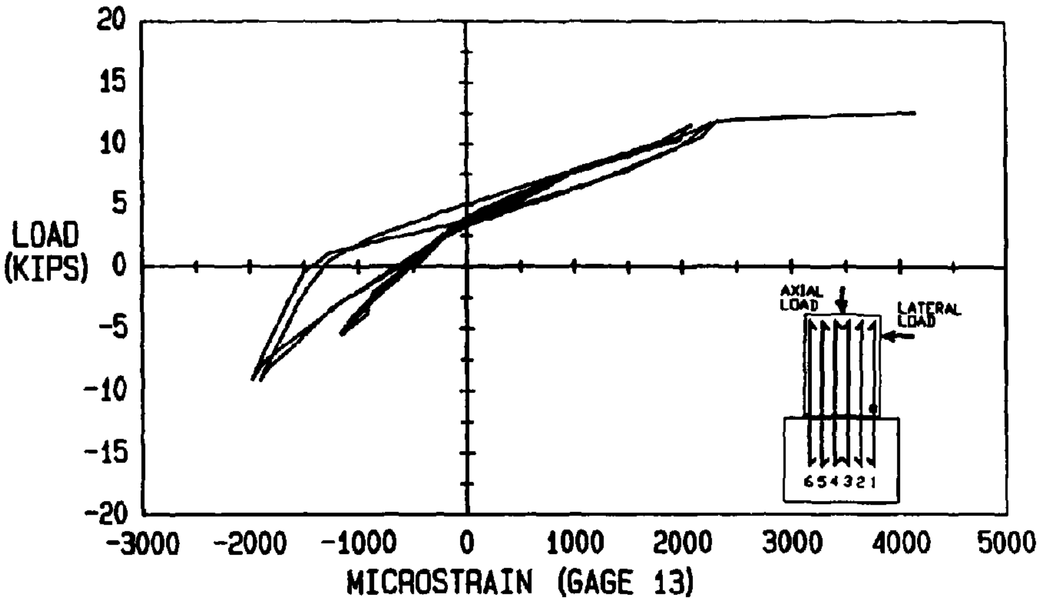

Figure 3-68. Load-Strain Diagram for SD2C, Bar 1 (Gage 13).

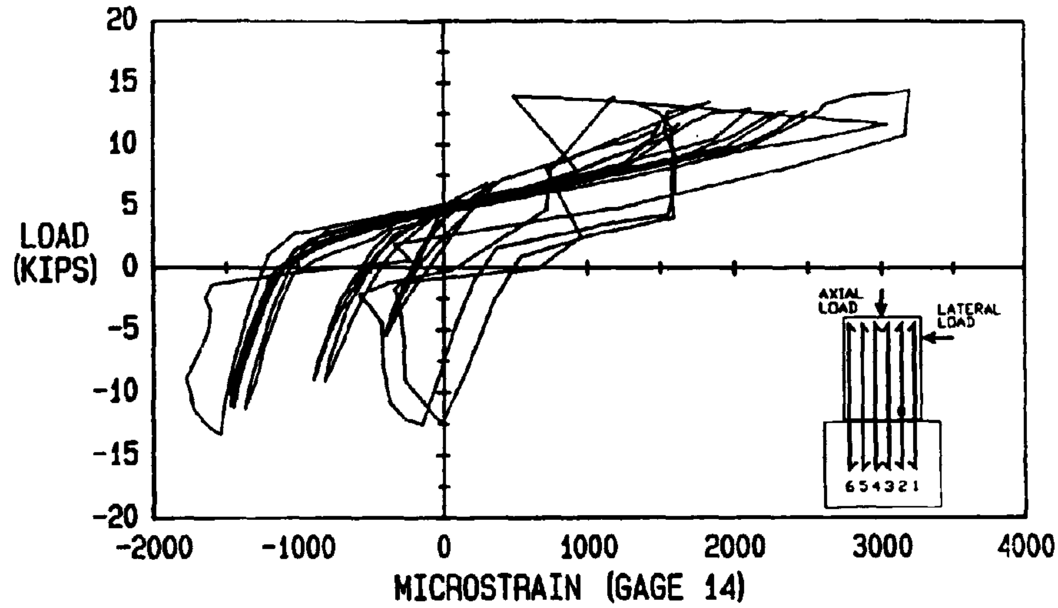

Figure 3-69. Load-Strain Diagram for SD2C, Bar 2 (Gage 14).

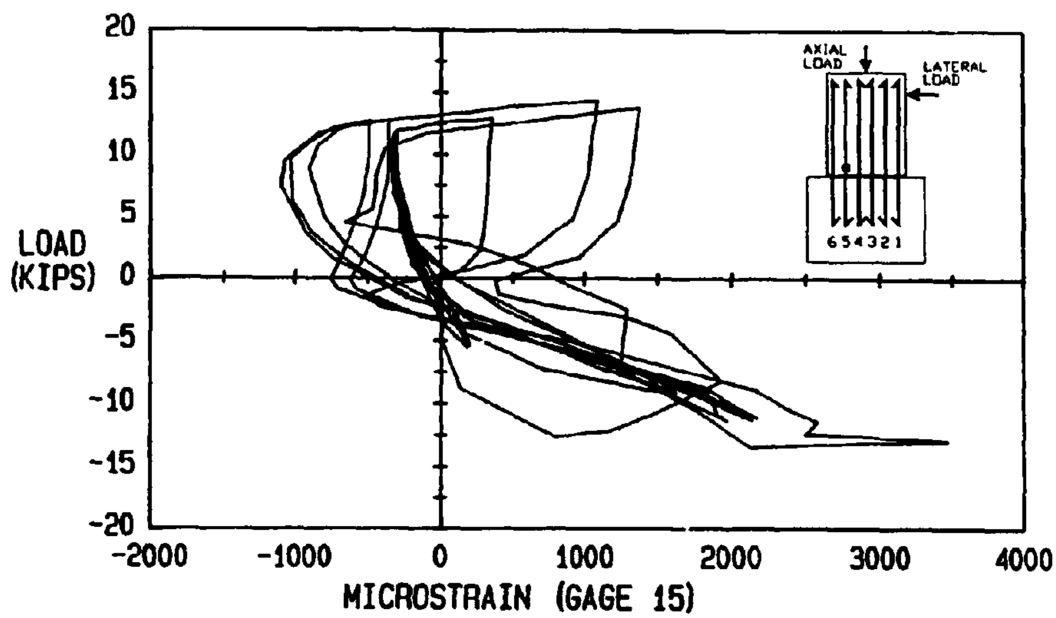

Figure 3-70. Load-Strain Diagram for SD2C, Bar 3 (Gage 15).

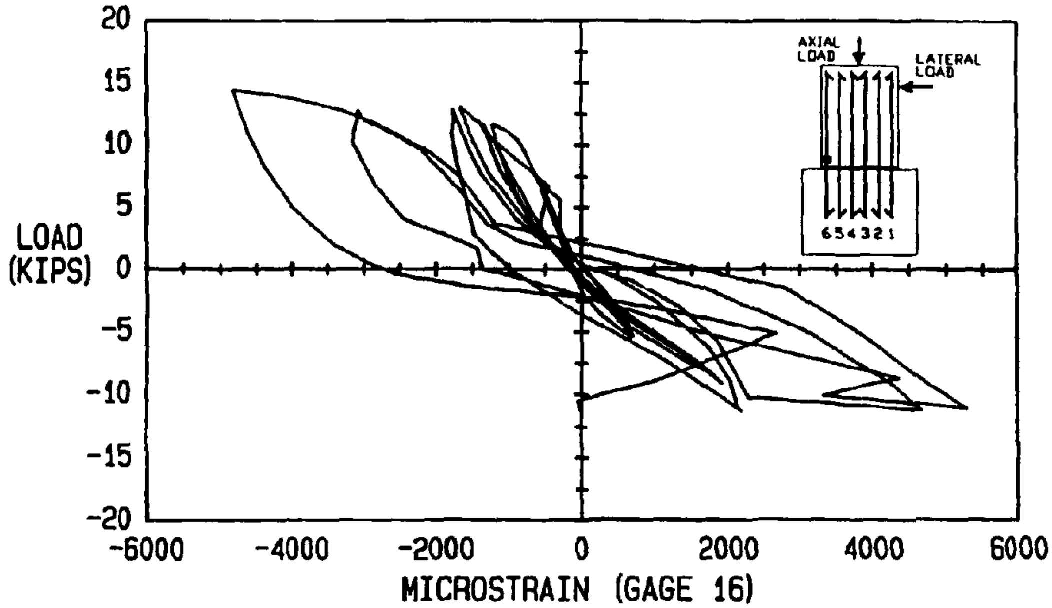

Figure 3-71. Load-Strain Diagram for SD2C, Bar 4 (Gage 16).

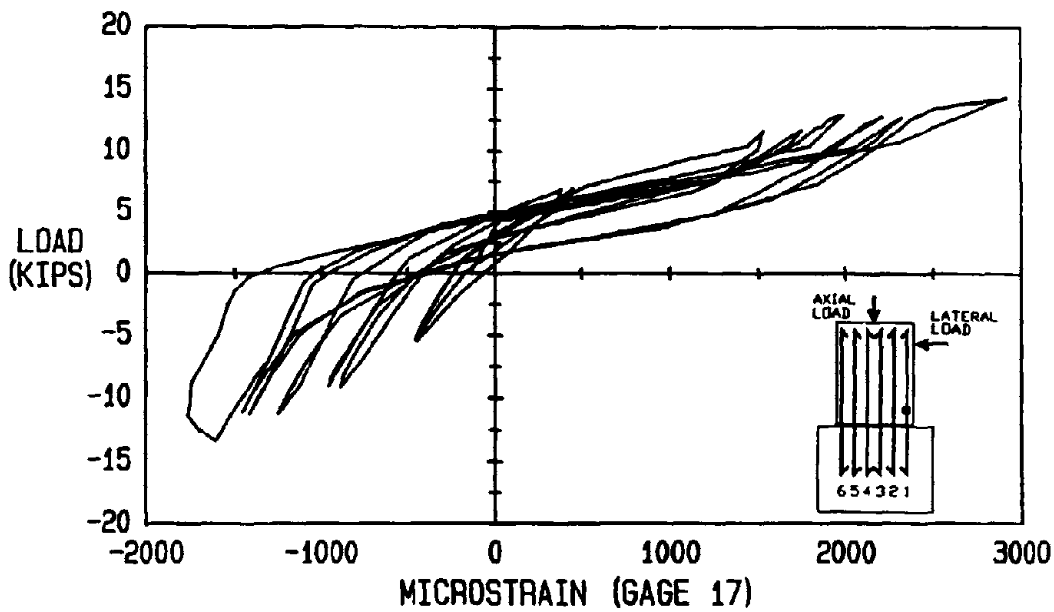

Figure 3-72. Load-Strain Diagram for SD2C, Bar 5 (Gage 17).

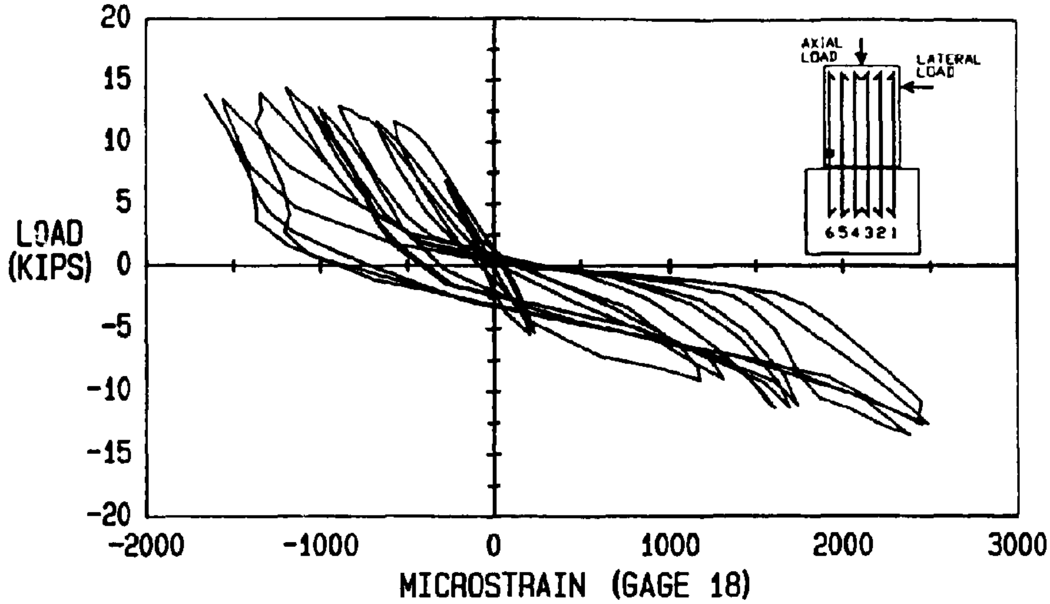

Figure 3-73. Load-Strain Diagram for SD2C, Bar 6 (Gage 18).

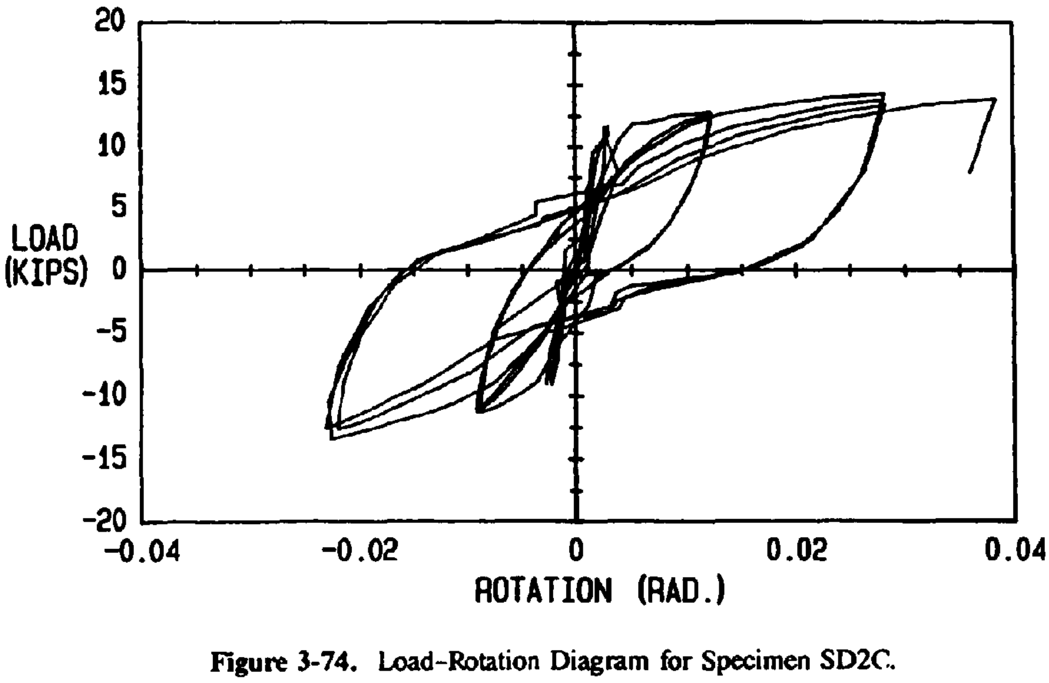

Figure 3-74. Load-Rotation Diagram for Specimen SD2C.

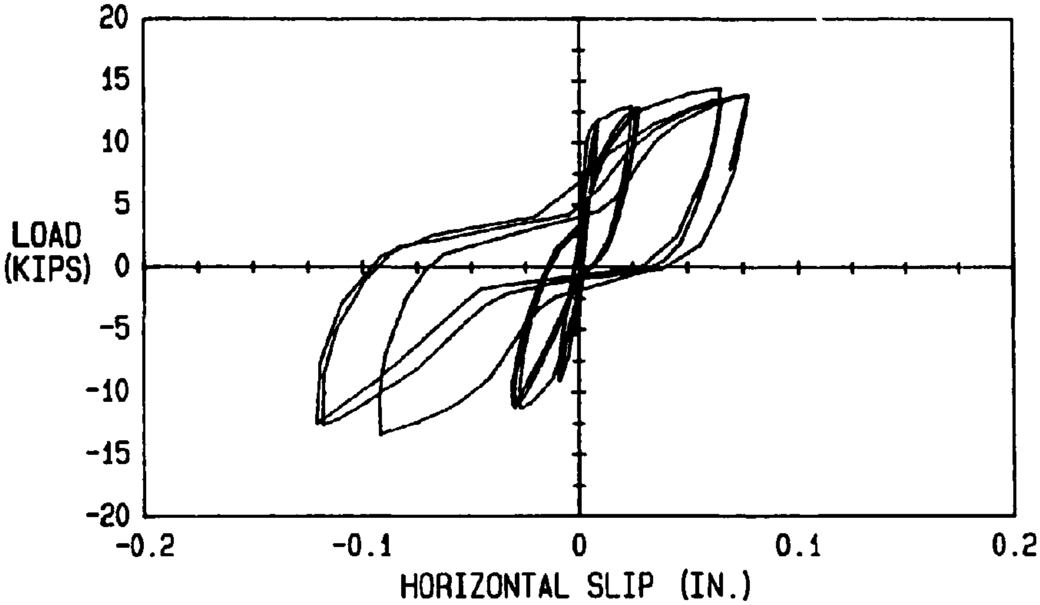

Figure 3-75. Load-Horizontal Slip Diagram for Specimen SD2C.

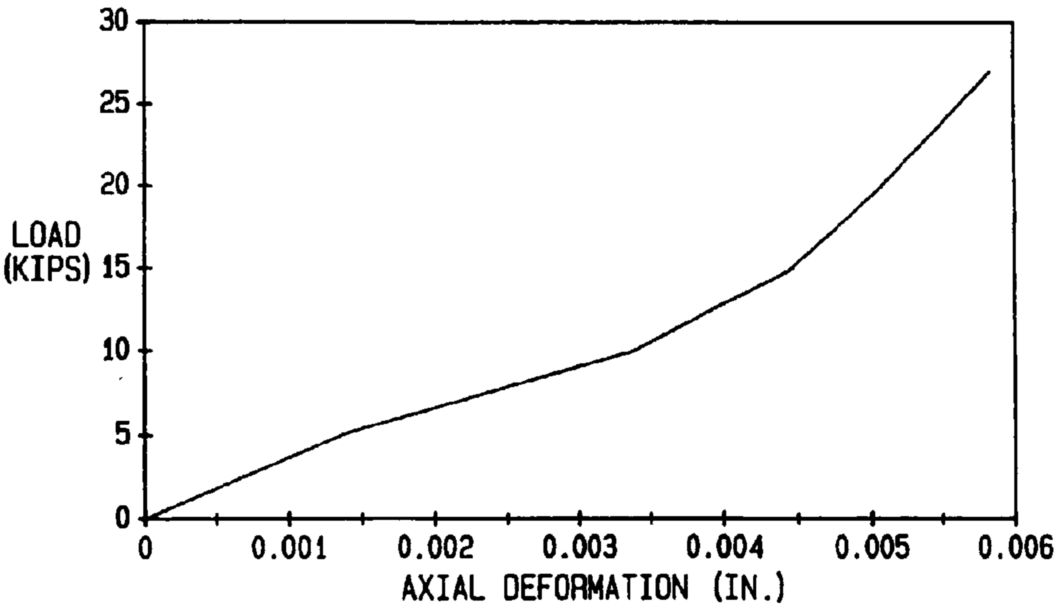

Figure 3-76. Axial Load-Deformation Diagram for Specimen SD2C.

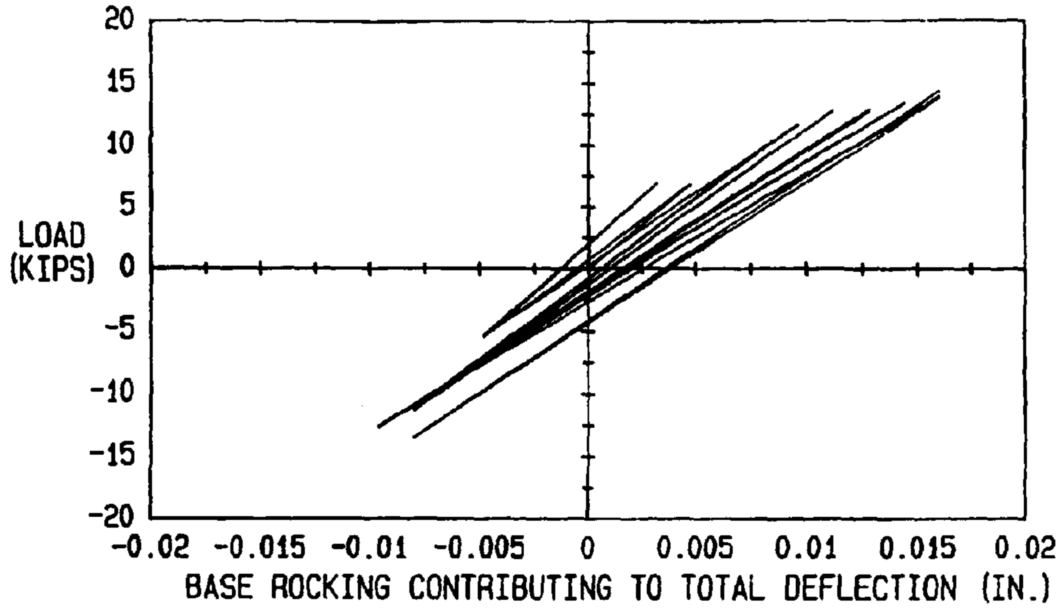

Figure 3-77. Load-Base Rotation Contributing to Total Deflection for SD2C.

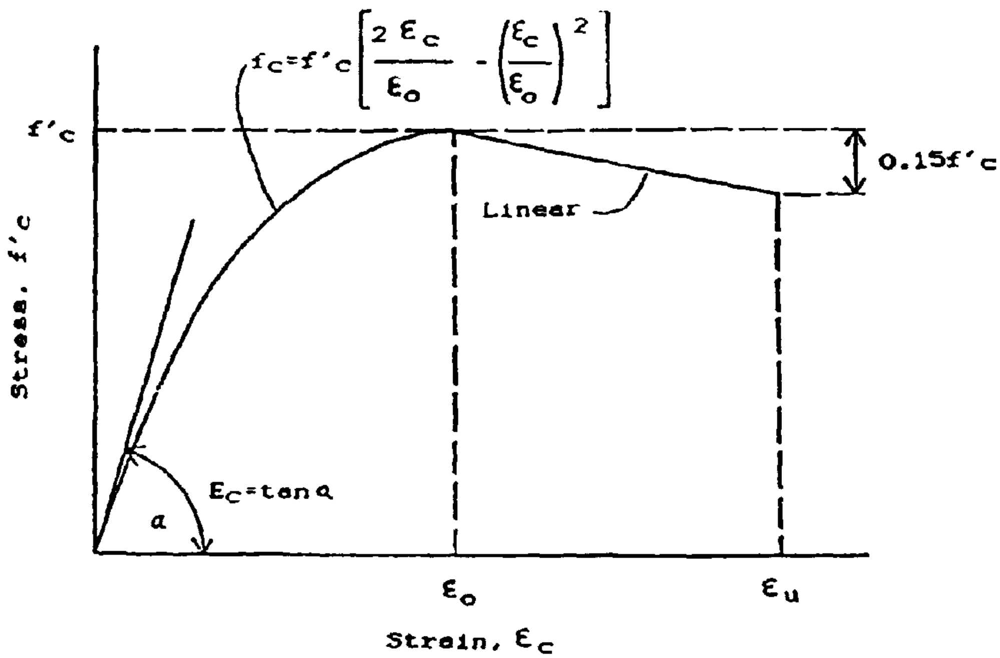

Figure 4-1. Idealized Stress-Strain Curve for Concrete.

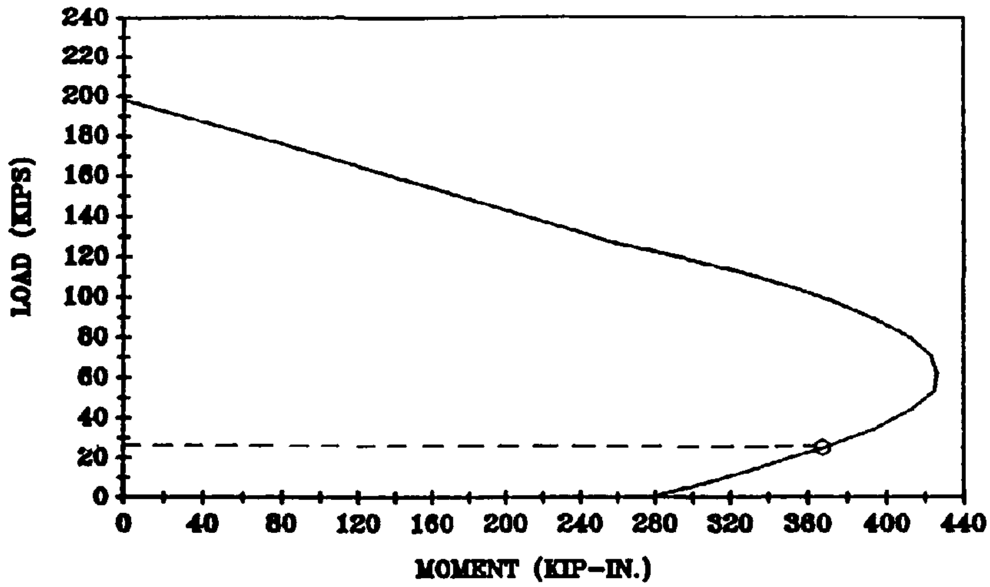

Figure 4-2. Axial Load-Moment Interaction Diagram for Specimen SD1M.

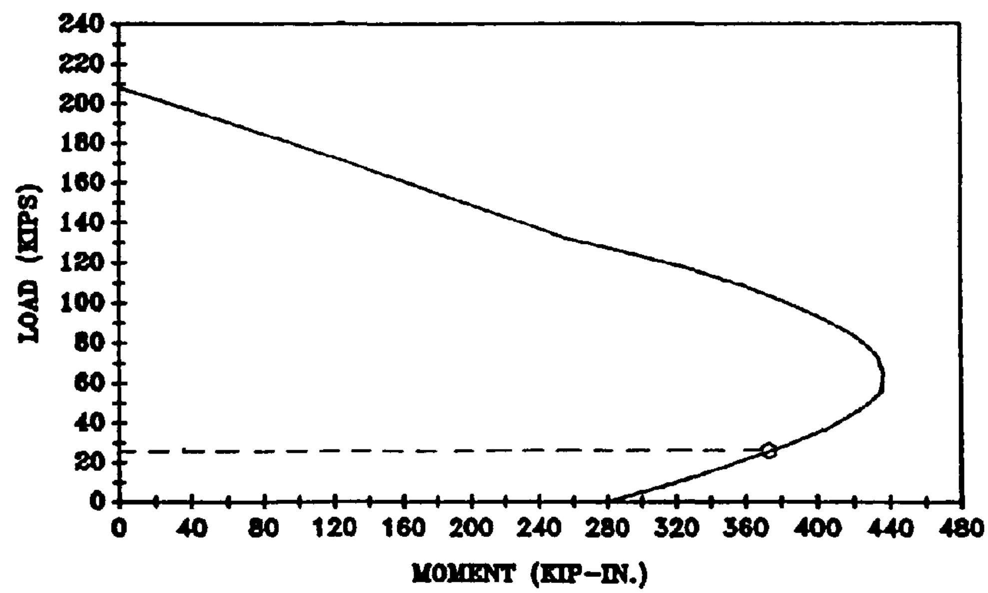

Figure 4-3. Axial Load-Moment Interaction Diagram for Specimen SD2M.

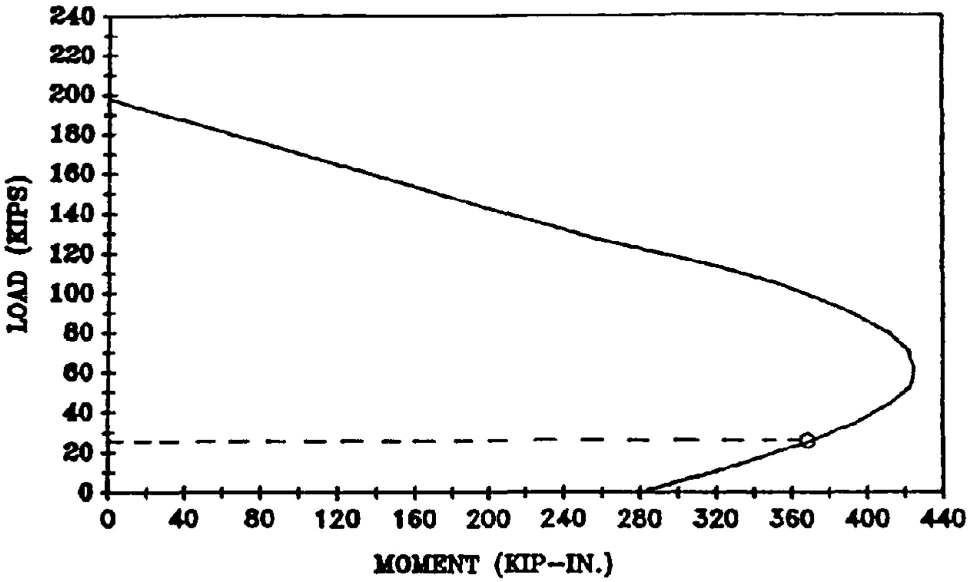

Figure 4-4. Axial Load-Moment Interaction Diagram for Specimen SD1C.

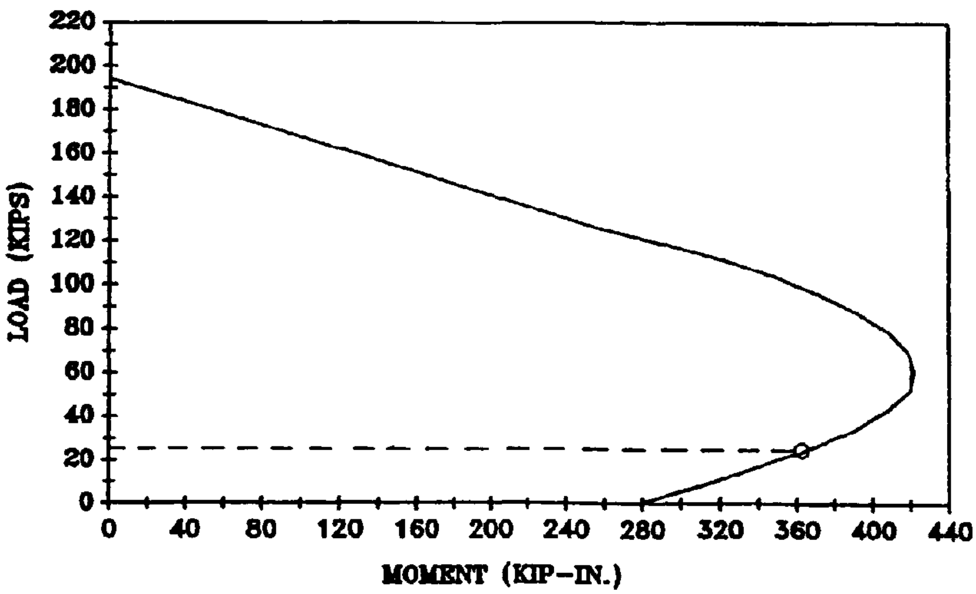

Figure 4-5. Axial Load-Moment Interaction Diagram for Specimen SD2C.

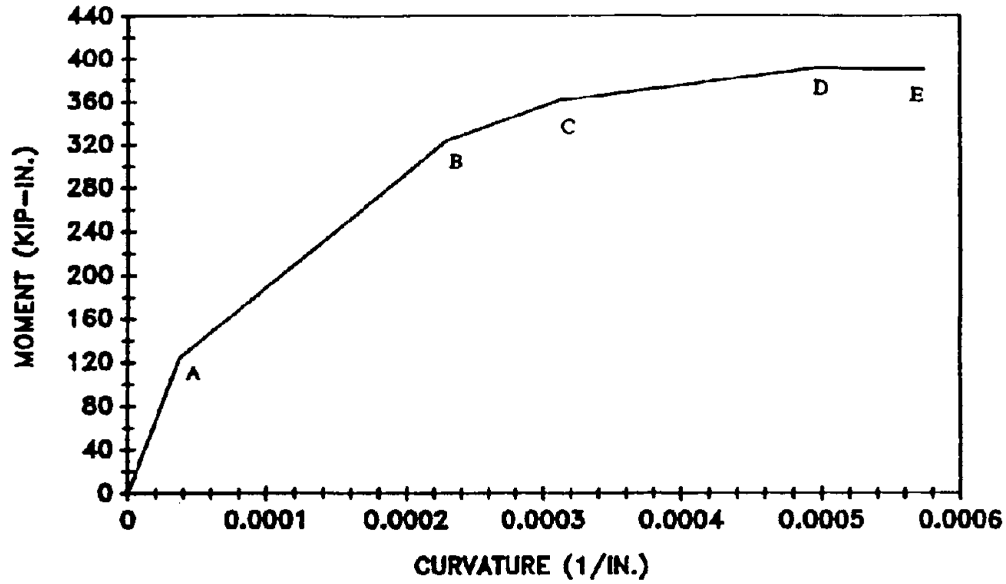

Figure 4-6. Moment-Curvature Diagram for Specimen SD1M.

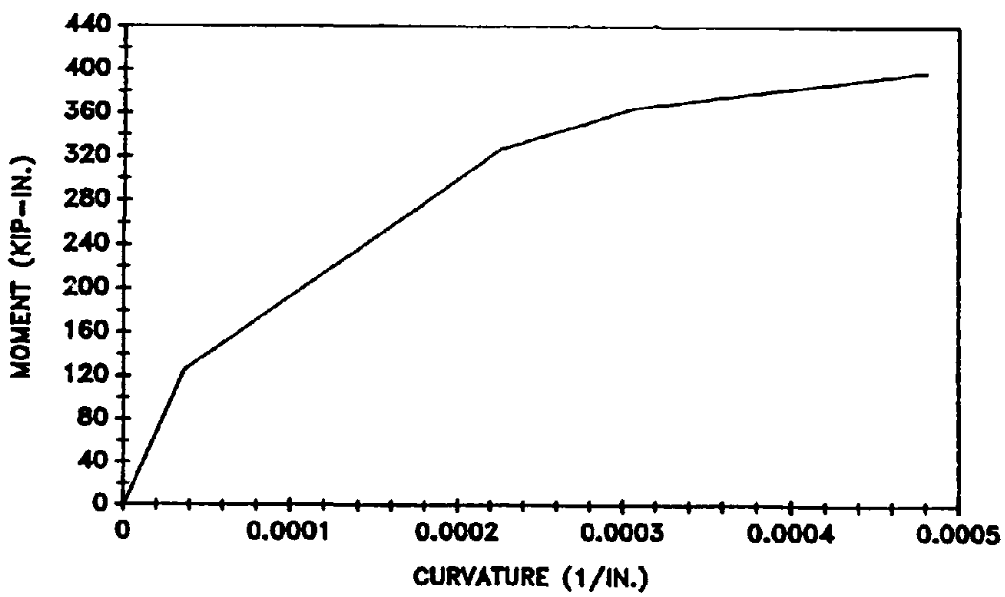

Figure 4-7. Moment-Curvature Diagram for Specimen SD2M.

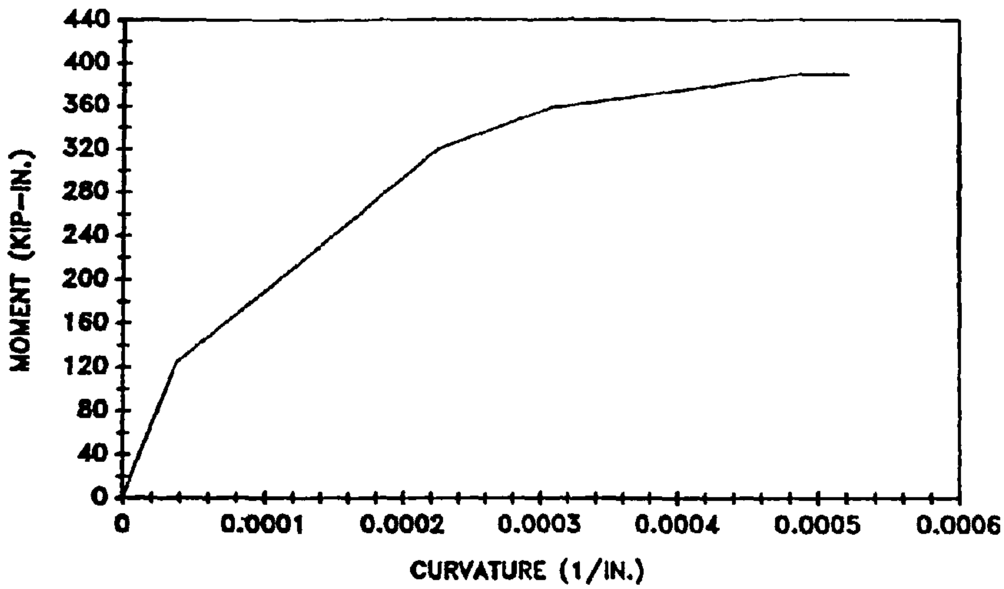

Figure 4-8. Moment-Curvature Diagram for Specimen SD1C.

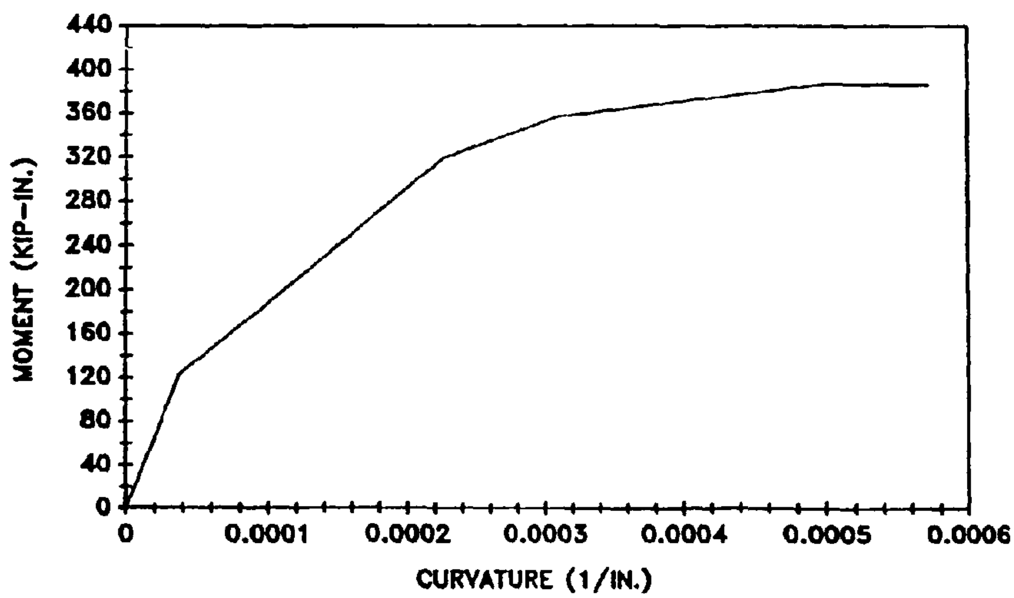

Figure 4-9. Moment-Curvature Diagram for Specimen SD2C.

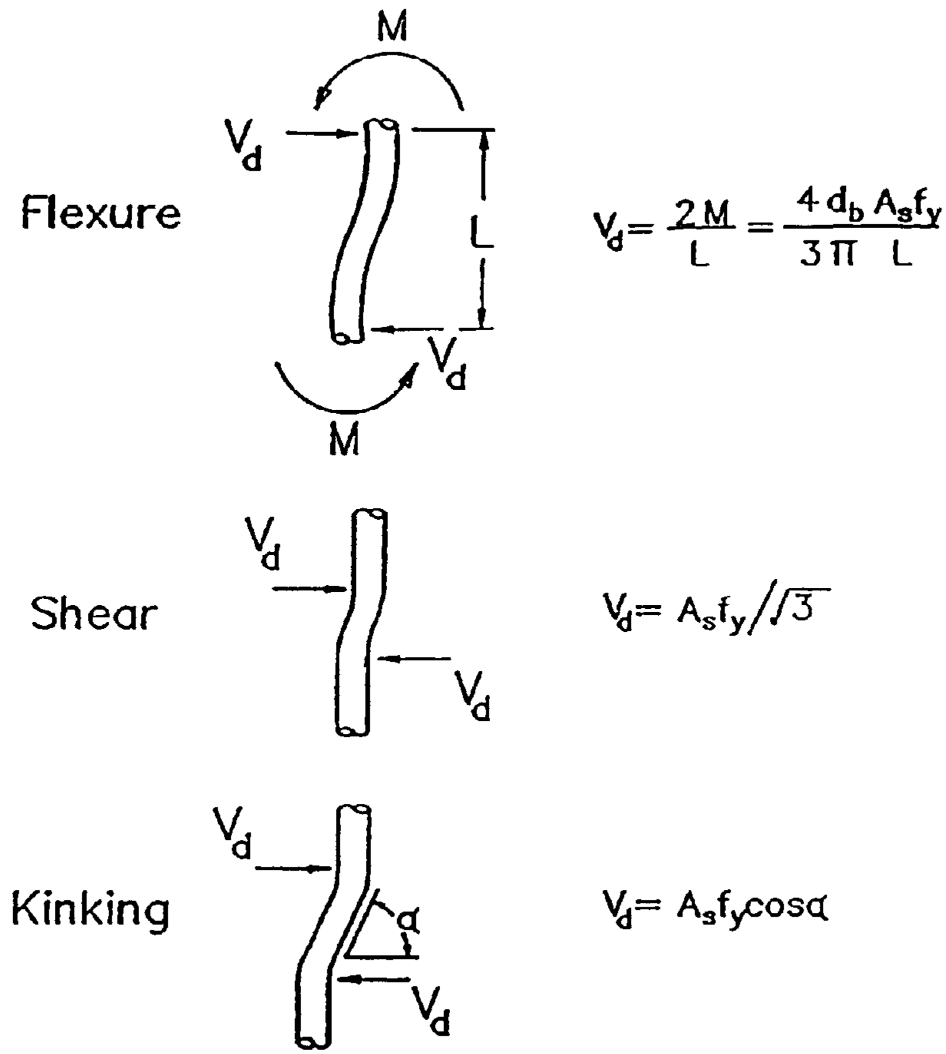

Figure 4-10. Mechanisms for Dowel Action.

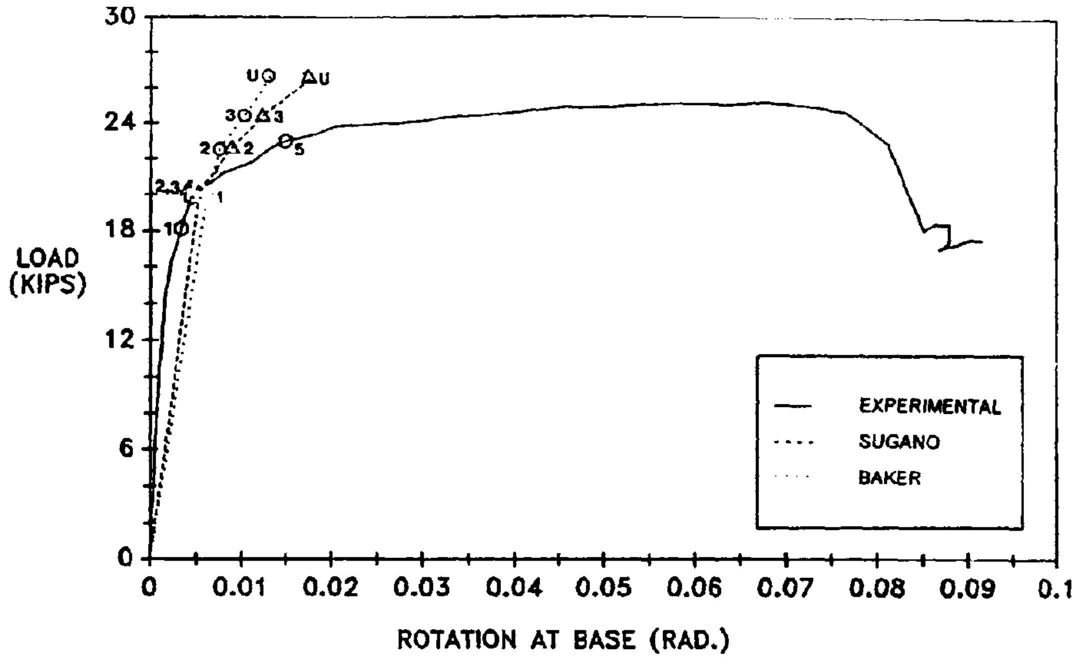

Figure 4-11. Measured versus Calculated Load-Rotation Diagrams for SD1M.

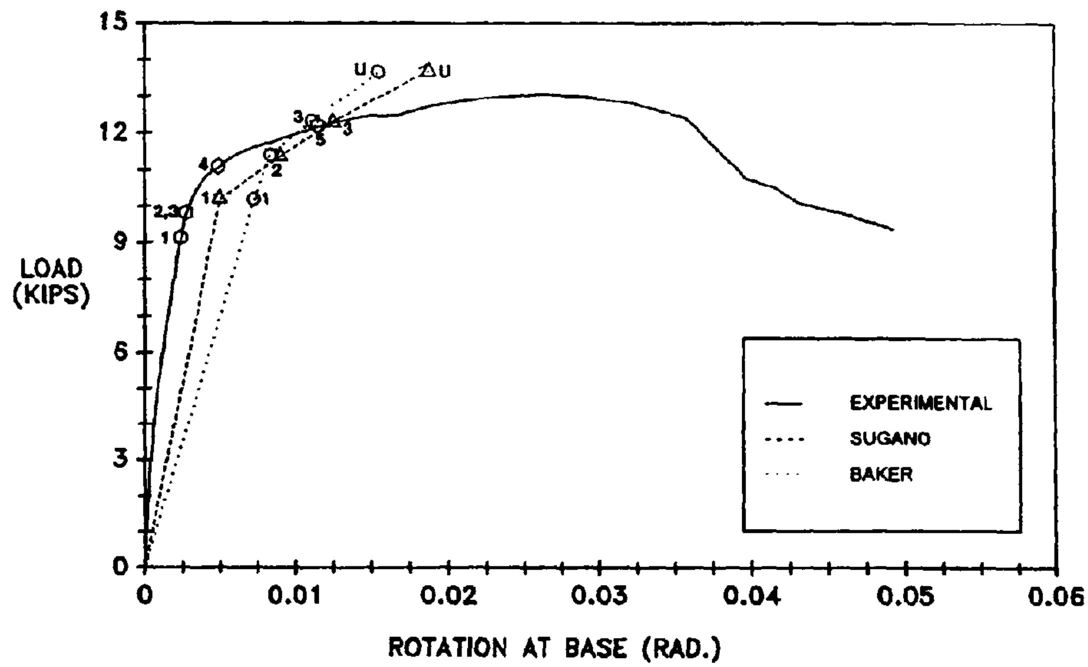

Figure 4-12. Measured versus Calculated Load-Rotation Diagrams for SD2M.

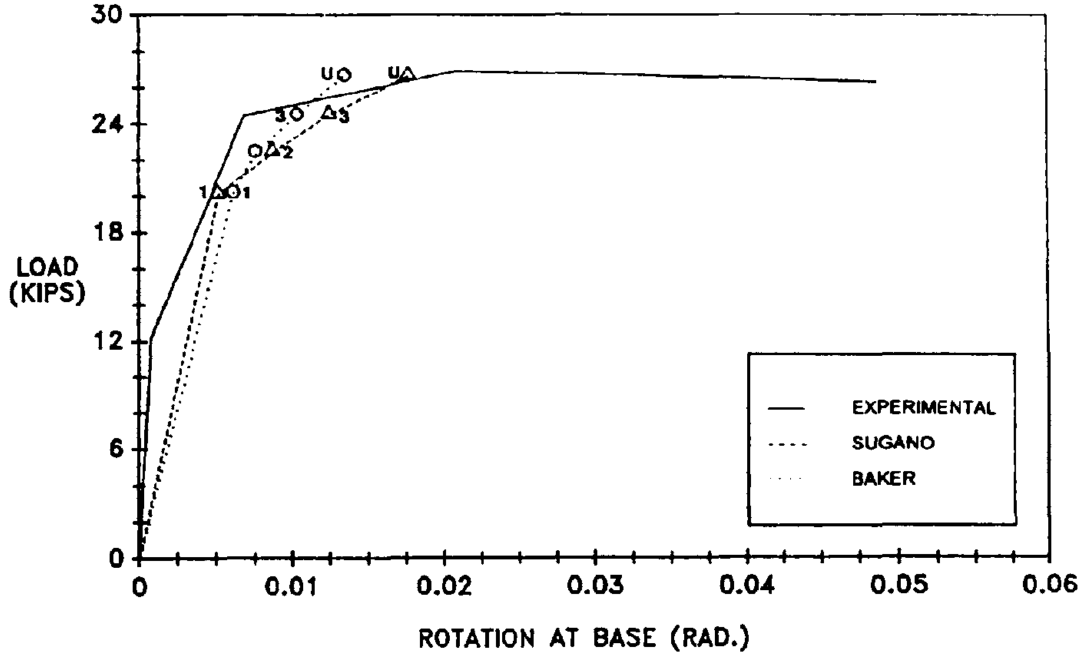

Figure 4-13. Measured versus Calculated Load-Rotation Diagrams for SD1C.

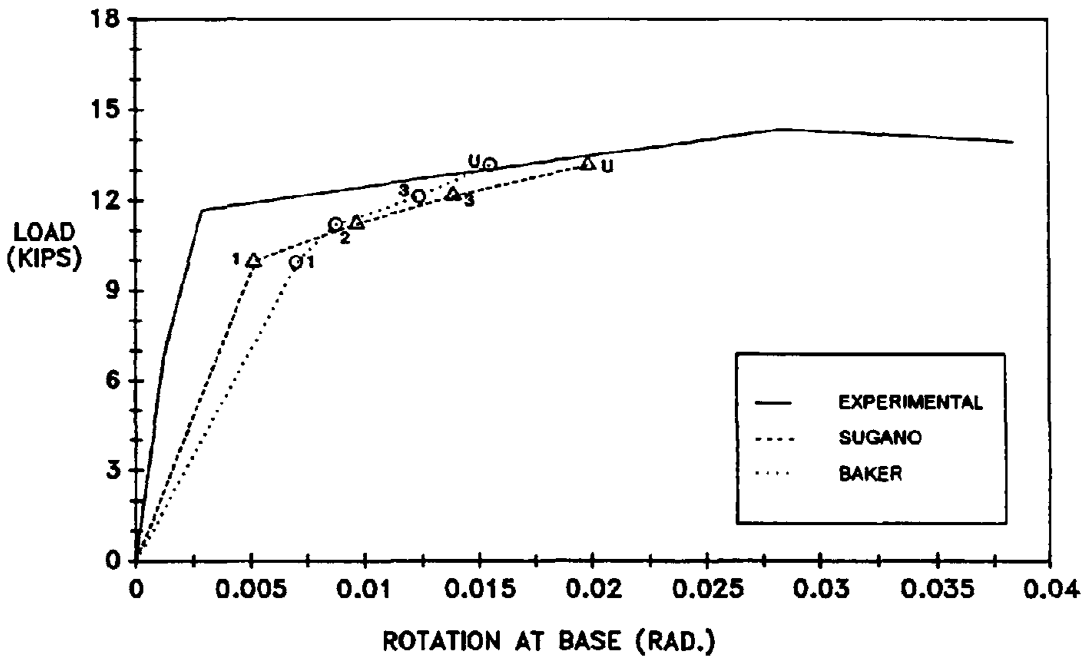

Figure 4-14. Measured versus Calculated Load-Rotation Diagrams for SD2C.

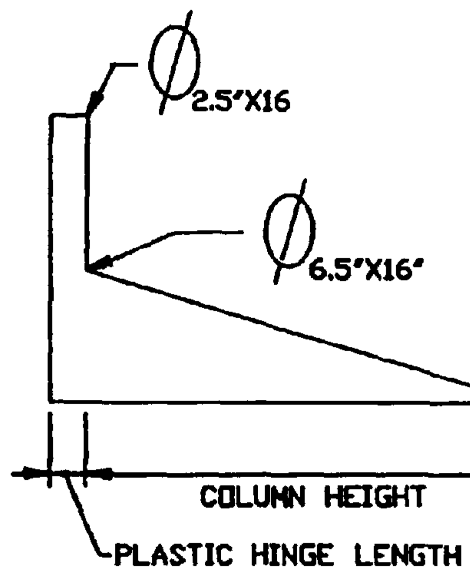

Figure 4-15. Idealized Curvature Distribution Along Cantilevered Element.

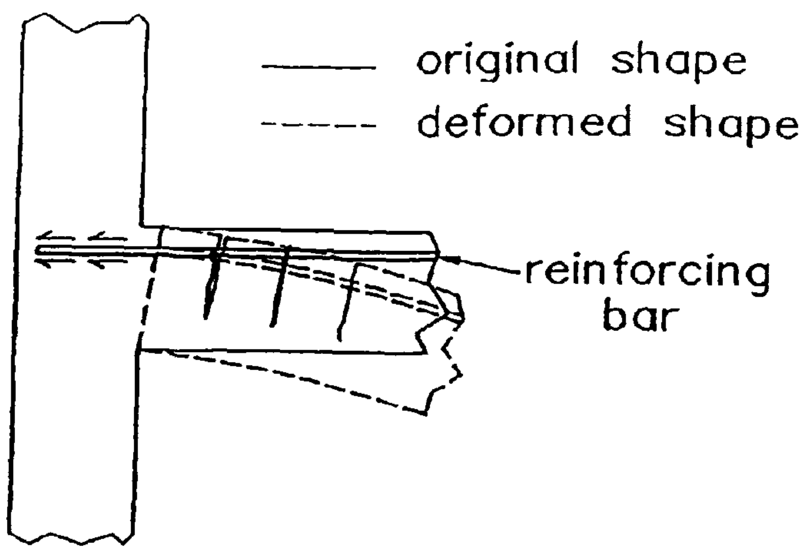

Figure 4-16. Bar Slip Mechanism in in a Typical Reinforced Concrete Beam.

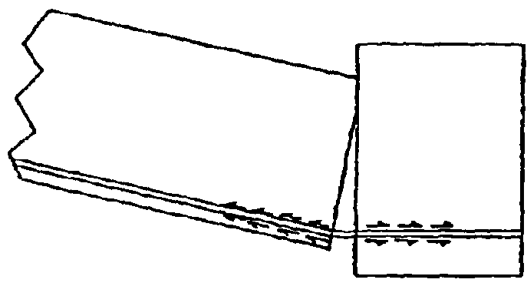

Figure 4-17. Assumed Bar Slip Mechanism in Hinged Specimens.

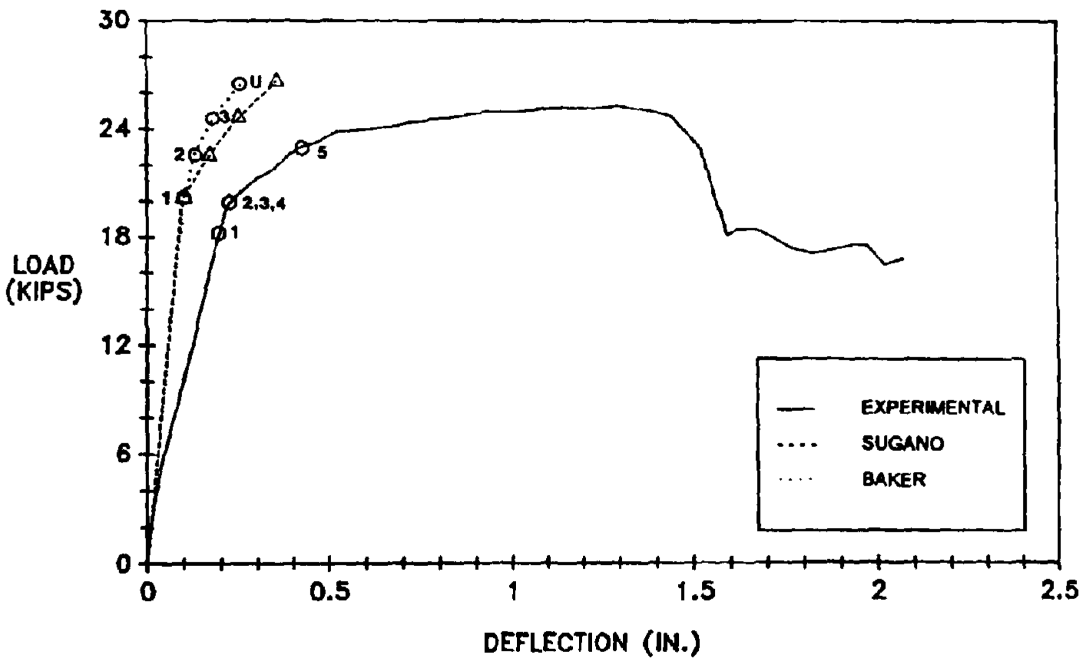

Figure 4-18. Measured versus Calculated Load-Deflection Diagrams for SD1M.

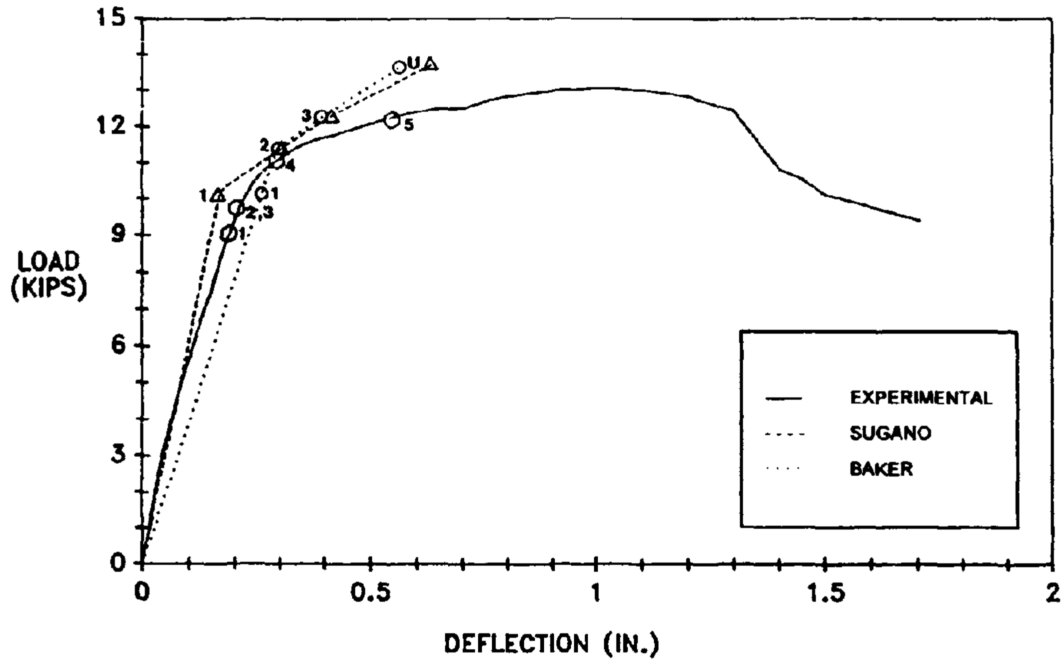

Figure 4-19. Measured versus Calculated Load-Deflection Diagrams for SD2M.

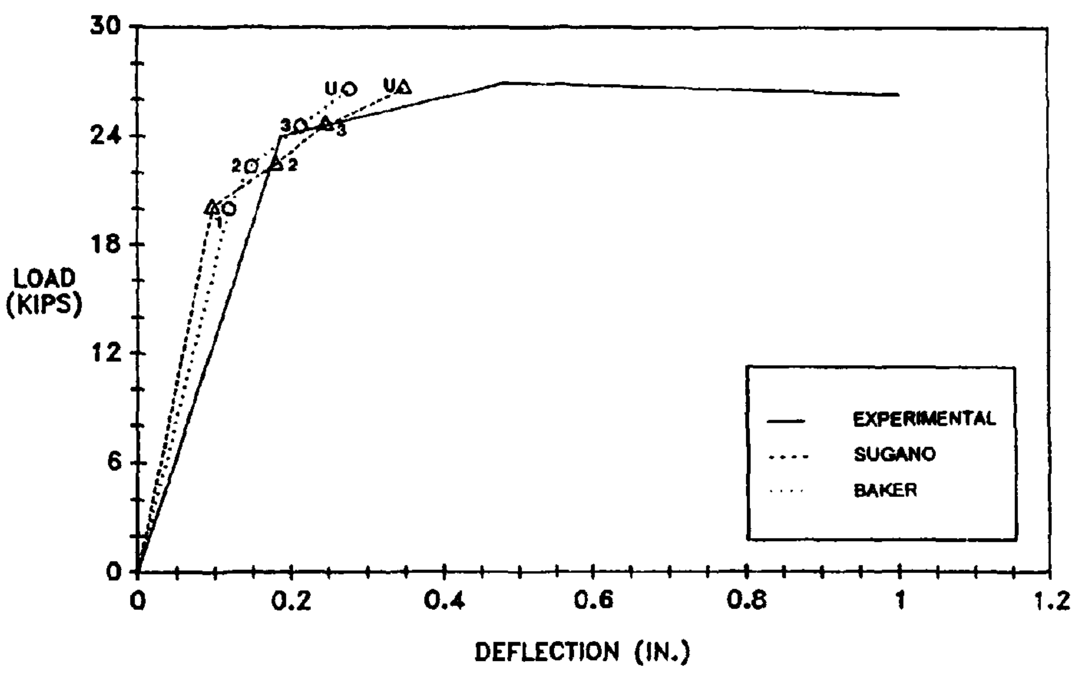

Figure 4-20. Measured versus Calculated Load-Deflection Diagrams for SD1C.

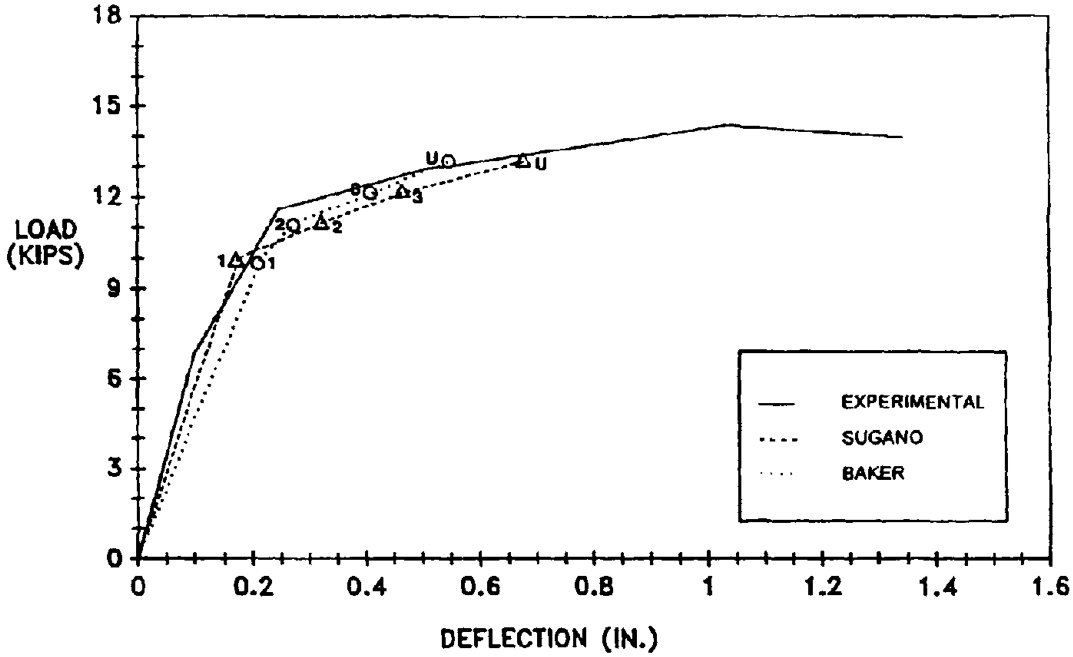

Figure 4-21. Measured versus Calculated Load-Deflection Diagrams for SD2C.

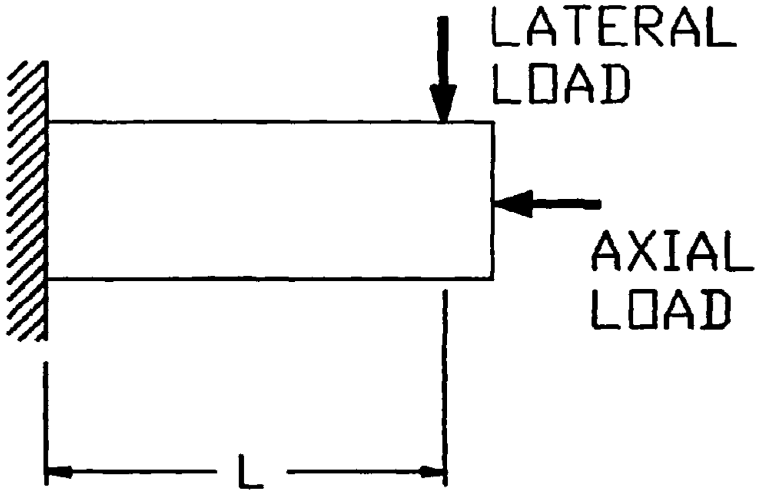

Figure 4-22. Cantilevered End Element.

Appendix A

Aggregate Properties

Coarse Aggregate:

Maximum Size	½ inch
Specific Gravity	2.52
Moisture Content	0.78%
Absorption Capacity	2.52%
Dry Rodded Weight	110 lb/ft^3

Fine Aggregate:

Specific Gravity	2.52
Moisture Content	7.95%
Absorption Capacity	3.08%
Fineness Modulus	3.16

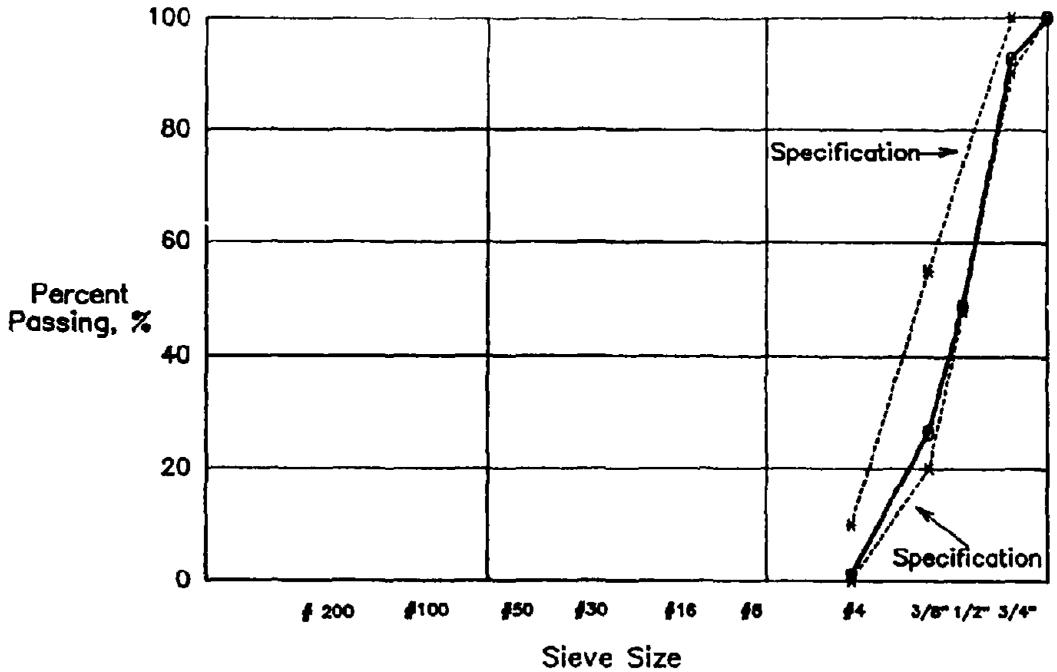

Figure A-1. Grading Chart for Coarse Aggregate.

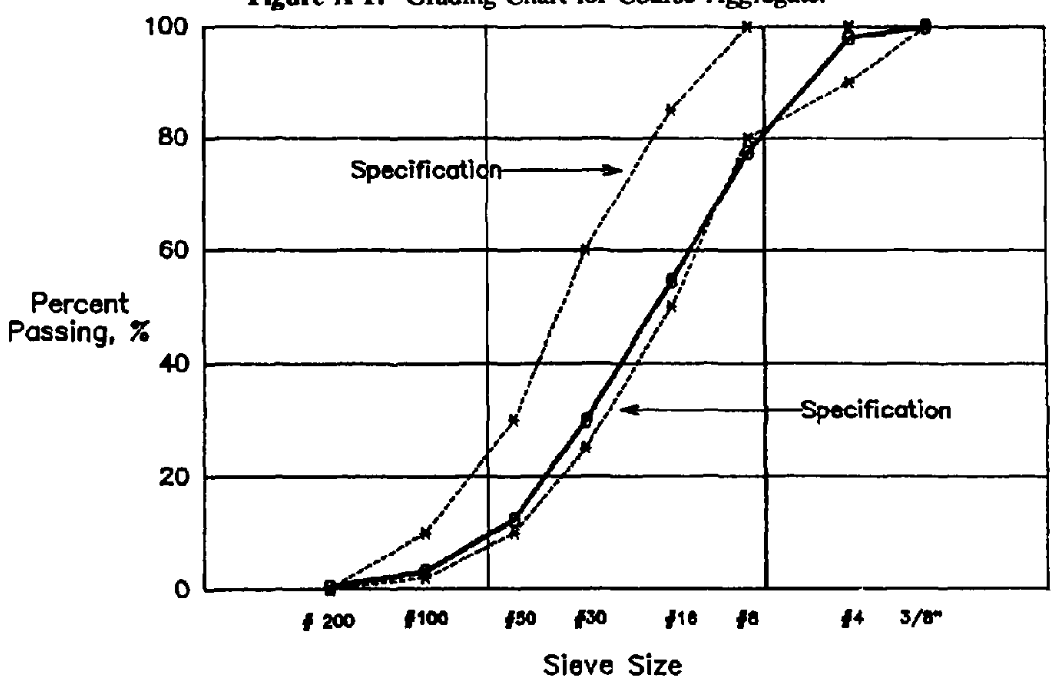

Figure A-2. Grading Chart for Fine Aggregate.

Appendix B

Concrete Mixture Design

Batch weights to make one cubic yard of concrete:

Water/Cement Ratio	0.40
Cement	738 lb/yd^3
Water	295 lb/yd^3
Coarse Aggregate	1377 lb/yd^3
Fine Aggregate	1195 lb/yd^3
Air Entraining Admixture	1 fl. oz. per 100 lbs. of cement

The concrete mixture was proportioned using the PCA Absolute Volume Method.

Appendix C

Concrete Properties

		Compressive Strength, f'_c			
		7-Days	28-Days	Day of Test	Slump
SD1M	Column	3750 psi	4070 psi	4690 psi	2 in.
	Footing	3540 psi	3710 psi	4600 psi	2 in.
SD2M	Column	4050 psi	4690 psi	5140 psi	2 in.
	Footing	4620 psi	4630 psi	4900 psi	2.5 in.
SD1C	Column	3550 psi	4330 psi	4440 psi	2.5 in.
	Footing	4100 psi	4610 psi	4950 psi	2.25 in.
SD2C	Column	2830 psi	4070 psi	4420 psi	2.5 in.
	Footing	3910 psi	4560 psi	4790 psi	2.25 in.

Appendix D

Reinforcing Steel Properties

Bars:	#3 Grade 60, Deformed
Diameter:	0.375 in.
Area:	0.11 in^2
Modulus of Elasticity:	29,000 ksi

	SD1M & SD2M	SD1C & SD2C
Yield Strength:	58 ksi	57 ksi
Yield Strain:	0.002	0.00197
Ultimate Strength:	83 ksi	87 ksi
Ultimate Strain:	0.232	0.274

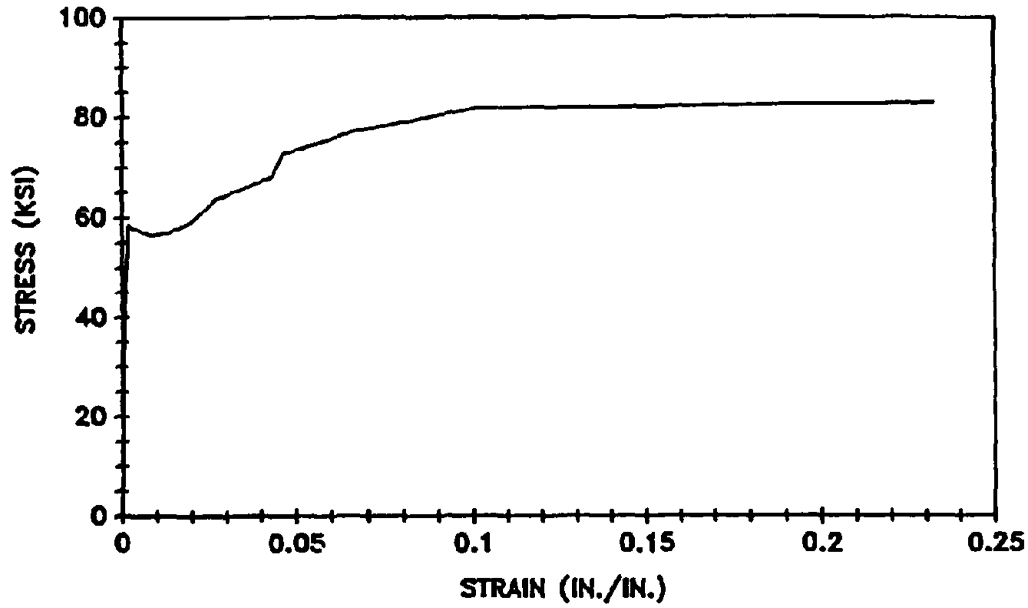

Figure D-1. Reinforcing Steel Stress-Strain Diagram for SD1M and SD2M.

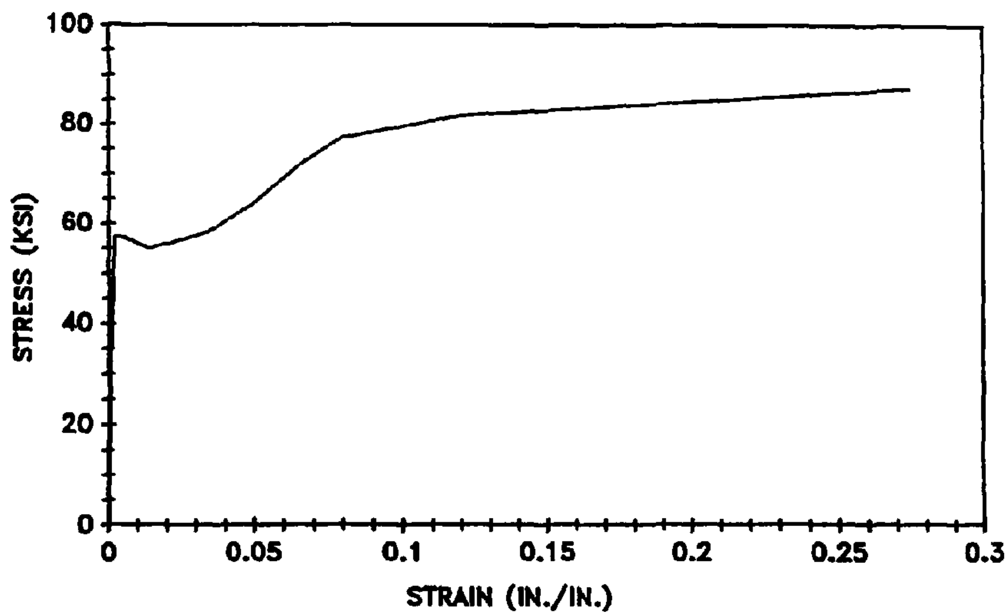

Figure D-2. Reinforcing Steel Stress-Strain Diagram for SD1C and SD2C.

Appendix E
Listing of *PIERHINGE* Computer Program

```
10    ! ------------------------------------------------------------------
20    ! ==================================================================
30    !                          Computer Program "PIERHINGE"
40    !                          Version 1.0
50    !                          By David L. Straw
60    !                          Civil Engineering Department
70    !                          University of Nevada, Reno
80    !                          March 1989
90    !   This computer program was written by David L. Straw by modifying
100   !   compter program "AQUIREDAT" written by James L. Orie [1].
110   !   The program was written to aquire data from testing of one-sixth
120   !   scale model bridge pier-to-foundation connections (one-way hinges)
130   !   in the strong direction during the spring of 1989. The computer
140   !   program is written in Hewlett-Packard Basic Version  4.0.
150   !   This program requires that the following HP equipment be turned on:
160   !   3437A System Voltmeter, 3456A Digital Voltmeter, 3497A Data
170   !   Aquistion System/Control Unit, Hp Thinkjet Printer, and HP 7470A
180   !   External Plotter.
190   !   Data is aquired using electronic resistance strain gages,
200   !   external LVDT's, and the MTS Structural Testing Machine (load
210   !   cell and ram arm).
220   !   The strain gages are located on reinforcing bars within the concrete
230   !   test specimens. 3-external LVDT'S are used to measure  the following:
240   !   (1) deflection of the pier relative to the foundation as the
250   !   specimen is being loaded (to monitor the rotation of the column) and
260   !   (2) slip of the column relative to foundation.
270   !   The MTS was used to load the R/C test specimen and the following
280   !   was recorded: (1) load from the load cell and (2) center span
290   !   displacement of the hydraulic ram.
300   !   The HP 7470A external plotter plotted lateral load vs. center
310   !   span deflection of the column during testing.
320   ! ==================================================================
330   ! ------------------------------------------------------------------
340   DIM Volt(300),V(300),Chan(300),Gf(30),Clvdt(300),Cf(30),Displ(300)
350   DIM Loadp(300),Defl(300),Sp(300,10),Dist(300,5),P(300),Dn(300),Disp(300)
360   DIM Title$[30],Titl$[30]
370   DIM U_ratio(300),S_ratio(300)
380   Ln=1         ! COUNTER FOR TESTING
390   D1=1         ! COUNTER FOR FILE1
400   D2=1         ! COUNTER FOR FILE2
410   Defl1=0
420   Load1=0
430   PRINTER IS 1
440   Gage$="gage"
450   !  TWO DATA FILES ARE CREATED FOR STORING TEST RESULT DATA.
460   !  FILE #1 IS THE STRAIN REFERENCE DATA AND FILE #2 IS THE STRAIN GAGE
470   !  OUTPUT, LVDT DISPLACEMENT OUTPUT, CENTER SPAN DEFLECTION OUTPUT,
480   !  AND FINALLY THE LATERAL LOAD FORCE.
490   OUTPUT KBD USING "#,K";CHR$(255)&"K"
500   INPUT "INPUT FILE NAME FOR REFERENCE DATA",File1$
```

```
510   PRINT
520   INPUT "INPUT FILE NAME FOR OUTPUT DATA FILE",File2$
530   PRINT
540   INPUT "ENTER THE TITLE OF THIS EXPERIMENT",Titl$
550   PRINT
560   !
570   PRINT "IS THIS THE READING TO BE USED AS A REFERENCE POINT FOR FUTURE MEAS
UREMENTS (Y/N) ?"
580   INPUT Rp$
590   Ng=18          ! INPUT THE NUMBER OF STRAIN GAGES USED IN EACH SPECIMEN
600   Num=3          ! INPUT THE NUMBER OF EXTERNAL LVDT'S USED
610   IF Rp$="Y" THEN GOTO 880
620   ! ****************************************************
630   !     SETTING THE TIME AND DATE
640   ! ****************************************************
650   OUTPUT KBD USING "#,K";CHR$(255)&"K"
660   INPUT "DO YOU WISH TO SET THE TIME AND DATE (Y/N) ?",Set$
670   IF Set$="N" THEN GOTO 720
680   INPUT "ENTER THE TIME OF DAY (HR:MIN:SEC)",Td$
690   INPUT "ENTER THE DATE (DAY MONTH YEAR)",Dd$
700   SET TIMEDATE DATE(Dd$)
710   SET TIME TIME(Td$)
720   PRINT "TIME=";TIME$(TIMEDATE)
730   PRINT "DATE=";DATE$(TIMEDATE)
740   OUTPUT KBD USING "#,K";CHR$(255)&"K"
750   CALL Plotter_i(Title$,X$,Y$,Minx,Maxx,Miny,Maxy)     ! INPUT GRAPH DATA FOR
EXTERNAL HP PLOTTER
760   CALL Printerin(Lowx,Higx,Lowy,Higy,Xticl,Xtich,Yticl,Ytich,Spacex,Spacey)
      ! INPUT GRAPH DATA FOR SCREEN PLOT
770 ! ***********************************************************************
780 ! RETRIEVING OLD REFERENCE VALUES
790 ! ***********************************************************************
800   ASSIGN @Path1 TO File1$
810   FOR I=1 TO Ng
820   ENTER @Path1,D1;U_ratio(I)
830   D1=D1+1
840   NEXT I
850   ASSIGN @Path1 TO *
860   CREATE BDAT File2$,6900,8
870   ASSIGN @Path2 TO File2$
880   COM /Hp3054/ Scn,Dvm,Svm,Prt,Error,Err$[6],Ercnt$[15]
890 ! *****************************************************************
900 ! SUBROUTINE TO ASSIGN CHANNELS TO THE STRAIN GAGES
910 ! THE STRAIN GAGE READINGS WILL BE ASSIGNED AUTOMATICALLY TO
920 ! CHANNELS BY THE COMPTER PROGRAM.
930 ! *****************************************************************
940   C1=20
950   C3=40
960   C4=60
970   FOR I=1 TO 8
980   Chan(I)=C1
990   Gf(I)=2.045
1000  C1=C1+1
1010  NEXT I
```

```
1020  FOR K=9 TO 16
1030  Chan(K)=C3
1040  Gf(K)=2.045
1050  C3=C3+1
1060  NEXT K
1070  FOR J=17 TO 18
1080  Chan(J)=C4
1090  Gf(J)=2.045
1100  C4=C4+1
1110  NEXT J
1120! ******************************************************************
1130! SUBROUTINE TO ASSIGN CHANNELS TO THE LVDT's.
1140! CHANNELS 2-4 WILL AUTOMATICALLY BE ASSIGNED TO THE EXTERNAL LVDT's.
1150! ******************************************************************
1160  C2=2
1170  FOR J=1 TO Num
1180  Cf(1)=10.091
1190  Cf(2)=10.019
1200  Cf(3)=20.773
1210  Clvdt(J)=C2
1220  C2=C2+1
1230  NEXT J
1240  ! ********************************************************************
1250  ! SUBROUTINE TO ASSIGN CHANNELS TO THE MTS LOAD CELL AND RAM ARM
1260  ! TO MONITOR CENTER SPAN DEFLECTION.
1270  ! ********************************************************************
1280  Cload=1              ! MTS LOAD CELL IS CHANNEL No.1
1290  Cfload=5.0           ! (+/-) 10 VOLTS = (+/-) 50 KIPS  ! CALIBRATION FACTOR
1300  Cdist=0              ! MTS LVDT IS CHANNEL No.0
1310  Cfdist=.3            ! (+/-) 10 VOLTS = (+/-) 3 INCHES ! CALIBRATION FACTOR
1320  ! ********************************************************************
1330  OUTPUT KBD USING "#,K";CHR$(255)&"K"       !  CLEAR CRT
1340  CALL Init(3456)
1350  IF Rp$="N" THEN GOTO 1580
1360  ! Get Bridge voltage, Excitation voltage, and Ratio for reference gages
1370  FOR K=1 TO Ng
1380    CALL Brmeas(Chan(K),Bridge,Excitation,Ratio)  ! Bridge Measurement
1390    U_ratio(K)=Ratio
1400    V(K)=Excitation
1410    PRINTER IS 701
1420    PRINT "REFERENCE RATIO GAGE ",K;U_ratio(K)
1430    PRINT "REFERENCE EXCITATION VOLTAGE";V(K)
1440  NEXT K
1450  WAIT 1
1460  OUTPUT KBD USING "#,K";CHR$(255)&"K"       !  CLEAR CRT
1470  !  **********************************************
1480  !  NOW STORING REFERENCE DATA
1490  !  **********************************************
1500  CREATE BDAT File1$,50,0
1510  ASSIGN @Path1 TO File1$
1520  CALL Datastor(@Path1,D1,Ng,U_ratio(*))
```

```
1530  GOTO 2550
1540  CALL Plotter_1(Title$,X$,Y$,Minx,Maxx,Miny,Maxy)
1550  !  **************************************************
1560  !   LOOP TO CALCULATE STRAINS
1570  !  **************************************************
1580   FOR J=1 TO Ng
1590    CALL Brmeas(Chan(J),Bridge,Excitation,Ratio)  ! Bridge Measurement
1600    S_ratio(J)=Ratio            ! Ratio of Bridge to Excitation Voltage
1610    P(J)=FNStrain(Gf(J),S_ratio(J),U_ratio(J)) !  Determines strain
1620    IF Ln=1 THEN GOTO 1680
1630    Sp(Ln,J)=P(J)-Sp(1,J)
1640    GOTO 1690
1650  ! ********************************************************************
1660  !  PRINTING STRAIN GAGE VALUES
1670  ! ********************************************************************
1680    Sp(Ln,J)=P(J)
1690    P(J)=Sp(Ln,J)
1700    PRINT "MICROSTRAIN";Sp(Ln,J)
1710   NEXT J
1720  ! *********************************************************************
1730  !  DETERMINING LATERAL LOAD AND CENTER SPAN DEFLECTION FROM MTS
1740  ! *********************************************************************
1750     Force=FNDcv(Cload)
1760     Loadp(Ln)=Force*Cfload
1770     IF Ln=1 THEN GOTO 1790
1780     Loadp(Ln)=Loadp(Ln)-Loadp(1)
1790     Load=Loadp(Ln)
1800     Dispt=FNDcv(Cdist)
1810     IF Ln=1 THEN GOTO 1830
1820     Dispt=Dispt-Defl(Ln)
1830     Defl(Ln)=Dispt*Cfdist
1840     Plotval=Defl(Ln)
1850  ! *********************************************************************
1860  ! SUBROUTINE TO PRINT RESULTS ON HP THINKJET PRINTER
1870  ! *********************************************************************
1880    CALL Dataprint(Ng,P(*),Chan(*),Load,Time$,Date$,Titl$,Ln,Plotval)
1890     FOR I=1 TO Num
1900  ! *********************************************************************
1910  ! SUBROUTINE TO DETERMINE LVDT DISPLACEMENTS
1920  ! *********************************************************************
1930    CALL Lvdt(I,Clvdt(I),Cf(I),Volt(I),Displ(I))
1940     NEXT I
1950     PRINTER IS 701
1960     FOR K=1 TO Num
1970     IF Ln>1 THEN GOTO 2000
1980     Dist(Ln,K)=Displ(K)
1990     GOTO 2010
2000     Dist(Ln,K)=Displ(K)-Dist(1,K)
2010     Dn(K)=Dist(Ln,K)
2020     PRINT "LVDT NO. ";K;"=";Dist(Ln,K);" IN."
2030     NEXT K
```

```
2040  ! ********************************************************************
2050  ! SUBROUTINE TO STORE TEST DATA ON COMPUTER HARD DRIVE
2060  ! ********************************************************************
2070   CALL Datasave(@Path2,D2,Ln,Load,Plotval,Ng,Num,P(*),Dn(*))
2080  PRINT "///////////////////////////////////////////////////////////////////
////////////"
2090  PRINTER IS 1
2100  PRINT
2110  ! CALL SUBROUTINE "Plotrplot":TO PLOT LOAD VS. CENTER SPAN DEFLECTION
2120  !                              ON EXTERNAL PLOTTER.
2130  CALL Plotrplot(Plotval,Load,Minx,Maxx,Miny,Maxy,Defl1,Load1)
2140  PRINT
2150  PRINT
2160       PRINT "WOULD YOU LIKE TO SEE A GRAPH ON THE SCREEN (Y/N) ?"
2170       INPUT Aa$
2180       IF Aa$="N" THEN GOTO 2240
2190  ! CALL SUBROUTINE "Printplot": TO PLOT LOAD VS. STRAIN ON CRT SCREEN.
2200       CALL Printplot(Lowx,Higx,Lowy,Higy,Xticl,Xtich,Yticl,Ytich,Spacex,Spac
ey,Ln,Sp(*),Loadp(*))
2210       PRINT "DO YOU WANT TO SEE ANOTHER GRAPH ON THE SCREEN (Y/N) ?"
2220       INPUT Resp$
2230       IF Resp$="Y" THEN 2200
2240  PRINT
2250  Ln=Ln+1
2260  PRINT
2270  PRINT "///////////////////////////////////////////////////////////////////
/////////////"
2280  PRINT
2290  PRINTER IS 1
2300  OUTPUT KBD USING "#,K";CHR$(255)&"K"
2310  PRINT
2320  PRINT
2330  PRINT "      ///////////////////////////////////////////////////////"
2340  PRINT "      /                 LOADING COMPLETED !!!                /"
2350  PRINT "      /  DO YOU WANT TO LOAD THE STRUCTURE AGAIN (Y/N) ?    /"
2360  PRINT "      / //////////////////////////////////////////////////////"
2370  INPUT F$
2380  IF F$="N" THEN 2450
2390  PRINT
2400  PRINT
2410  PRINT "           LOAD THE STRUCTURE AND PRESS {CONTINUE}"
2420  PAUSE
2430  GOTO 1560
2440  PRINT
2450  PRINT
2460  OUTPUT KBD USING "#,K";CHR$(255)&"K"
2470  PRINT "     <<<<<<<<<<<<<<<<<<<<<<<<<<<<<<<<<<<<<<<<<<<<<<<<<<<<<<<"
2480  PRINT "     <  WARNING: THIS WILL TERMINATE PROGRAM OPERATION.  <"
2490  PRINT "     <  IS THIS WHAT YOU REALLY WANT TO DO !!!! (Y/N) ?  <"
2500  PRINT "     <<<<<<<<<<<<<<<<<<<<<<<<<<<<<<<<<<<<<<<<<<<<<<<<<<<<<<<"
2510  INPUT Agg$
2520  IF Agg$="N" THEN 2300
2530  PRINT
2540  PRINT
```

```
2550  PRINT "                        END OF TESTING !!!!"
2560  END
2570  ! ***********************************************************
2580  ! SUBPROGRAM Datastore TO STORE REFERENCE VALUES TO FILE #1.
2590  ! ***********************************************************
2600  SUB Datastor(@Path1,D1,Ng,U_ratio(*))
2610    FOR K=1 TO Ng
2620      OUTPUT @Path1,D1;U_ratio(K)   ! STORE REFERENCE VALUES
2630      D1=D1+1
2640    NEXT K
2650  SUBEND
2660  !**************************************************
2670  ! SUBPROGRAM Dataprint TO PRINT DATA ON PRINTER
2680  !**************************************************
2690  SUB Dataprint(Ng,P(*),Chan(*),Load,Time$,Date$,Titl$,Ln,Plotval)
2700    PRINTER IS 701
2710    PRINT CHR$(27);CHR$(38);CHR$(107);CHR$(48);CHR$(83)   !  NORMAL PRINT
2720    PRINT
2730    PRINT "/////////////////////////////////////////////////////////////////
//////////////"
2740    PRINT "TEST SPECIMEN IS = ";Titl$
2750    PRINT "Electrical Strain Gages   (Microstrain)"
2760    Time$=TIME$(TIMEDATE)
2770    Date$=DATE$(TIMEDATE)
2780    PRINT "TIME= ";Time$
2790    PRINT "DATE= ";Date$
2800    PRINT
2810    PRINT "LOAD= ";Load;"KIPS"
2820    PRINT "CENTER SPAN DEFLECTION= ";Plotval;"IN."
2830    PRINT
2840    PRINT "LOAD NUMBER=";Ln
2850    PRINT
2860    PRINT "-----------------------------------------------------------------
----------"
2870    PRINT "     GAGE      CHANNEL   STRAIN    *      GAGE       CHANNEL
  STRAIN"
2880    PRINT "-----------------------------------------------------------------
----------"
2890    FOR K=1 TO Ng-1 STEP 2
2900    M=K+1
2910    PRINT "     GAGE";K,Chan(K),P(K),"      GAGE";M,Chan(M),P(M)
2920    NEXT K
2930    PRINT "-----------------------------------------------------------------
----------"
2940 !  PRINT "/////////////////////////////////////////////////////////////////
//////////"
2950    PRINT
2960    PRINTER IS 1
2970  SUBEND
2980  ! *****************************************************************
2990  ! SUBROUTINE FOR INITIALIZING THE VOLTMETERS
3000  ! *****************************************************************
3010  SUB Init(Dvmeter)                       ! 200 SERIES COMPUTER   02/02/83
3020    COM /Hp3054/ Scn,Dvm,Svm,Prt,Error,Err$[6],Ercnt$[15]
3030    DIM Message$[50]       ! STRING CONTAINING USER MESSAGE
3040    INTEGER Address        ! HOLDS HPIB ADDRESS DURING BUS SCAN
3050    INTEGER Bstatus        ! HPIB STATUS REG CONTENTS
```

```
3060    Prthere=0              ! PRINTER FLAG
3070    Error=0                ! ERROR CODE #'S
3080    Ercnt$="0000000000000000"! ERROR MASK
3090    Err$=""                ! ERROR SUB NAME
3100  ! INITIALIZE  DEVICE ADDRESSES
3110    Scn=709                ! 3497A SCANNER ADDRESS
3120    Dvm=722                ! 3456A DIGITAL VOLTMETER ADDRESS
3130    Svm=724                ! 3437A SYSTEM VOLTMETER ADDRESS
3140    Prt=701                ! SYSTEM PRINTER ADDRESS
3150    Bus=Scn DIV 100        ! HPIB SELECT CODE
3160    Initdvm=Dvm            ! TEMP. STORAGE FOR HP3456 ADDRESS
3170  ! VERIFY THAT INTERFACE IS HP-IB
3180    Message$="THE NUMBER "&VAL$(Bus)&" IS NOT A VALID SELECT CODE"
3190    IF Bus<7 OR Bus>31 THEN Terminate
3200    Message$="NO INTERFACE FOUND AT SELECT CODE "&VAL$(Bus)
3210    ON ERROR GOTO Terminate
3220    STATUS Bus,0;Bstatus
3230    Message$="THE INTERFACE AT SELECT CODE "&VAL$(Bus)&" IS NOT HP-IB"
3240    IF Bstatus<>1 THEN Terminate
3250    ON TIMEOUT Bus,1 GOTO Time
3260    CONTROL Bus,0;1        ! CLEAR THE INTERFACE
3270    SEND Bus;UNL           ! UNLISTEN THE BUS
3280    OFF TIMEOUT
3290    OFF ERROR
3300    CLEAR Bus              ! SENDS DEVICE CLEAR (DCL)
3310    IF (Dvmeter<>3456) AND (Dvmeter<>3497) THEN Abort
3320    IF Dvmeter=3497 THEN Dvm=Scn
3330  ! CHECK FOR EQUIPMENT ON BUS AT ALL ADDRESSES AND PRINT DEVICE NAMES
3340    OUTPUT 1 USING "@,/,10X,K,DD";" EQUIPMENT PRESENT ON BUS #";Bus
3350    OUTPUT 1 USING "10X,""----------------------------"",/"
3360    FOR Address=Bus*100 TO Bus*100+30
3370      OUTPUT Address USING "#"  ! ADDRESS DEVICE TO LISTEN
3380      STATUS Bus,7;Bstatus      ! SEE IF IT LISTENED
3390      IF (NOT BIT(Bstatus,13)) THEN Nxt  ! BIT 13 TRUE IF DEVICE PRESENT
3400      Message$="        Device Unknown"
3410      IF Address=Scn THEN Message$="3497A  Mainframe"
3420      IF Address=Initdvm THEN Message$="3456A  Digital Voltmeter"
3430      IF Address=Svm THEN Message$="3437A  System Voltmeter"
3440      IF (Dvm=Scn) AND (Address=Scn) THEN Message$=Message$&", DVM"
3450      IF Address=Prt THEN
3460        Message$="        System Printer"
3470        Prthere=1
3480      END IF
3490      OUTPUT 1 USING Fmt;Message$,Address MOD 100
3500 Nxt:NEXT Address
3510    STATUS Bus,3;Bstatus
3520    OUTPUT 1 USING Fmt;"        System Computer",BINAND(Bstatus,31)
3530 Fmt:IMAGE 6X,24A," at address ",2Z
3540    IF NOT Prthere THEN Prt=1
3550    SUBEXIT
3560 Time:CONTROL Bus,0;1    ! RESET INTERFACE
```

```
3570    Message$="NO DEVICES RESPOND OVER HP-IB SELECT CODE "&VAL$(Bus)
3580 Terminate:OUTPUT 1 USING Fmt2;"CAUTION!","PROGRAM TERMINATED BECAUSE:"
3590 Fmt2:IMAGE @,5/,K,2/,K,/
3600    OUTPUT 1 USING "5X,K,"""";Message$
3610    STOP
3620 Abort:Error=2
3630    Err$="Init"
3640    CALL Warn
3650   SUBEND
3660   ! ****************************************************************
3670   ! SUBPROGRAM FOR RECORDING BRIDGE MEASUREMENT
3680   ! ****************************************************************
3690   SUB Brmeas(Channel,Bridge,Excitation,Ratio)    ! 200 SERIES        02/02/83
3700    COM /Hp3054/ Scn,Dvm,Svm,Prt,Error,Err$[6],Ercnt$[15]
3710    Exc_chn=Channel
3720    Bridge=9.E+19
3730    Excitation=9.E+19
3740    Ratio=9.E+19
3750    OUTPUT Dvm USING "#"
3760    STATUS Dvm DIV 100,7;Here1
3770    Here2=8192*(Scn<>0)
3780    IF Dvm=Scn THEN Chk
3790    OUTPUT Scn USING "#"
3800    STATUS Scn DIV 100,7;Here2
3810 Chk:Error=2*((Channel<0) OR (Channel>999) OR (Channel MOD 20)=10))
3820    Error=Error+16*((NOT BIT(Here2,13)) OR (NOT BIT(Here1,13)) AND (Dvm=Scn)
)
3830    Error=Error+32*((NOT BIT(Here1,13)) AND (Dvm<>Scn))
3840    IF Error THEN Abort
3850 Read:OUTPUT Scn;"AC";INT(Exc_chn);"ST0" !CLOSE CHAN. & WAIT UNTIL EXECUTED
3860    IF Dvm=Scn THEN OUTPUT Dvm;"VR1VR5VN1VA1VF1VD5VC0VS0VW0VT3" !3497 SETUP &
 TRG
3870    IF Dvm<>Scn THEN OUTPUT Dvm;"HR2R11STI6ST6T3"        !3456 SETUP & TRG
3880    ENTER Dvm;Excitation
3890    IF Channel<>Exc_chn THEN Done
3900    Bridge=Excitation
3910    Exc_chn=(Channel DIV 10)*10+10       !COMPUTE EXCITATION CHANNEL NUMBER
3920    GOTO Read
3930 Done:IF ABS(Bridge)>.119 THEN Error=128     ! BRIDGE VOLT. NOT READ ON .1V
RANGE
3940    IF (ABS(Excitation)<.01) OR (ABS(Excitation)>5.4) THEN Error=Error+256!E
XCIT. VOLT.  TEST
3950    IF Error THEN Abort
3960    Ratio=Bridge/Excitation
3970    SUBEXIT
3980 Abort:Err$="Brmeas"
3990    CALL Warn
4000   SUBEND
4010   ! ****************************************************************
4020   ! USER DEFINED FUNCTION FOR COMPUTING VALUES OF STRAIN.
4030   ! ****************************************************************
4040   DEF FNStrain(Gf,S_ratio,U_ratio) ! 200 SERIES
4050    COM /Hp3054/ Scn,Dvm,Svm,Prt,Error,Err$[6],Ercnt$[15]
4060    Dif=S_ratio-U_ratio
4070    Error=Error+128*((Dif<-.25) OR (Dif>1) OR (S_ratio=9.E+19))
```

```
4080    IF Error THEN Abort
4090    Strain=-(4*Dif)/(Gf*(1+2*Dif))      ! 1/4 BRIDGE EQUATION
4100    RETURN SGN(Strain)*INT(ABS(Strain*1.E+6)+.5)       ! RETURN MICROSTRAIN
4110 Abort:Err$="Strain"
4120    CALL Warn
4130    RETURN 9.E+19
4140  FNEND
4150  ! ********************************************************************
4160  ! SUBPROGRAM FOR DETECTING ERRORS
4170  ! ********************************************************************
4180  SUB Warn                                  ! 200 SERIES COMPUTER 02/02/83
4190    COM /Hp3054/ Scn,Dvm,Svm,Prt,Error,Err$[6],Ercnt$[15]
4200    COM /Hp3054_warn/ Da$[14],Erm$(0:14)[65],Aster$[80]
4210    INTEGER Max_warns,Flag,Index,Nerrs,Bstatus,Line_len,Gap
4220    Max_warns=2              ! MAXIMUM NUMBER OF WARNINGS ON EACH ERROR ( <=9 )
4230    OFF INTR                 ! PREVENTS WARN FROM BEING EXITTED EARLY
4240    Flag=0
4250    Nerrs=0
4260    Line_len=80
4270    IF LEN(Ercnt$)<>15 THEN Ercnt$="000000000000000"! FILL Ercnt$ IF NECESSA
RY
4280    FOR Index=0 TO 14                             ! ANY ERRORS THAT NEED WARNINGS?
4290      IF BIT(Error,Index) AND (VAL(Ercnt$[Index+1,Index+1])<Max_warns) THEN
Flag=Flag+2^Index
4300    NEXT Index
4310    IF Flag=0 THEN Exit                                           ! NO...RETURN
4320    READ Erm$(*),Aster$                                          ! YES...DO SETUP
4330    IF Prt=1 THEN Line1
4340    ON ERROR GOTO Noprt
4350    ON TIMEOUT Prt DIV 100,1 GOTO Noprt
4360    OUTPUT Prt USING "#"
4370    STATUS Prt DIV 100,7;Bstatus
4380    IF BIT(Bstatus,13) THEN Nocheck! PRINTER PRESENT
4390 Noprt:Prt=1
4400 Line1:STATUS Prt,9;Line_len
4410 Nocheck:ON ERROR GOTO Nodate
4420    ON TIMEOUT Scn DIV 100,1 GOTO Nodate
4430    OUTPUT Scn USING "#"
4440    STATUS Scn DIV 100,7;Bstatus
4450    IF NOT BIT(Bstatus,13) THEN Nodate
4460    OUTPUT Scn;"TD"
4470    ENTER Scn;Da$
4480    IF Da$="01:01:00:00:00" THEN Nodate! Sorry if it's Dec.31,23:59:59+1 sec
4490    Gap=INT((Line_len-30)/2)
4500    OUTPUT Prt USING Fmt;Aster$[1,Gap];Da$[1,2],Da$[4,5],Da$[7,14],Aster$[1,
Gap]
4510 Fmt:IMAGE K," Date: ",K,"/",K,"   Time: ",K,X,K
4520    GOTO Warnout
4530 Nodate:OFF TIMEOUT
4540    OFF ERROR
4550    OUTPUT Prt;Aster$[1,Line_len]
4560 Warnout:OFF ERROR
4570    OFF TIMEOUT
4580    OUTPUT Prt;"WARNING:    SUBPROGRAM "&Err$&" WAS NOT EXECUTED"
```

```
4590    FOR Index=0 TO 14                          ! IDENTIFY THE INDIVIDUAL ERRORS
4600      IF (NOT BIT(Flag,Index)) THEN Next_indx
4610      Ercnt$[Index+1,Index+1]=VAL$(VAL(Ercnt$[Index+1,Index+1])+1)! INCREMEN
T
4620      Nerrs=Nerrs+1
4630      OUTPUT Prt USING "S(K)";" ERROR CODE #",Index,":",".    ",Erm$(Index)
4640      IF VAL(Ercnt$[Index+1,Index+1])=Max_warns THEN
4650      . OUTPUT Prt;"  This is the last warning for this error."
4660      END IF
4670 Next_indx:NEXT Index
4680    OUTPUT Prt USING "#,K,6A,K";"SEE THE ",Err$," DOCUMENTATION FOR AN"
4690    IF Nerrs<>1 THEN OUTPUT Prt;" EXPLANATION OF THESE ERRORS"
4700    IF Nerrs=1 THEN OUTPUT Prt;" EXPLANATION OF THIS ERROR"
4710    OUTPUT Prt;Aster$[1,Line_len]
4720    DATA " Passed  array  is dimensioned  improperly."!ERROR MESS'ES IN ORDE
R
4730    DATA " First  pass  parameter out of  range."
4740    DATA " Second  pass parameter out of  range."
4750    DATA " Third  pass  parameter out of  range."
4760    DATA " 3497A does not respond to bus  commands."
4770    DATA " 3456A does not respond to bus  commands."
4780    DATA " 3437A does not respond to bus  commands."
4790    DATA " Measurement out of range."
4800    DATA " Reference temp. or excitation  voltage out of range."
4810    DATA " The axis endpoints equal each  other."
4820    DATA "Scaling value is <= 0 on a log axis."
4830    DATA "Datapoint <= 0 on a log axis."
4840    DATA "Level crossing not found."
4850    DATA "User definable error."
4860    DATA "User definable error."
4870    DATA "*****************************************************************
*************"
4880 Exit:SUBEND
4890    ! *****************************************************************
4900    ! USER DEFINED FUNCTION FOR RECORDING A DC VOLTAGE
4910    ! *****************************************************************
4920   DEF FNDcv(Channel)                          ! 200 SERIES COMPUTER 02/02/83
4930    COM /Hp3054/ Scn,Dvm,Svm,Prt,Error,Err$[6],Ercnt$[15]
4940    OUTPUT Dvm USING "#"
4950    STATUS Dvm DIV 100,7;Here1
4960    Here2=8192*(Scn<>0)               ! MAKE A DEVICE NOT THERE CLEAR BIT 13
4970    IF (Dvm=Scn) OR (Channel=-1) THEN Chk
4980    OUTPUT Scn USING "#"
4990    STATUS Scn DIV 100,7;Here2
5000 Chk:Error=2*(((Channel<0) OR (Channel>999)) AND (Channel<>-1))
5010    Error=Error+16*((NOT BIT(Here2,13)) OR (NOT BIT(Here1,13)) AND (Dvm=Scn)
)
5020    Error=Error+32*((NOT BIT(Here1,13)) AND (Dvm<>Scn))
5030    IF Error THEN Abort
5040    IF Channel<>-1 THEN OUTPUT Scn;"AC";INT(Channel);"ST0"! CLOSE CHANNEL &
WAIT UNTIL EXECUTED
5050    IF Dvm=Scn THEN OUTPUT Dvm;"VR5VN1VA1VF1VD5VC0VS0VW0VT3"!3497 SETUP & TR
G
5060    IF Dvm<>Scn THEN OUTPUT Dvm;"H1STIGSTGT3"               !3456 SETUP & TRG
5070    ENTER Dvm;Reading
5080    RETURN Reading
5090 Abort:Err$="Dcv"
```

```
5100     CALL Warn
5110     RETURN 9.E+19
5120   FNEND
5130   !*****************************************************************
5140   ! SUBPROGRAM Lvdt FOR TAKING LVDT MEASUREMENTS
5150   !*****************************************************************
5160   SUB Lvdt(J,Channel,Cal,Meas,Dist)
5170   COM /Hp3045/ Scn,Dvn,Prt,Error,Err$[6],Ercnt$[15]
5180      Meas=FNDcv(Channel)
5190      Dist=Meas/Cal
5200      PRINT "LVDT VOLTAGE FOR LVDT #";J;Meas
5210      PRINT "DISPLACEMENT FOR LVDT #";J;Dist
5220      PRINT
5230   SUBEND
5240   !****************************************************************
5250   ! SUBPROGRAM Plotter_i FOR PLOTTING GRAPH ON PLOTTER FOR
5260   ! LATERAL LOAD VS DISPLACEMENT.
5270   !****************************************************************
5280   SUB Plotter_i(Title$,X$,Y$,Minx,Maxx,Miny,Maxy) ! Routine To Plot Graph On
 Plotter '
5290     PRINT
5300     PRINT "    <<<<<<<<<<<<<<<<<<<<<<<<<<<<<<<<<<<<<<<<<<<<<<<"
5310     PRINT "    <  ENTER PLOT PARAMETERS FOR GRAPH ON PLOTTER  <"
5320     PRINT "    >          (AXIS AND MAJOR/MINOR TICK MARKS)    >"
5330     PRINT "    >>>>>>>>>>>>>>>>>>>>>>>>>>>>>>>>>>>>>>>>>>>>>>>"
5340     PRINT
5350     INPUT "INPUT NAME OF TEST SPECIMEN",Title$
5360     PRINT
5370     INPUT "INPUT PLOT AXIS LIMITS (Minx,Maxx,Miny,Maxy)",Minx,Maxx,Miny,Maxy
5380     PRINT
5390     INPUT "INPUT NUMBER OF MAJOR AND MINOR TICK MARKS (Txmaj,Txmin,Tymaj,Tym
in)",Txmaj,Txmin,Tymaj,Tymin
5400     Spacx=(Maxx-Minx)/(Txmaj*Txmin)
5410     Spacy=(Maxy-Miny)/(Tymaj*Tymin)
5420     GINIT
5430     PLOTTER IS 705,"HPGL"    !  Specifies external two pen plotter as plotter
5440                              !  device
5450     OUTPUT 705;"SP1"     ! SELECTS PEN ON LEFT SIDE
5460     LORG 6                        ! Label Origin
5470     X_gdu_max=100*MAX(1,RATIO)    ! SCREEN SIZE LIMITS
5480     Y_gdu_max=100*MAX(1,1/RATIO) ! "      "        "
5490 !   LABELING TITLE
5500     FOR I=-.3 TO .3 STEP .1
5510     MOVE X_gdu_max/2+I,Y_gdu_max    ! gdu's - GRAPHICS DISPLAY UNITS
5520     LABEL "LOAD VS. DEFLECTION"
5530     NEXT I
5540     CSIZE 4
5550     MOVE X_gdu_max/2,.95*Y_gdu_max
5560     LABEL Title$
5570 !   LABELING X AND Y AXES TITLES
5580     DEG
5590     LDIR 90                         ! LABEL DIRECTORY
5600     CSIZE 3.5                       ! CHARACTER SIZE
```

```
5610    MOVE 0,Y_gdu_max/2
5620    LABEL "LOAD (KIPS)"
5630    LDIR 0
5640    MOVE X_gdu_max/2,.07*Y_gdu_max
5650    LABEL "DEFLECTION (IN.)"
5660    VIEWPORT .1*X_gdu_max,.90*X_gdu_max,.15*Y_gdu_max,.9*Y_gdu_max
5670    WINDOW Minx,Maxx,Miny,Maxy
5680    AXES Spacx,Spacy,Minx,Miny,Txmin,Tymin,3
5690    AXES Spacx,Spacy,Maxx,Maxy,Txmin,Tymin,3
5700  ! NUMBERING X AND Y AXES
5710    CLIP OFF    ! CAN NOW LABEL OR PLOT OUTSIDE VIEWPORT LIMITS
5720    CSIZE 2.6,.5
5730    LORG 6
5740    FOR I=Minx TO Maxx+Spacx STEP Spacx*Txmin
5750       MOVE I,Miny
5760       LABEL USING "K";I
5770       NEXT I
5780       LORG 8
5790       FOR I=Miny TO Maxy STEP Spacy*Tymin
5800       MOVE Minx,I
5810       LABEL USING "K,X";I
5820       NEXT I
5830       MOVE 0,Miny
5840       DRAW 0,Maxy
5850       MOVE Minx,0
5860       DRAW Maxx,0
5870       CLIP ON     ! NOW CAN ONLY LABEL OR PLOT WITHIN VIEWPORT LIMITS
5880     SUBEND
5890  !*********************************************************************
5900  ! SUBPROGRAM Printplot FOR PLOTTING DATA ON CRT SCREEN AS TEST PROCEEDS
5910  !*********************************************************************
5920  SUB Printplot(Lowx,Higx,Lowy,Higy,Xticl,Xtich,Yticl,Ytich,Spacex,Spacey,Ln
,Sp(*),Loadp(*))
5930    OUTPUT KBD USING "#,K";CHR$(255)&"K"
5940    PRINT
5950    PRINT "DO YOU WANT TO CHANGE PLOTTING LIMITS FOR CRT GRAPH (Y/N) ?"
5960    INPUT Answ$
5970    IF Answ$="Y" THEN GOTO 5990
5980    GOTO 6050
5990    INPUT "INPUT PLOT AXES LIMITS (Lowx,Higx,Lowy,Higy)",Lowx,Higx,Lowy,Higy
6000    PRINT
6010    PRINT
6020    INPUT "INPUT NUMBER OF MAJOR AND MINOR TICK MARKS (Txmaj,Txmin,Tymaj,Tymi
n)",Xtich,Xticl,Ytich,Yticl
6030    Spacex=(Higx-Lowx)/(Xticl*Xtich)
6040    Spacey=(Higy-Lowy)/(Yticl*Ytich)
6050    ALLOCATE X(400),Y(400)
6060    ON ERROR GOSUB Recov
6070    OUTPUT KBD USING "#,K";CHR$(255)&"K"
6080    PRINT "                    ***********************************"
6090    PRINT "                    *     PLOT OF LOAD VS. STRAIN      *"
6100    PRINT "                    * -------------------------------- *"
6110    PRINT "                    *   NOTE: TO PROCEED AFTER GRAPH   *"
```

```
6120   PRINT "                    *          PRESS <CONTINUE> !        *"
6130   PRINT "                    **********************************"
6140   PRINT
6150   INPUT "INPUT NUMBER OF STRAIN GAGE TO BE PLOTTED",Xnum
6160   FOR I=1 TO Ln
6170       X(I)=Sp(I,Xnum)
6180       Y(I)=Loadp(I)
6190     NEXT I
6200   Xn$="Gage"
6210   OFF ERROR
6220   OUTPUT KBD USING "#,K";CHR$(255)&"K"     ! CLEAR CRT
6230   ON ERROR GOTO Recov
6240   GINIT
6250   PLOTTER IS CRT,"INTERNAL"
6260   GRAPHICS ON
6270   LORG 6
6280   X_gdu_max=100*MAX(1,RATIO)
6290   Y_gdu_max=100*MAX(1,1/RATIO)
6300 ! LABELING TITLE
6310   FOR I=-.3 TO .3 STEP .1
6320   MOVE X_gdu_max/2+I,Y_gdu_max
6330   LABEL "LOAD VS. STRAIN"
6340   NEXT I
6350 ! LABELING X AND Y AXES TITLES
6360   DEG
6370   LDIR 90
6380   CSIZE 3.5
6390   MOVE 0,Y_gdu_max/2
6400   LABEL "LOAD (KIPS)"
6410   LDIR 0
6420   MOVE X_gdu_max/2,.07*Y_gdu_max
6430   LABEL "MICROSTRAIN"
6440 ! LABEL WHICH GAGE IS BEING PLOTTED
6450   LORG 2
6460   CSIZE 2.8
6470   MOVE .05*X_gdu_max,.02*Y_gdu_max
6480   LABEL Xn$;Xnum
6490   VIEWPORT .1*X_gdu_max,.9*X_gdu_max,.15*Y_gdu_max,.9*Y_gdu_max
6500   WINDOW Lowx,Higx,Lowy,Higy
6510   AXES Spacex,Spacey,Ldwx,Lowy,Xticl,Yticl,3
6520   AXES Spacex,Spacey,Higx,Higy,Xticl,Yticl,3
6530   OFF ERROR
6540 ! NUMBERING X AND Y AXES
6550   CSIZE 2.6,.5
6560   CLIP OFF
6570   LORG 6
6580   FOR I=Lowx TO Higx+Spacex STEP Spacex*Xticl
6590       MOVE I,Lowy
6600       LABEL USING "K";I
6610    NEXT I
6620    LORG 8
```

```
6630    FOR I=Lowy TO Higy STEP Spacey*Yticl
6640       MOVE Lowx,I
6650       LABEL USING "K,X";I
6660    NEXT I
6670    MOVE 0,Lowy
6680    DRAW 0,Higy
6690    MOVE Lowx,0
6700    DRAW Higx,0
6710    MOVE 0,0
6720    FOR I=1 TO Ln
6730        PLOT X(I),Y(I)
6740    NEXT I
6750    DEALLOCATE X(*),Y(*)
6760    OUTPUT KBD USING "#,K";CHR$(255)&"K"   !CLEAR CRT
6770    PAUSE
6780    GOTO 6840
6790 Recov:         !
6800    PRINT "UNEXPECTED ERROR. PLOTTING SEQUENCE WILL BE REPEATED."
6810    PRINT "NEED TO CHANGE PLOTTING LIMITS"
6820    PRINT
6830    WAIT 2
6840    GCLEAR                          ! CLEAR GRAPHICS SCREEN
6850   SUBEND
6860   !*****************************************************************
6870   ! SUBPROGRAM Plotrplot FOR PLOTTING DATA ON PLOTTER AS TEST PROCEEDS
6880   !*****************************************************************
6890   SUB Plotrplot(Plotval,Load,Minx,Maxx,Miny,Maxy,Defl1,Load1)
6900   PLOTTER IS 705,"HPGL"
6910   OUTPUT 705;"SP2"
6920   X_gdu_max=100*MAX(1,RATIO)
6930   Y_gdu_max=100*MAX(1,1/RATIO)
6940   WINDOW Minx,Maxx,Miny,Maxy
6950   PLOT Defl1,Load1
6960   PLOT Plotval,Load   ! PLOT LOAD VERSUS LVDT DISPLACEMENT
6970   PENUP
6980   Defl1=Plotval
6990   Load1=Load
7000   SUBEND
7010   !****************************************************************
7020   ! SUBROUTINE Printerin FOR INPUTING GRAPH DATA FOR SCREEN GRAPH
7030   !****************************************************************
7040    SUB Printerin(Lowx,Higx,Lowy,Higy,Xticl,Xtich,Yticl,Ytich,Spacex,Spacey)
7050    OUTPUT KBD USING "#,K";CHR$(255)&"K"
7060    PRINT "  <<<<<<<<<<<<<<<<<<<<<<<<<<<<<<<<<<<<<<<<<<<<<<<<<<<<"
7070    PRINT "  <   ENTER PLOT PARAMETERS FOR GRAPH ON CRT SCREEN  <"
7080    PRINT "  >          (AXIS AND MAJOR/MINOR TICK MARKS)       >"
7090    PRINT "  >>>>>>>>>>>>>>>>>>>>>>>>>>>>>>>>>>>>>>>>>>>>>>>>>>>>"
7100    PRINT
7110    INPUT "INPUT PLOT AXES LIMITS (Lowx,Higx,Lowy,Higy)",Lowx,Higx,Lowy,Higy
7120    INPUT "INPUT NUMBER OF MAJOR AND MINOR TICK MARKS (Txmaj,Txmin,Tymaj,Tymi
n)",Xtich,Xticl,Ytich,Yticl
7130    Spacex=(Higx-Lowx)/(Xticl*Xtich)
```

```
7140   Spacey=(Higy-Lowy)/(Yticl*Ytich)
7150   SUBEND
7160  ! ***************************************************************
7170  ! SUBPROGRAM Datasave STORES DATA IN FILE2$ FOR TEST RESULTS
7180  ! ***************************************************************
7190  SUB Datasave(@Path2,D2,Ln,Load,Plotval,Ng,Num,P(*),Dn(*))
7200    OUTPUT @Path2,D2;Ln              ! STORE LOAD NUMBERS
7210      D2=D2+1
7220    OUTPUT @Path2,D2;Load            ! STORE LOADS
7230      D2=D2+1
7240    OUTPUT @Path2,D2;Plotval         ! STORE CENTER SPAN DEFLECTIONS
7250      D2=D2+1
7260      FOR K=1 TO Ng
7270    OUTPUT @Path2,D2;P(K)            ! STORE STRAIN VALVES
7280      D2=D2+1
7290      NEXT K
7300      FOR K=1 TO Num
7310    OUTPUT @Path2,D2;Dn(K)           ! STORE LVDT DISPLACEMENTS
7320      D2=D2+1
7330      NEXT K
7340    SUBEND
```

Appendix F
PIERHINGE User's Guide

PIERHINGE is a general program for collecting, storing, and processing test data using a Hewlett-Packard series 9000 microcomputer and a series 3000 data acquisition unit. The program collects data from strain gages and linear variable differential transformers (LVDT's) attached to the test specimen and from a load cell and LVDT to measure axial load and lateral deflection. The collected data is stored on the computer's hard drive for later processing. Data collected from the load cell and the LVDT mounted in the hydraulic ram arm are plotted during testing. A screen plot of the applied lateral load versus strain gage readings is also available.

Before testing can commence, certain parameters must be entered: file names to tell the program where to store the data, the date and time of the test, and measurements for plotter scaling. Other information required by the program is coded into the software. This information includes:

1. The total number of strain gages and LVDT's used to record test data.

2. Gage factors and calibration factors for the strain gages, the LVDT's and the load cell.

3. Channel assignments for the input devices.

During testing, data collection involves triggering the system and recording strain, displacement, and load values. These values are converted from voltage measurements by an analog-to-digital (A/D) converter. The test data is stored on the hard drive and sent to the printer to provide a log of strains, displacements, and loads. A plot of the axial load versus lateral displacement hysteresis curve is made during the test to provide "visual feedback." After testing is complete, the user can view plots of the test data on the computer's monitor. The program was designed to allow the to operator to trigger one data point at a time, and is not set up for continuous real-time data aquisition. *PIERHINGE* was written in Hewlett-Packard Basic. Comments, denoted by a leading "!", are provided throughout the program to to document the logic flow.

The following is a line-by-line explanation of the program:

<u>10-330</u>

Comments on initial equipment set-up and basic testing operation.

<u>340-570</u>

Variable initialization. The program prompts the user to input the names of the stain gage reference data file, the output file name for the test data, and the title of the experiment.

590-600

Input the number of stain gages and LVDT's.

650-730

Set the date and time of the test.

750

The subprogram "Plotter_i" is called to ask the user to enter information about the load versus lateral displacement plot. "Plotter_i" sets up the graphics for the hard copy plot on the HP 7470A plotter. The user is asked to enter the *x*- and *y*-axis plot limits, and the number of major and minor tick marks. Plot axis limits refer to the minimum and maximum load and displacement limits. After inputting the required data the plot axes will be drawn and the graph will be labeled.

760

The user is now asked for plotting information from subprogram "Printerin," which sets up the on-screen plotting of load versus strain. Plot axis limits and tick marks are inputed from the computer. Viewport limits are set to maximum.

800-880

Retrieve the reference strain gage values taken prior to the start of the test. Reference values are obtained for each strain gage. These reference values are subtracted from test readings to obtain true values.

Memory is allocated for a maximum of 300 data points. Space is provided for 18 strain gages, 3 LVDT's, 1 load cell, and 1 LVDT located on the MTS hydraulic ram arm.

940-1310

The program automatically assigns channels to the strain gages, LVDT's, load cell, and the LVDT located on the MTS ram. Also, within these lines are the gage and calibration factors for each device.

1340

The HP-IB interface bus is initialized for proper communications. The following message will appear on the screen:

```
          Equipment Present on Bus #7
     3497A Mainframe               at address 09
     3456A Digital Voltmeter       at address 22
     3437A System Voltmeter        at address 24
     System Computer               at address 21
     System Printer                at address 01
```

1380-1460

Read unstrained bridge imbalance-to-excitation voltage ratio and excitation voltage for each strain gage, and print the results. Lines 1340 and 1380-1460 are executed initially to obtain the reference strain gage data and each time a data point is triggered during the test.

1500-1520

Store the reference strain gage data for later use.

1560-1710

Calculate actual strain gage values with respect to the reference readings and print the values.

1750-1840

Compute lateral force and horizontal displacement from the load cell and LVDT located on the MTS ram. These values are used for the load versus displacement plot.

1860-1890

Print the test data.

1930-2030

Call subroutine "Lvdt," whichcalculates the external LVDT's displacements and then prints the results.

2050-2070

Call subroutine "Datasave" to save the test data on the hard drive.

2570-2650

Subroutine "Datastor;" saves the strain gage reference data.

2660-2940

Subroutine "Dataprint;" prints the following test data: test specimen name; time and date; lateral load; center span deflection; load number; strain gage number, channel, and the strain for each gage; and the LVDT number displacement.

3010-3650

Subroutine "Init." All of the system voltmeters are initialized and the interface bus is cleared for transfer of data from the controller to the computer. This portion of the program initializes the HP-IB, assigns device names to select codes, and lists the instruments connected to the HP-IB with their address.

3690-4000

Subroutine "Brmeas." Takes a strain gage bridge measurement in conjunction with the user defined function DEF FNStrain to perform a complete strain gage measurement. This subroutine is called before stress is applied to the gage; after stress is applied to the gage, the subroutine is again called for a second set of measurements. This information is passed to DEF FNStrain to calculate the strain.

4040-4140

User defined function DEF FNStrain.

4180-4880

Subroutine "Warn." This subroutine detects errors, such as when a strain gage fails during testing. An error message will be printed (the message will only be printed once, when the gage fails.), and subsequent readings from the failed gage will be printed with a value of 9.E+19 printed. This error, however, will not halt program execution.

4920-5120

User defined function DEF FNDcv(Channel). A user defined function for recording DC voltages.

5160-5230

Subroutine "Lvdt." In line 5180 a voltage measurement for the LVDT is taken by the user defined function DEF FNDcv. The voltage is converted to displacement by dividing the voltage by the appropriate calibration factor.

5280-5880

Subroutine "Plotter_i."

5920-6860

Subroutine "Printplot."

6890-7000

Subroutine "Plotrplot."

7040-7150

Subroutine "Printerin."

7190-7340

Subroutine "Datasave."

Appendix G

List of CCEER Publications

Report No.	Publication
CCEER-84-1	Saiidi, M., and R. A. Lawver. "User's manual for LZAK-C64, a computer program to implement the Q-model on Commodore 64." *Report number CCEER-84-1*. Reno: University of Nevada, Department of Civil Engineering. January 1984.
CCEER-84-2	Douglas, B. M., and T. Iwasaki. "Proceedings of the first USA-Japan bridge engineering workshop," held at the Public Works Research Institute, Tsukuba, Japan. *Report number CCEER-84-2*. Reno: University of Nevada, Department of Civil Engineering. April 1984.
CCEER-84-3	Saiidi, M., J. D. Hart, and B. M. Douglas. "Inelastic static and dynamic analysis of short R/C bridges subjected to lateral loads." *Report number CCEER-84-3*. Reno: University of Nevada, Department of Civil Engineering. July 1984.
CCEER-84-4	Douglas, B. "A proposed plan for a national bridge engineering laboratory." *Report number CCEER-84-4*. Reno: University of Nevada, Department of Civil Engineering. December 1984.
CCEER-85-1	Norris, G. M., and P. Abdollaholiaee. "Laterally loaded pile response: Studies with the strain wedge model." *Report number CCEER-85-1*. Reno: University of Nevada, Department of Civil Engineering. April 1985.
CCEER-86-1	Ghusn, G. E., and M. Saiidi. "A simple hysteretic element for biaxial bending of R/C columns and implementation in NEABS-86." *Report number CCEER-86-1*. Reno: University of Nevada, Department of Civil Engineering. July 1986.
CCEER-86-2	Saiidi, M., R. A. Lawver, and J. D. Hart. "User's manual of ISADAB and SIBA, computer programs for nonlinear transverse analysis of highway bridges subjected to static and dynamic lateral loads." *Report number CCEER-86-2*. Reno: University of Nevada, Department of Civil Engineering. September 1986.
CCEER-87-1	Siddharthan, R. "Dynamic effective stress response of surface and embedded footings in sand." *Report number CCEER-87-1*. Reno: University of Nevada, Department of Civil Engineering. June 1987.

CCEER-87-2 Norris, G., and R. Sack. "Lateral and rotational stiffness of pile groups for seismic analysis of highway bridges." *Report number CCEER-87-2*. Reno: University of Nevada, Department of Civil Engineering. June 1987.

CCEER-88-1 Orie, J., and M. Saiidi. "A preliminary study of one-way reinforced concrete pier hinges subjected to shear and flexure." *Report number CCEER-88-1*. Reno: University of Nevada, Department of Civil Engineering. January 1988.

CCEER-88-2 Orie, D., M. Saiidi, and B. Douglas. "A micro-CAD system for seismic design of regular highway bridges." *Report number CCEER-88-2*. Reno: University of Nevada, Department of Civil Engineering. June 1988.

CCEER-88-3 Orie, D., and M. Saiidi. "User's manual for Micro-SARB, a microcomputer program for seismic analysis of regular highway bridges." *Report number CCEER-88-3*. Reno: University of Nevada, Department of Civil Engineering. October 1988.

CCEER-89-1 Douglas, B., M. Saiidi, R. Hayes, and G. Holcomb. "A comprehensive study of the loads and pressures exerted on wall forms by the placement of concrete." *Report number CCEER-89-1*. Reno: University of Nevada, Department of Civil Engineering. February 1989.

CCEER-89-2a Richardson, J., and B. Douglas. "Dynamic response analysis of the Dominion Road Bridge test data." *Report number CCEER-89-2*. Reno: University of Nevada, Department of Civil Engineering. March 1989.

CCEER-89-2b Vrontinos, S., M. Saiidi, and B. Douglas. "A simple model to predict the ultimate response of R/C beams with concrete overlays." *Report number CCEER-89-2*. Reno: University of Nevada, Department of Civil Engineering. June 1989.

CCEER-89-3 Ebrahimpour, A., and P. Jagadish. "Statistical modeling of bridge traffic loads: A case study." *Report number CCEER-89-3*. Reno: University of Nevada, Department of Civil Engineering. December 1989.

CCEER-89-4 Shields, J., and M. Saiidi. "Direct field measurement of prestress losses in box girder bridges." *Report number CCEER-89-4*. Reno: University of Nevada, Department of Civil Engineering. December 1989.

CCEER-90-1 Saiidi, M., E. Maragakis, G. Ghusn, Jr., Y. Jiang, and D. Schwartz. "Survey and evaluation of Nevada's transportation infrastructure, task 7.2—highway bridges, final report." *Report number CCEER-90-1*. Reno: University of Nevada, Department of Civil Engineering. October 1990.

CCEER-90-2 Abdel-Ghaffar, S., E. Maragakis, and M. Saiidi. "Analysis of the response of reinforced concrete structures during the Whittier earthquake of 1987." *Report number CCEER-90-2*. Reno: University of Nevada, Department of Civil Engineering. October 1990.

CCEER-91-1 Saiidi, M., E. Hwang, E. Maragakis, and B. Douglas. "Dynamic testing and analysis of the Flamingo Road Interchange." *Report number CCEER-91-1*. Reno: University of Nevada, Department of Civil Engineering. February 1991.

CCEER-91-2 Norris, G., R. Siddharthan, Z. Zafir, S. Abdel-Ghaffar, and P. Gowda. "Soil-foundation-structure behavior at the Oakland Outer Harbor Wharf." *Report number CCEER-91-2*. Reno: University of Nevada, Department of Civil Engineering. July 1991.

CCEER-91-3 Norris, G. M. "Seismic lateral and rotational pile foundation stiffness at Cypress." *Report number CCEER-91-3*. Reno: University of Nevada, Department of Civil Engineering. August 1991.

CCEER-91-4 O'Connor, D. N., and M. Saiidi. "A study of protective overlays for highway bridge decks in Nevada, with emphasis on polyester-styrene polymer concrete." *Report number CCEER-91-4*. Reno: University of Nevada, Department of Civil Engineering. October 1991.

CCEER-91-5 O'Connor, D. N., and M. Saiidi. "Laboratory studies of polyester-styrene polymer concrete engineering properties." *Report number CCEER-91-5*. Reno: University of Nevada, Department of Civil Engineering. November 1991.

CCEER-92-1 Straw, D. L., and M. "Saiid" Saiidi. "Scale model testing of one-way reinforced concrete pier hinges subjected to combined axial force, shear and flexure." *Report number CCEER-92-1*. Reno: University of Nevada, Department of Civil Engineering. March 1992.